file — research reports
(key word: framing angle connection tests)

1400

STRENGTH AND BEHAVIOR OF CONNECTION ELEMENTS

Prepared for

American Institute of Steel Construction
400 North Michigan Avenue
Chicago, Illinois 60611

by

David J. Irish
Reidar Bjorhovde

author

of

The Department of Civil Engineering
and Engineering Mechanics
THE UNIVERSITY OF ARIZONA
Tucson, Arizona 85721

1983

STRENGTH AND BEHAVIOR OF CONNECTION ELEMENTS

by

David Irish

and

Reidar Bjorhovde

Report Submitted to
American Institute of Steel Construction, Inc.
400 N. Michigan Avenue
Chicago, Illinois

Department of Civil Engineering
University of Arizona
Tucson, Arizona

June, 1983

~~Rod~~
~~Sett~~
file

It doesn't appear that Reidar changed his shear test approach.

I agree with N.T. I think we have a problem Norton

~~Bob D~~

ACKNOWLEDEMENTS

The findings that are presented in this report were developed in the research project "Strength and Stiffness of Connection Components", funded by the American Institute of Steel Construction under grant no. 21.79. The authors are sincerely appreciative of the financial support, as well as the helpful technical comments made by Messrs. R. O. Disque, W. A. Milek and R. M. Richard. Laboratory assistance was rendered by Messrs. K. H. Hamm, D. A. Rabern, G. C. Williams and Mun-Foo Leong.

TABLE OF CONTENTS

		Page
	ACKNOWLEDGMENTS	ii
	LIST OF ILLUSTRATIONS	v
	LIST OF TABLES	vi
	ABSTRACT	vii
1.	INTRODUCTION	1
2.	SCOPE OF THE STUDY	3
3.	PREVIOUS STUDIES	4
4.	DESCRIPTION OF TEST SPECIMENS AND TESTING PROCEDURES	7
	4.1 General Information	7
	4.2 Test Specimens	8
	4.3 Instrumentation and Data Acquisition	9
	4.4 Loading Procedure	11
5.	TEST RESULTS	21
	5.1 General Information	21
	5.2 Results of Shear Tests	22
	5.3 Results of the Compression Tests	23
	5.4 Results of the Tension Tests	23
	5.5 Other Results	27
6.	DISCUSSION AND APPLICATION OF TEST RESULTS	29
	6.1 Graphing and Plotting of Test Results	29
	6.2 Orthotropic Failure Surface	30

TABLE OF CONTENTS--Continued

		Page
7.	THEORETICAL ANALYSIS.	36
	7.1 General Information	36
	7.2 Finite Element Analysis	36
8.	SUMMARY AND CONCLUSIONS	38
	APPENDIX A: LEAST-SQUARES CURVE FITS FOR THE DATA REQUIRED.	40
	APPENDIX B: VARIATION IN LOAD-DEFORMATION CURVES WITH RESPECT TO A CHANGE IN THE LOAD-BEARING PLATE THICKNESS	74
	APPENDIX C: VARIATION IN LOAD-DEFORMATION CURVES WITH RESPECT TO A CHANGE IN ANGLE THICKNESS.	86
	APPENDIX D: VARIATION IN LOAD-DEFORMATION CURVES WITH RESPECT TO A CHANGE IN GAGE LENGTH.	96
	APPENDIX E: VARIATION IN LOAD-DEFORMATION CURVES WITH RESPECT TO BOLT DIAMETER OR STATE OF STRESS	106
	APPENDIX F: EXPLANATION OF THE RICHARD CURVE	109
	REFERENCES	111

LIST OF ILLUSTRATIONS

Figure		Page
4.1a	Typical Specimen Configurations for Tension Tests (Front View).	13
4.1b	Typical Specimen Configurations for Tension Tests (Side View)	14
4.1c	Typical Specimen Configurations for Compression Tests (Front View).	15
4.1d	Typical Specimen Configurations for Compression Tests (Side View)	16
4.1e	Typical Specimen Configurations for Shear Test.	17
4.2	Base Plate for the Three Angle Sizes.	18
4.3	Sizes of Angles Used in Testing Program	19
4.4	Load-Bearing Plates for Tension, Compression and Shear	20
6.1	Typical Curve with Richard Parameters	31
6.2	Diagram of Orthotropic Failure Surface.	33

LIST OF TABLES

Table		Page
5.1	Location of Failure for all the Tension Tests.	28
6.1	Tension Test Data.	34
6.2	Compression Test Data	35
6.3	Shear Test Data	35

ABSTRACT

Double angle gusset plate connection elements were tested in compression, shear, and tension, and load-deformation curves were produced. A least-squares curve fit program was used to analyze the data and provide empirical curves and curve parameters. The parameters define the load-deformation curves so that these may be used as input into a finite element analysis program.

The influence of load-bearing plate thicknesses, angle thicknesses, gage lengths, and bolt diameters was also evaluated, and an orthotropic failure surface developed. Its use in the analysis of the connections is detailed.

CHAPTER 1

1. INTRODUCTION

Among the most difficult problems faced in the analysis of complex connections is the incorporation of realistic material and fastener properties. In a one-dimensional approach, a material behaves according to its stress-strain characteristics. For real connections and other areas where the state of strain is better characterized as two- or three-dimensional, the stress-strain curve is not sufficient. On the other hand, the development of connection behavior models that incorporate the multidimensional characteristic of the material are highly complex. This is even further complicated by the fact that dissimilar materials are used in connections: The behavior and strength of bolts, welds and basic structural steel can be very different. Naturally, the geometry of the joint plays a major role as well.

It is fortunate that for practical purposes it is not necessary to know the individual compoments of load-deformation that can be attributed to each of the basic materials, the welds, bolts, and other fastening elements. Insofar as the overall connection behavior and strength are concerned, it is the <u>total response</u> of the

fastening detail that is important. Once its load-deformation characteristic is known, it can be used as part of the analytical procedure for the connection as a whole.

Limited load-deformation data are available on the behavior of double angles that are bolted or welded to plates or other structural elements. The results are almost exclusively based on double beam-to-column connection tests, for which two or more bolts were used. The usefulness of the data is also limited because they were obtained from overall connection tests, which to a certain degree masks the behavior of the angles, bolts, and plates. Consequently, the load-deformation data derived from these tests are not accurate enough to be used in the analysis of realistic connections. For example, if a finite element approach is utilized, in order for the program to be of any value to the structural engineer, the load-deformation curve that is used in the program must be modeled as closely as possible to the actual behavior of the connection element. The only way this can be achieved is to test the appropriate elements for the conditions to which they will be subjected in the structure.

The value of this information can be appreciated when considering the size of the gusset plate connections that are used in large industrial-type structures. It is not unusual for these plates to span a sizable fraction of the clear span between the girders of different floors. Thus, one may see that the results of these tests may lead to a more efficient and economical utilization of materials.

CHAPTER 2

2. SCOPE OF THE STUDY

To gather the necessary data for input into the finite element program, this investigation will consist of an experimental study of the load-deformation characteristics of double angles, bolted to a plate and a supporting member. To provide the proper and complete data for the theoretical analysis of connections that use such elements, the connections will be loaded to produce the three basic types of load-deformation data. The first curve will be the double angles in tension, the second for double angles in compression, and the third a curve for double angles in shear. The combination of these tests will be used to develop what is termed a failure envelope, to be discussed with the load-deformation curves in Chapter Six.

CHAPTER 3

3. PREVIOUS STUDIES

Most of the experimental studies on connections that have been undertaken have dealt primarily with the behavior of the connections when end moments are induced (Rathburn, 1935; Sommer, 1969; Munse, Bell, and Chesson, 1959; and Lewitt, Chesson, and Munse, 1966). As a result, the data that was collected led to conclusions on elastic moment resistance (Rathbun, 1935), moment-rotation characteristics of the connection as a whole (Sommer, 1969), the general behavior of beam-to-column connections when assembled with both rivets and bolts (Munse, Bell and Chesson, 1959), and the development of the actual end moment (Lewitt, Chesson, and Munse, 1966).

In the study of welded header plate connections by W. H. Sommer (1969), load-deformation data of the connection itself were not taken. However, references and conclusions were made with respect to the size of the connection and how the number of rows of bolts affected the behavior. He observed that high tension and shear forces were transmitted to the bolts of deep connections; severe outward deformation occurred at the top of such connections.

Munse, Bell and Chesson (1959) conducted tests of beam-to-column connections, and observed that they failed by tearing of the angles without rupture of the fasteners. Also, because the behavior

of the connections during loading, they determined that the tearing of the angles in tension results primarily from the bending moment. With these results in mind, it was felt that the tension specimens of the present study would fail at relatively low loads when compared to the compression tests. Failure would take place in the angles themselves and not in the high-strength bolts, even though the specimens had been designed for pure tension.

To fully understand the application of the tests and their use in finite element model analysis, it must be noted that it was assumed that flexible connection behavior can be adequately represented by using a number of flexible elements that are connected to the model through appropriate boundary conditions. It should thus be possible to obtain the required load-deformation characteristics of the connection by testing different segments of similar geometry for the three basic load types: tension, compression, and shear. This, in turn, implies that there is no difference in behavior between a length of angle segment containing a fastener and a length of angle segment that does not. Lewitt, Chesson, and Munse (1966) also used these assumptions, and found them to be reasonably accurate. For example, they found that a six inch segment with two bolts, three inches between centers and one and a half inches from each end, was a little more than twice as stiff as a three inch segment with one bolt in the center. Obviously, the geometry of the angle, the sizes and locations of the holes from the heel, and the bolt were all similar, otherwise, the comparison would not be valid. Unfortunately, they did not run a sufficient number of tests with respect

to varying angle sizes, load-bearing plate thicknesses, and bolt diameters for the compression and tension tests to develop conclusive results about the load-deformation characteristics of double angle connections.

CHAPTER 4

DESCRIPTION OF TEST SPECIMENS AND TESTING PROCEDURES

4.1 General Information

Figure 4.1 shows the testing configuration for the three basic types of loading; tension, compression and shear. The test specimens were designed to model double angles bolted to a stiff supporting member. The stiff supporting member was a thick rectangular plate designed to be relatively rigid with respect to the angles. Holes were then bored through the plate and recessed at one end to accommodate the head of the bolt, so the specimen could lay flat as shown in Figure 4.2. However, when putting the specimens together, the bolt used for tightening the horizontal leg to the supporting member did not leave enough room for the wrench to tighten the bolt on the vertical leg. The bolt was therefore turned around and the nut fit in the recessed end.

Four different sizes of angles were selected for the testing program to give a variation in gage length and a constant pitch. The angles are shown in Figure 4.3 with all their geometric properties. All of the angles were made three inches long, to model the spacing of bolts in typical connections.

Three different thicknesses of load-bearing plates were also used to determine if the distance between the vertical legs of the angles as well as the relative stiffness of the load-bearing plate would give any variations in the load-deformation data. The three plate thicknesses were 1/4 inch, 3/8 inch, and 1/2 inch. This range was obtained by using a simple plate for the tension tests and a structural tee (WT) for the compression and shear tests, as shown in Figure 4.4.

Both 3/4 inch and 7/8 inch diameter A325 structural bolts were used in the compression tests where the load-bearing plate was either 3/8 inch or 1/2 inch. This was done to evaluate how the size of the bolt, the size of the hole, and the tension in the bolt would affect the load-deformation data. It must be noted, however, that the two different bolt diameters were not used together in the same test; either 3/4 inch or 7/8 inch diameter bolts were used for the entire connection.

Milling was performed at Stanley Structures of Tucson using standard fabrication techniques and assembly of the test specimens was performed in the lab.

4.2 Test Specimens

The compression tests were relatively easy to make and install for testing. The horizontal leg of both angles were bolted to a large rectangular plate, 1-1/2 inches thick to resemble a supporting member, as discussed earlier, and shown in Figure 4.2. A structural tee (WT) of desired stem thickness was bolted between the

vertical legs of the double angles to transfer the load through the bolt and to the angles. The three sizes of the WT sections were: WT 9x35.5, WT 8x25, WT 8x13.

The tension tests were the most difficult to design, but were actually relatively easy to make and install. A specially fabricated tension plate, shown in Figure 4.4, was bolted between the vertical legs of the double angles to transmit the load through the bolts and to the angles. The tension plate was mounted to a jig that extended through the jaws of the testing machine and was fastened to the top crosshead. The horizontal legs were bolted to the base plate, modeled as the supporting member. The base plate then had a plate, similar to the plate bolted between the vertical legs, welded to the bottom to transfer the load to another jig that was fastened to the bottom crosshead.

The shear tests, however, were run slightly differently. The two angles to be tested were placed on their sides, and a structural tee (WT) was bolted between what would have been the vertical legs, as shown in Figure 4.1. For this model, no supporting member was used; it was felt that this would give the same results as the compression tests, since failure was expected to occur in the load-bearing plate, the bolt, or the hole, and not in the angles themselves as in the tension tests.

4.3 Instrumentation and Data Acquisition

Dial gages of 0.001 inch accuracy were used instead of strain gages on the specimens because large deformations were anticipated,

especially in the tension tests. Since strain gages cannot record large deformations reliably, dial gages were used to achieve the desired accuracy.

For the tension and compression specimens, the dial gages measured the amount of deformation in the vertical angle legs, the bolt and the load-bearing plate material to a point just above the top of the vertical angle legs, as shown in Figure 4.1. Since the shear specimens were tested differently, the dial gages measured a slightly different deformation. In the shear tests, the deformation also took place in the bolt and in a portion of the load-bearing plate. However, the deformation of the angles was perpendicular to the deformation measured in the tension and compression tests. It was felt, however, that the compression and shear tests would yield similar load-deformation curves.

The dial gages were read in the same order each time so that any error as a consequence of reading the dials would be kept to a minimum. Then, the readings from the two dial gages were averaged to give the "true" deformation at the centerline of the specimen. When the specimens were unloaded, the dial gages were read again. This would give an indication as to the amount of permanent deformation that had taken place.

Pre-prepared data sheets were used when recording the data for all three test types. This simplified the process of documentation and reduced the chances of recording the right information in the wrong place, since the specimens were marked and catalogued before the bulk of the testing started.

4.4 Loading Procedure

A Tinius Olsen 200 kip universal testing machine was used because it gave the desired capacity and load scales for the different test types. For the compression and shear tests, loads of up to 80 kips were expected. For the tension tests, loads were not expected to exceed 50 kips.

The bolts were tightened according to their locations. The bolts that held the horizontal legs of the angles to the supporting member were tightened with a spud wrench until secure. The bolt that transmitted the load from the load-bearing plate to the vertical angle legs was also tightened using a spud wrench, but in addition was also tightened one-half turn using the turn-of-nut method. After the nut was secured, marks were made on both sides of the vertical angle legs and also on both the nut and the head of the bolt. The mark on the angle on the side of the nut was used to judge when one-half turn had been completed. The mark on the angle on the side of the bolt head was used to determine if the bolt rotated when the nut was tightened with the torque wrench. It must be noted, however, that the load-bearing bolt was not tightened with the torque wrench until an initial load of five kips for both the compression and shear tests and 2.5 kips for tension tests was applied. This initial load allowed the bolt, the load-bearing plate and the two vertical angle legs to be "seated" and eliminate the influence of slip on the load-deformation readings that were recorded.

A spherical head was used for the compression and shear tests to ensure that the load-bearing tee was loaded as uniformly as possible. Any eccentricity of the load about the centerline of the test specimen thus was reduced to a minimum.

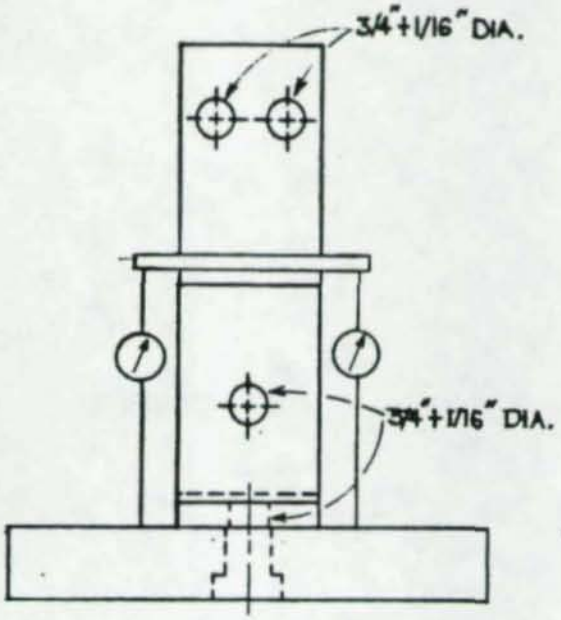

FIGURE 4.1a

TYPICAL SPECIMEN CONFIGURATIONS FOR TENSION TESTS

Front View

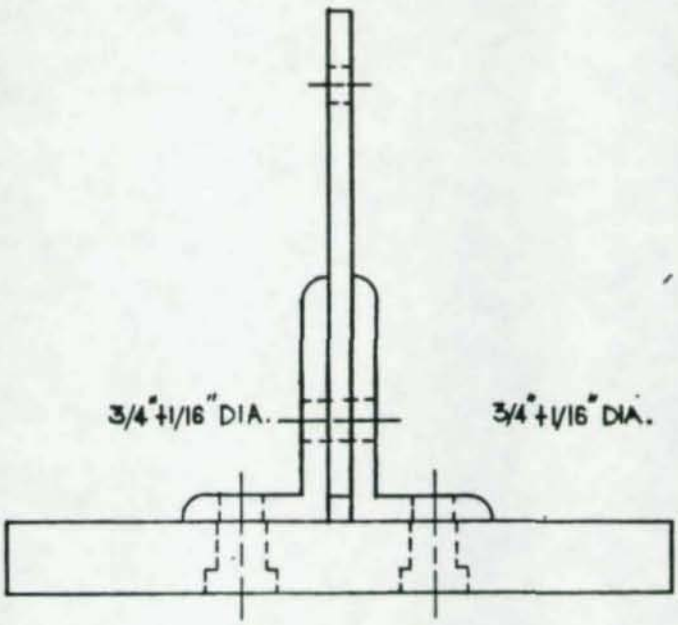

FIGURE 4.1b

TYPICAL SPECIMEN CONFIGURATIONS FOR TENSION TESTS

Side View

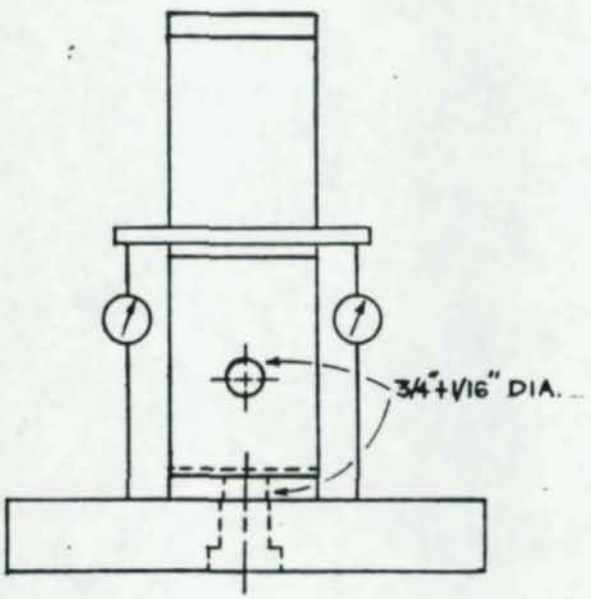

FIGURE 4.1c

TYPICAL SPECIMEN CONFIGURATIONS FOR COMPRESSION TESTS

Front View

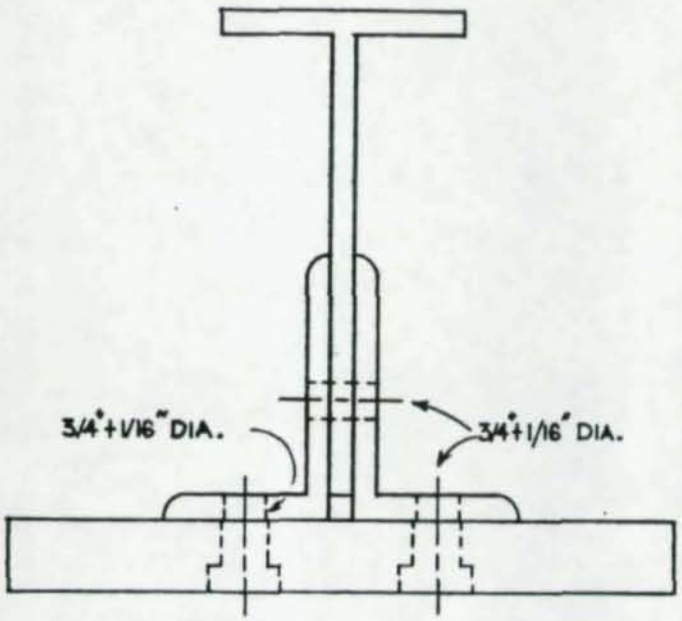

FIGURE 4.1d

TYPICAL SPECIMEN CONFIGURATIONS FOR COMPRESSION TESTS

Side View

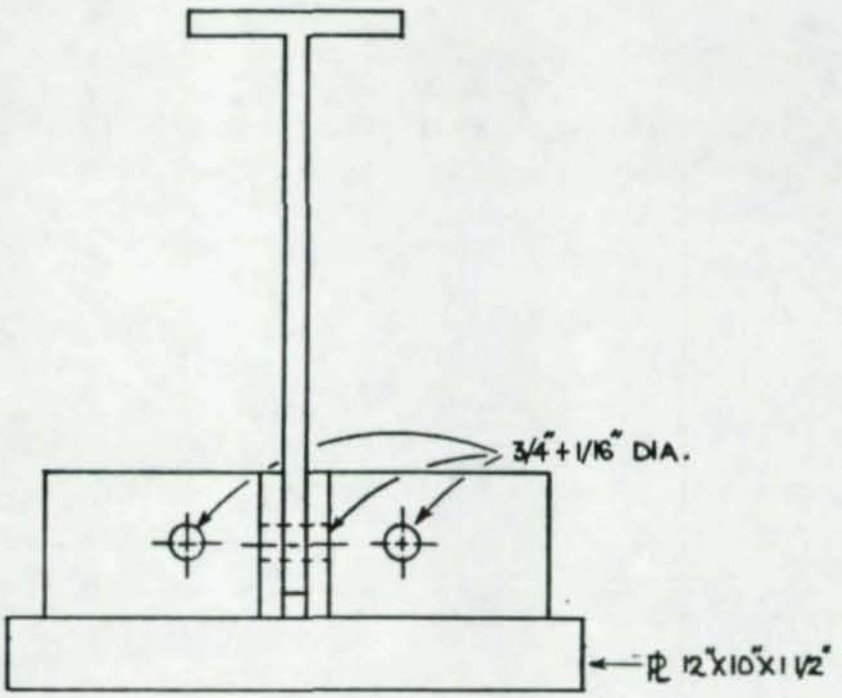

FIGURE 4.1e

TYPICAL SPECIMEN CONFIGURATIONS FOR SHEAR TEST

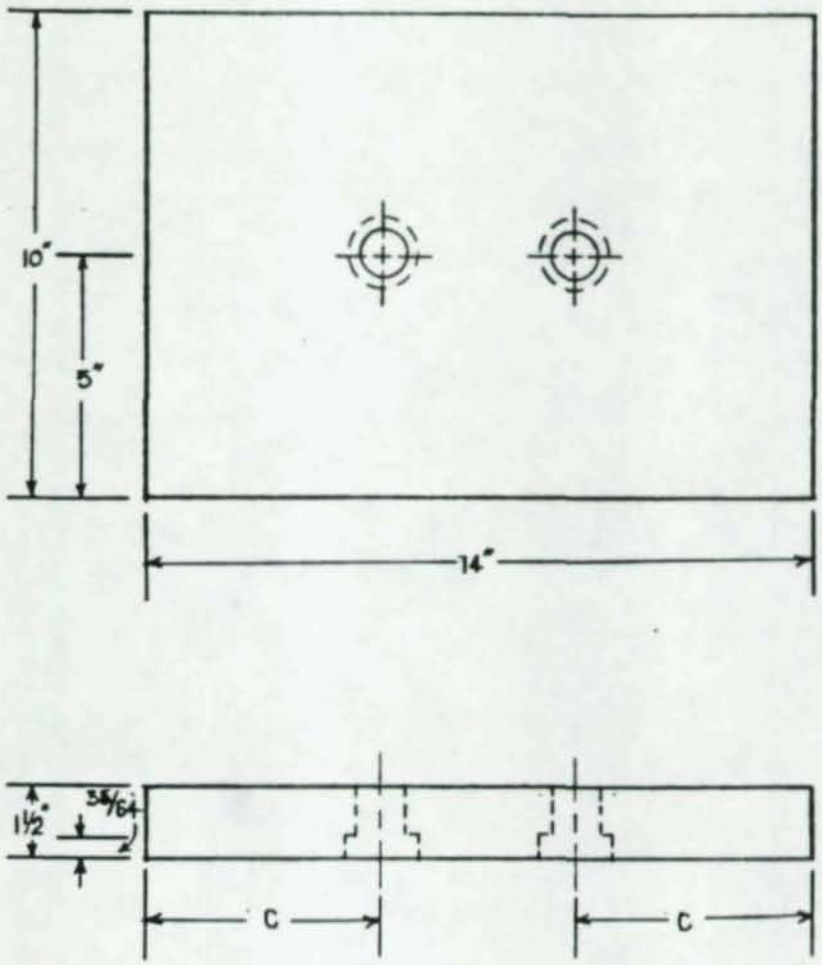

FIGURE 4.2

BASE PLATE FOR THE THREE ANGLE SIZES

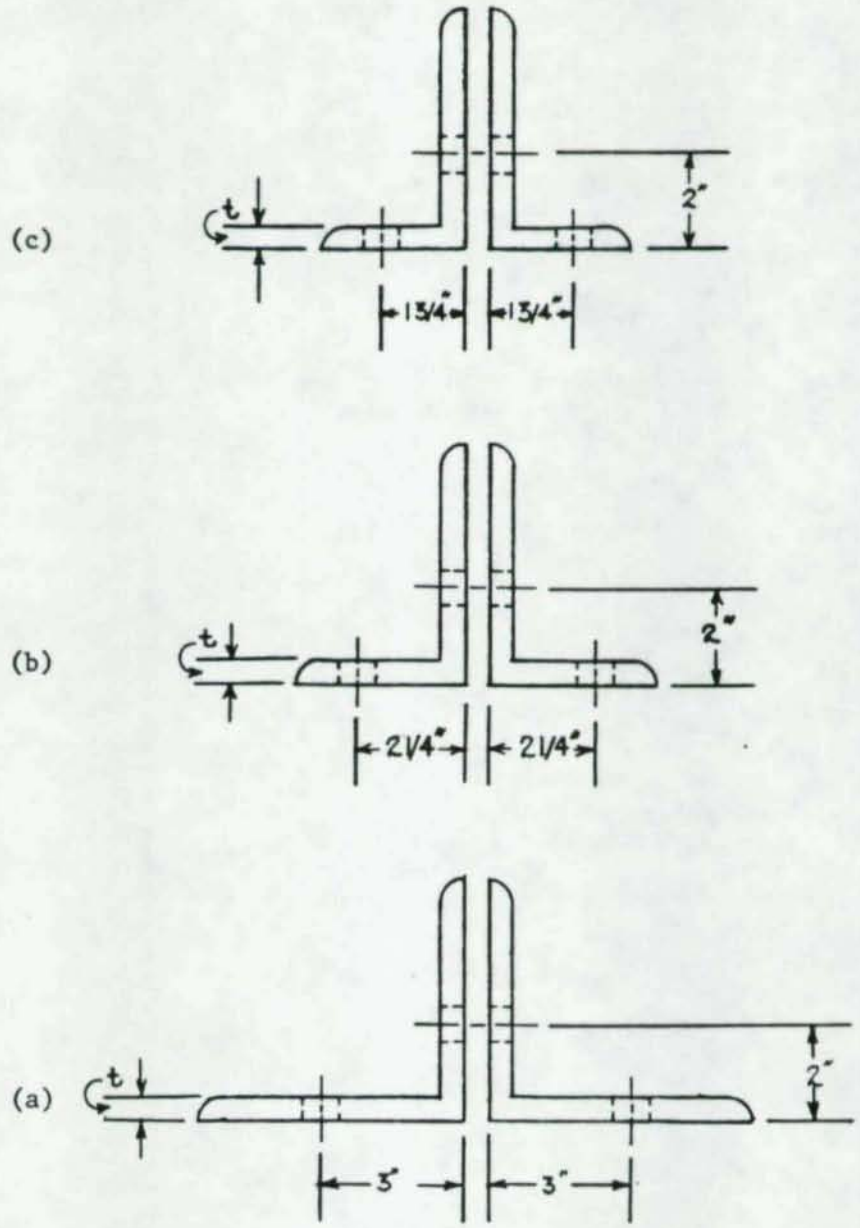

FIGURE 4.3

SIZES OF ANGLES USED IN TESTING PROGRAM:
(a) 5x5xt, (b) 5x3-1/2xt, (c) 5x3xt
(t is the thickness of the angle: t=1/2", 3/8", 5/16", and 1/4")

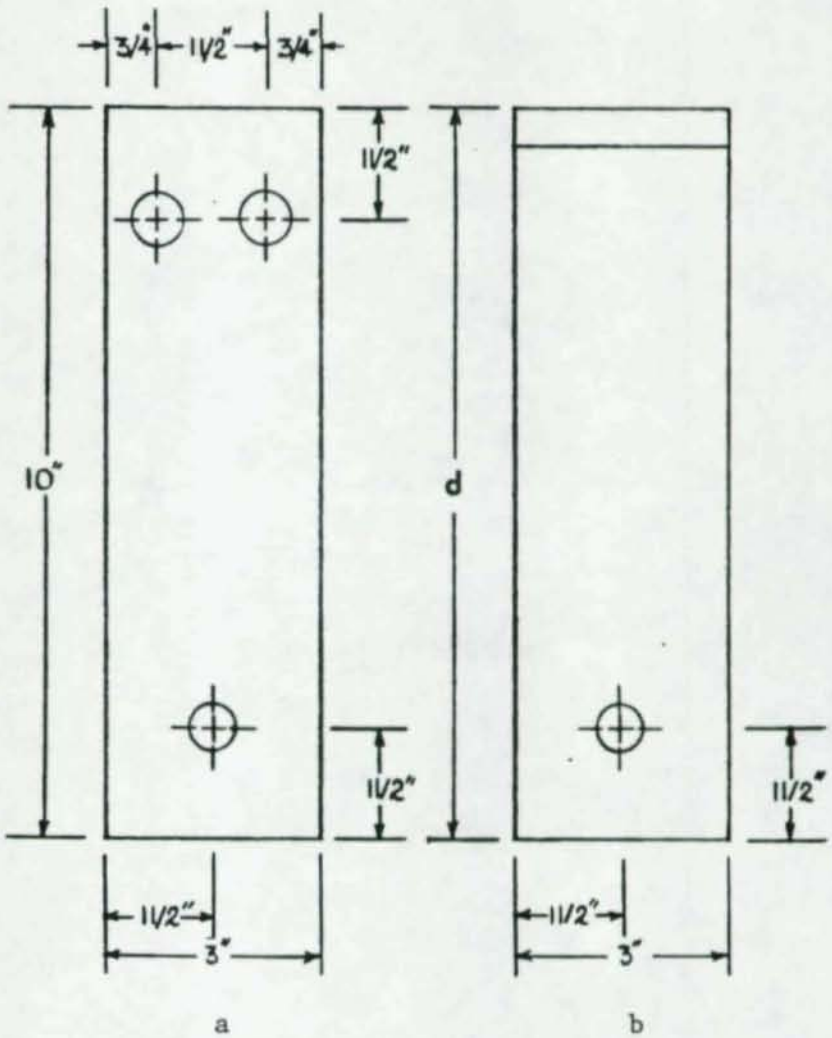

FIGURE 4.4

LOAD BEARING PLATES FOR (a) TENSION, (b) COMPRESSION AND SHEAR

CHAPTER 5

5. TEST RESULTS

5.1 General Information

The maximum loads for each of the three test types were as expected. Thus, the shear and the compression tests of similar plate and angle leg thicknesses and bolt diameter had approximately the same failure load, reaching about 75 kips. The tension tests had a maximum load of about 55 kips. For the shear test and all of the compression tests, the load-bearing plate and the bolt showed signs of large permanent deformation. Thus, yielding occurred either in the bolt or in the load-bearing plate, but not noticeably in the angles.

The failure characteristics of the tension tests also were as expected. The load-bearing plate below the bolt on the vertical legs of the angles tore, or the bolt head tore through the horizontal angle leg after the heel of the angle exhibited large deflection and/or rotation with respect to the base plate. In none of the tension tests did the bolt in the vertical angle legs exhibit large deformation. However, a new bolt was used for each tension test because that bolt had been pretensioned, as explained previously. The replacement of the bolt was done to eliminate any uncertain influences.

On the plots showing only the load-deformation curves or the specimens, the curves end where the data end. Thus, data extrapolation beyond the actual measurements is not used.

The identifying numbers for the curves of Appendix B represent the thickness of the load-bearing plate, in inches. The numbers on the plots of Appendix C represent the thickness of the angle, in inches. For the plots of Appendix D, the numbers represent the three angle types, as explained in the section on the results of the tension tests. For the two plots of Appendix E, the number on the first plot are bolt diameters, in inches, and the letters on the second plot stand for "shear" and "compression".

The method of curve fitting for all of the data is explained in Chapter 6, section 6.1.

5.2 Results of Shear Tests

Because it was felt that the shear and compression tests would yield similar curves, as shown in Appendix E, only one shear test was run. Thus, evaluation of the effect of varying the load-bearing plate thickness, angle thickness, and gage is not possible in these tests. The shear test data did resemble the compression test results for specimens of similar geometry, although the method of curve fitting did not work as well as it did on many of the compression and tension tests. The curve fit of the data of the shear test is given in Appendix A, and the diagram comparing the plots of the shear test of similar geometry is given in Appendix E.

5.3 Results of the Compression Tests

The least-squares curve fit of the compression test results, are in general, very good. However, for the 7/8 inch diameter bolts, the method of determining the initial slope is not accurate, and generally produces values that are too large. These curves, therefore, could be improved. The curve fit of the data are shown in Appendix A.

The variations in the load-deformation curves for the compression tests are as expected: The thicker the load-bearing plate, the stiffer the connection as a whole. This was true for both the 3/4 inch and 7/8 inch bolts. Plots of the curves for the different load-bearing plate thicknesses are located in Appendix B. The connection with 7/8 inch diameter bolts was stiffer than the connection of similar geometry with 3/4 inch bolts. This was expected because of the larger bending and shear stiffness of the larger diameter bolts. The plot comparing these two curves is given in Appendix E.

Since the compression tests were run with only one type of angle geometry, comparisons cannot be made with respect to a change in gage and/or a change in angle thickness. However, this is not of importance for these tests, because the plate thickness was such that it governed the overall behavior and strength.

5.4 Results of the Tension Tests

The tension tests were run using three different gage lengths; namely, 3, 2-1/4, and 1-3/4 inches. These gages will be referred to as Type 1, Type 2, and Type 3, respectively, for simplicity. Figures 4.3 show the details of the specimens.

The method for determining the initial slope of the curve (as explained in Chapter 6, section 6.1) for the data of the Type 1 angle tests worked well. However, for the test data of 3/8 and 1/4 inch angles, the initial slope should be raised significantly to achieve a better curve fit. This would also change the Richard curve parameters explained in Chapter 6, section 6.1.

The variation in the load-deformation curves for the three angle thicknesses, with respect to a change in the load-bearing plate thickness is small, up to 0.10 inches of total deformation for the Type 1 angle. Thus, until about 0.10 inches of deformation, the Type 1 angles of any thickness will exhibit similar load-deformation characteristics for the three load-bearing plate thicknesses. The plots showing the variation in the load-deformation curves for a given angle with the three diferent load-bearing plates are given in Appendix B.

The variation of the load-deformation curves due to differences in angle thickness are as expected for the Type 1 angles. Thus, as the angle becomes heavier, the connection as a whole becomes noticeably stiffer for each of the three load-bearing plate thicknesses. Unfortunately, 5/16 inch thick angles were delivered instead of 1/4 inch thick angles, and the difference in the curves for the 5/16 and 3/8 inch angles is small. Extrapolating to obtain the load-deformation curve for the 1/4 inch thick angle is therefore difficult. These plots are given in Appendix C. Of the type 1 angle tests, all specimens with a 5/16 inch angle thickness and the 3/8 inch load-bearing plate thickness showed signs of strain hardening of the

connection as a whole. Since the bolts did not deform very much, the strain hardening would appear to have occurred in the angles and/or the load-bearing plate.

The curve fits for the data of the Type angles, shown in Appendix A, are better than the curve fits for the Type 1, although there is more scatter of the data points in some cases. As in the Type 1 tests, the variation in the load-deformation curves with respect to differing load-bearing plate thicknesses is small, up to about 0.10 inches of deformation. Furthermore, only on the curves for the 1/2 inch angle with the different load-bearing plates is there a pattern after about 0.10 inches of deformation. The plot shows that as the load-bearing plate becomes thicker, the connection becomes stiffer. This pattern was not found in the Type 1 angle tests or in the 1/4 inch thick Type 2 angle tests. For the 3/8 inch Type 2 angle, this pattern may be seen after about 0.25 inches of deformation. The plots showing this pattern are given in Appendix B.

As with the Type 1 angles, the Type 2 angles exhibited a stiffer load-deformation curve with increasing thickness of the angle for all three load-bearing plate thicknesses. These curves are given in Appendix C. Interpolations for angle thicknesses not run may be made, if needed.

Of the Type 2 angles, only the 1/4 inch thick angle with 1/2 and 3/8 inch load-bearing plate thicknesses showed any signs of strain hardening. It must be kept in mind, however, that the tests were limited to 1.0 inches of deformation, although many of the specimens fialed long before the dials reached their full stroke.

Of the three angle types, the curve fits for the Type 3 angle data yielded the smallest error for the least-squares curve fits. None of the tests exhibited much scatter or showed any prominent signs of strain hardening. The curve fit data are contained in Appendix A.

Except for the 1/4 inch angle, the Type angle showed the same pattern of the curves for an angle with different load-bearing plate thicknesses as Type 1 and 2. The test for the 1/2 inch angle and 1/4 inch load-bearing plate was not run, because it was felt that an adequate deformation could not be reached before the load-bearing plate yielded below the bolt. These plots are also given in Appendix B.

As with the Type and Type 2 angles, the Type 3 angle connection became stiffer with an increase in angle leg thickness for all three load-bearing plate thicknesses. These plots are shown in Appendix C. Again, interpolations for angle thickness not run may be obtained, if needed.

The variation of the load-deformation curves with respect to a change in the gage length is as was expected for all the combinations of angle and load-bearing plate thicknesses. Four of the plots show only two curves, however, because three of the angle groups delivered were of the wrong intended thickness, and one of the angle groups were not run, as explained earlier. Briefly, the shorter the gage length, the stiffer the connection as a whole. These plots are shown in Appendix D.

Failure of the tension specimens was always in one of two areas; namely, either in the vicinity of the bolt head on the horizontal leg of the angle, or secondly, below the bolt in the load-bearing plate. Failure of the load-bearing plate occurred without the effects of "dishing", as the plate tore beneath the bolt and the two sides separated. Failure of the horizontal leg of the angle may be attributed to the large deflection of the heel of the angle.

Thus, failure of the connection in tension may be grouped into three categories: (1) no failure, full stroke of the dial gages was achieved, (2) failure by tearing of the load-bearing plate, and (3) failure of the horizontal leg of the angle by tearing or pulling through the bolt head. If no failure occurred, per se, the connection exhibited large deformations when load, and large permanent deformation when unloaded. Failure occurred in the load-bearing plate when the angles, together, were stiffer than the plate. When this occurred, the load-bearing plate was not stiff enough to pull the heel of the angle far enough off the base plate and thus induce failure around the head of the bolt on thehorizontal leg. The type of failure that occurred in each test group was recorded, and indicated in Table 5.1.

5.5 Other Results

Tests were not run for combined tension and shear or compression and shear, due to financial and time limitations. The effect of combined stresses on the stiffness of a connection will be evaluated in Chapter 6.

TABLE 5.1

LOCATION OF FAILURE FOR ALL THE TENSION TESTS

Angle Type	Angle Thickness	Plate Thickness	No Failure	Plate Failure	Angle Failure
1 Gage = 3"	1/2"	1/2"	X		
		3/8"		X	
		1/4"		X	
	3/8"	1/2"	X		
		3/8"	X		
		1/4"		X	
	5/16"	1/2"			X
		3/8"			X
		1/4"			X
2 Gage = 2-1/4"	1/2"	1/2"		X	
		3/8"		X	
		1/4"		X	
	3/8"	1/2"	X		
		3/8"		X	
		1/4"		X	
	1/4"	1/2"			X
		3/8"			X
		1/4"			X
3 Gage = 1-3/4"	1/2"	1/2"		X	
		3/8"		X	
		1/4"	Not	Run	
	3/8"	1/2"		X	
		3/8"		X	
		1/4"		X	
	1/4"	1/2"			X
		3/8"			X
		1/4"			X

CHAPTER 6

6. DISCUSSION AND APPLICATION OF TEST RESULTS

6.1 Graphing and Plotting of Test Results

The initial slopes for the least-squares curve fits were computed on the basis of two parts. The first represented the contribution of the plate action, K_{PL}, similar to that of a single plate framing connection (Richard, Gillett, Kriegh, and Lewis, 1980). The second, $K_{\measuredangle}$, was based on the stiffness of a beam, fixed at both ends, with equal and opposite end moments, reflecting the contribution of the angles. Equations 6.1 and 6.2 give the derivation of the initial slope.

$$K_{PL} = 4E\,\frac{t_1 t_2}{t_1+t_2} = 12\times10^4\,\frac{t_1 t_2}{t_1+t_2} \qquad \text{Equation 6.1}$$

$$K_{\measuredangle} = 2 \times \frac{12EI}{L^3} = 2 \times 12 \times (30 \times 10^3) \times \left(\frac{1}{12} \times 3 \times \left(\frac{t_1}{g}\right)^3\right)$$

$$= 18 \times 10^4 \left(\frac{t_1}{g}\right)^3 \qquad \text{Equation 6.2}$$

Where: t_1 = thickness of angle

t_2 = thickness of load-bearing plate

E = Young's Modulus

I = moment of inertia

g = L = gage length

It is assumed, therefore, that the combined stiffness, K, may be

found from: Equation 6.3

$$\frac{1}{K} = \frac{1}{K_{PL}} + \frac{1}{K_{\%}}$$

This initial slope was then used as input for a computer program developed at the University of Arizona. This program, RCFIT (Gillett and Hornby, 1978), by trial and error, zeroes in on what are referred to as the Richard parameters by means of the smallest value for the error in the least-squares curve fit. The equation used in the program is detailed in Appendix F. Figure 6.1 shows a curve with its Richard parameters. These parameters define the curvature of the "knee" of the curve, the final slope of the curve, and the value defining where the final slope of the curve would intersect the y-axis if it were extended back that far. Thus the data give a curve that consist of two straight lines and a "knee". These parameters, as well as the initial slope, are then used as input for another program that plots any number of curves on the same set of axes, but without the data points included. Thus, load-deformation curves with variations in geometry, bolt sizes, and/or similar tests may be easily compared. Tables 6.1, 6.2, and 6.3 show the values for the initial slope and the curve parameters.

6.2 Orthotropic Failure Surface

The theory behind the orthotropic failure surface is analogous to that of a failure envelope. On the interior of the envelope, a point may represent a possible state of stress. On the curve that defines the envelope, a state of the failure exists. Points on the

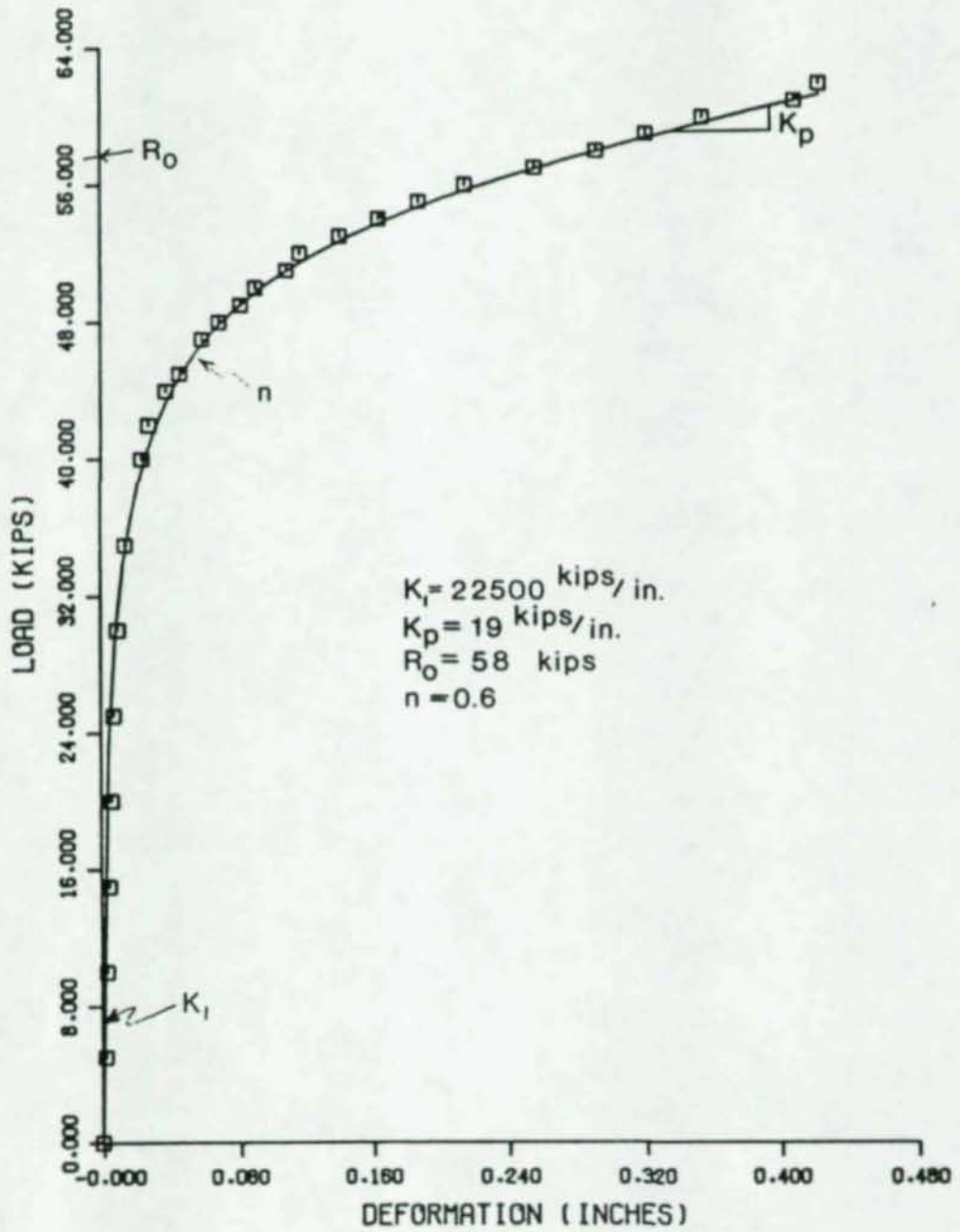

FIGURE 6.1

TYPICAL CURVE WITH RICHARD PARAMETERS

exterior of the envelope represent impossible states of stress because they lie beyond the boundary that defines failure.

The failure envelope for the connection elements of this study is made up of two parts; first, one-half of a circle, and secondly, one-half of an ellipse. It is illustrated in Figure 6.2. The half-circle represents the portion of the envelope that is defined by compression and shear. As has already been discussed, tests were run on connection elements for shear or compression. These curves, given in Appendix E, show that shear and compression tests yield very similar load-deformation curves and failure loads, and thus may be considered as producing the required half circle for their portion of the failure ellipse.

The tension specimens, on the other hand, did not reach the same failure loads and the failure envelope for this condition cannot be represented by a circle. Instead, the boundary on the side that represents failure of the tension specimens may be considered to be an ellipse, with the major axis equal to the diameter of the circle defined by shear and compression.

The surface of the envelope defines the failure boundary for all states of combined stress. For example, the failure load for a specimen in combined tension and shear may be determined by simply plotting lines parallel to the x- and y-axes from a single point on the boundary, and reading the respective values for tension and shear. Another way of using the failure envelope is to determine the magnitude of the shear force that may be taken by the connection when a given amount of tension already exists.

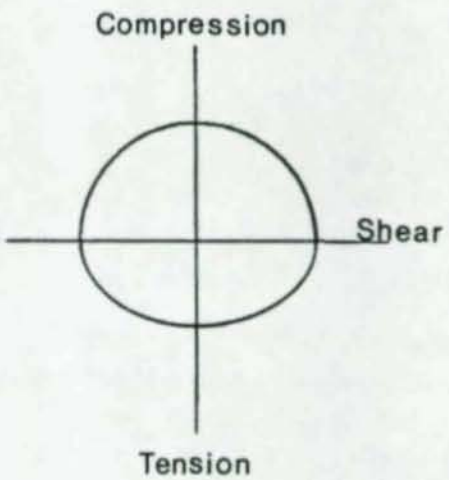

FIGURE 6.2

DIAGRAM OF ORTHOTROPIC FAILURE SURFACE

There are three primary properties that have to be developed for the envelope. In the first, the envelope must be defined on the basis of the correct gage length; secondly, on the basis of the correct angle thickness; and thirdly, on the basis of the correct bolt diameter. Thus, a large number of diagrams should be available for design or analysis purposes.

TABLE 6.1

TENSION TEST DATA

Angle Type	Angle Thickness	Plate Thickness	K	Kp	Ro	n
1	1/2"	1/2"	810	24	18	1.2
		3/8"	807	24	19	1.4
Gage = 3"		1/4"	800	19	22	1.2
	3/8"	1/2"	347	11	10	1.7
		3/8"	346	5	17	0.8
		1/4"	345	19	10	1.9
	5/16"	1/2"	201	9	9	14.0
		3/8"	201	11	9	6.6
		1/4"	201	14	8	10.3
2	1/2"	1/2"	1853	22	35	0.7
		3/8"	1834	15	32	0.8
Gage = 2-1/4"		1/4"	1797	6	29	0.8
	3/8"	1/2"	806	22	20	1.2
		3/8"	803	15	28	0.7
		1/4"	796	13	21	1.3
	1/4"	1/2"	244	10	7	3.6
		3/8"	243	15	6	3.5
		1/4"	242	18	6	1.8
3	1/2"	1/2"	3683	28	45	0.9
		3/8"	3609	14	41	1.2
Gage = 1-3/4"		1/4"	Not	Run		
	3/8"	1/2"	1657	28	29	0.9
		3/8"	1642	16	31	0.8
		1/4"	1612	10	28	1.1
	1/4"	1/2"	512	24	9	4.3
		3/8"	510	24	9	2.3
		1/4"	507	14	19	0.6

K = initial slope
Kp = final slope, in kips/inch
Ro = y-intercept, in kips
n = shape parameter

TABLE 6.2

COMPRESSION TEST DATA

Bolt Diameter	Angle Thickness	Plate Thickness	K	Kp	Ro	n
3/4"	3/8"	1/2"	25700	40	76	0.5
		3/8"	22500	19	58	0.6
		1/4"	18000	3	38	0.7
7/8"	3/8"	1/2"	25700	60	65	0.5
		3/8"	22500	28	72	0.5

K = initial slope
Kp = final slope, in kips/inch
Ro = y-intercept, in kips
n = shape parameter

TABLE 6.3

SHEAR TEST DATA

Bolt Diameter	Angle Thickness	Plate Thickness	K	Kp	Ro	n
3/4"	3/8"	1/2"	25700	67	65	0.5

CHAPTER 7

7. THEORETICAL ANALYSIS

7.1 General Information

Research at the University of Alberta in Canada and at the University of Arizona has examined connection elements similar to those tested in this program. The Canadian studies evaluated the performance of double angle beam-to-column connections (Bjorhovde, 1983a), and also incorporated full-size gusset plate tests where double angle connections were used (Bjorhovde, 1983b). The data generated in these two studies, along with the results of the present research program, give extensive and varied information on the strength and behavior of double angle connections, used for beams as well as other types of joints.

7.2 Finite Element Analysis

The results of this study will be used in further finite element analysis of gusset plate connections. Thus, the program can determine the behavior and strength of the plates in an accurate fashion because of the improved input data for the boundary conditions. The curves can also represent the stiffness of the connection at a given point, although the load-deformation curves are no longer

linear. Yielding of the connection is taken into account using the shape parameter n, the final slipe of the curve Kp, and the intercept R_o. Thus, even after the connection has yielded, the load-deformation relationship can be found.

CHAPTER 8

8. SUMMARY AND CONCLUSIONS

The purpose of this study has been to gather data on the strength and behavior of connection elements, to be used in further analyses of full-scale connections. Load-deformation curves for 27 different connection element geometries in tension, five different compression element geometries, including two different bolt diameters, and a shear test were obtained. The following conclusions and summaries can be given:

1. Compression tests of similar geometry were stiffer for 7/8 inch diameter bolts than for 3/4 inch diameter bolts.
2. The smaller the gage, the stiffer the connection.
3. The thicker the angle for any given load-bearing plate thickness, the stiffer the connection.
4. The shear and compression tests of similar geometry yielded almost identical curves.
5. A least-squares curve fit was used to the data to obtain optimal curve parameters.
6. The initial slope of the curve was determined by considering the contribution of the plate alone and then the contribution of the angles alone.

8. A failure envelope was developed using the information on the three test types; tension, compression, and shear.

Probably the only thing that can be added to this study would be the testing of combined shear and tension, and combined shear and compression. However, due to financial and time limitations, these were not feasible for this program.

APPENDIX A

LEAST-SQUARES CURVE FITS

FOR THE DATA RECORDED

The numbers in this Appendix, at the bottom of the Figure represent the following:

Compression

C - compression
- test number for that group
- 3 for 3/4" bolts, 7 for 7/8" in diameter bolts
- number identifying load-bearing plate thickness

Tension

T - tension
- test number for that group
- angle type
- angle thickness
- load-bearing plate thickness

For identifying angle or load-bearing plate thickness, using the following scale:

4 = 1/2"
5 = 3/8"
6 = 5/16"
7 = 1/4"

Examples:

1. C235 is a compression test using test number 2, 3/4 inch diameter bolts, and a 3/8 inch load-bearing plate.

2. T1145 is a tension test using test number 1, angle type 1, 1/2 inch thick angle, and a 3/8 inch thick load-bearing plate.

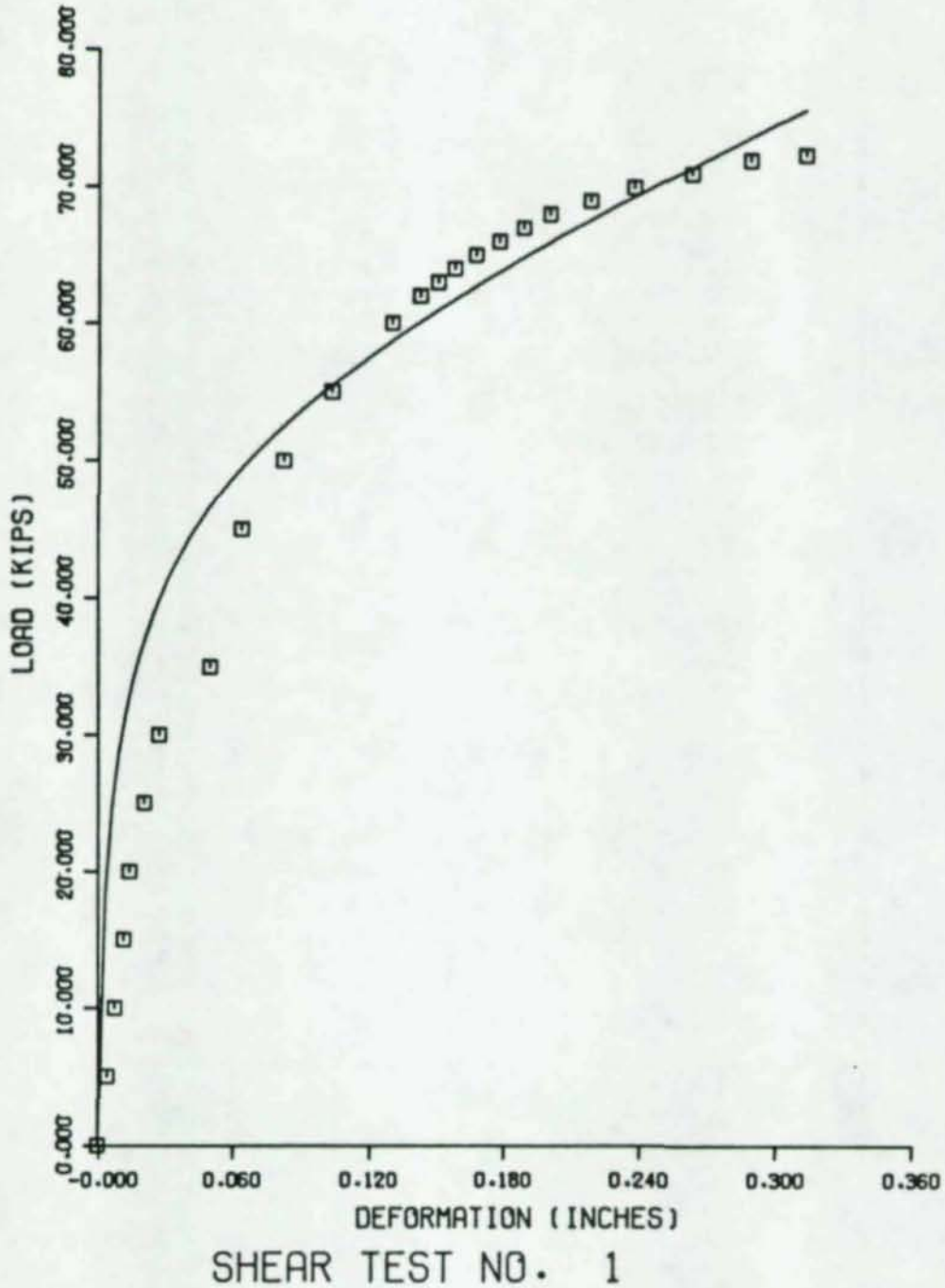

Figure A-1

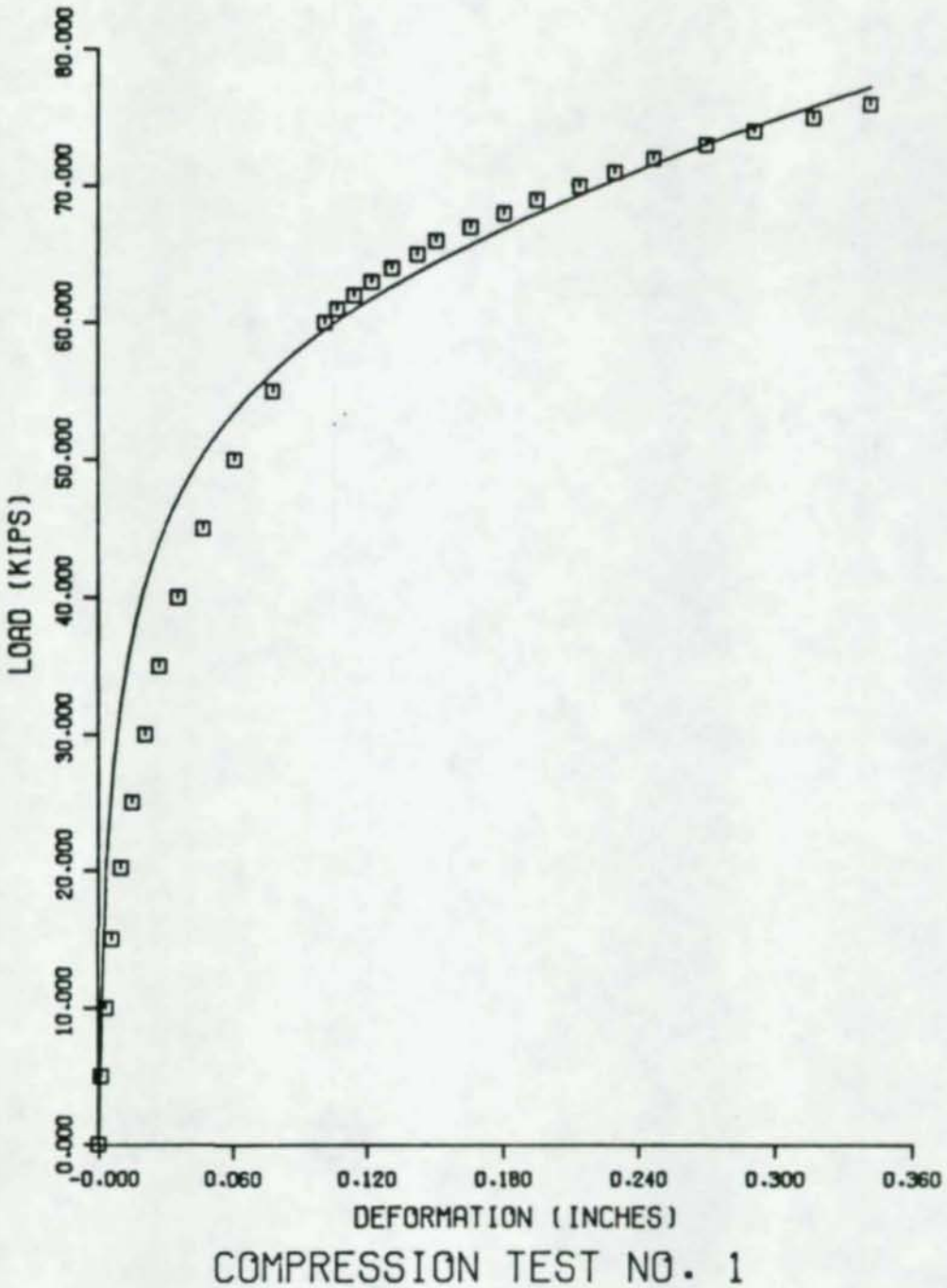

Figure A-2

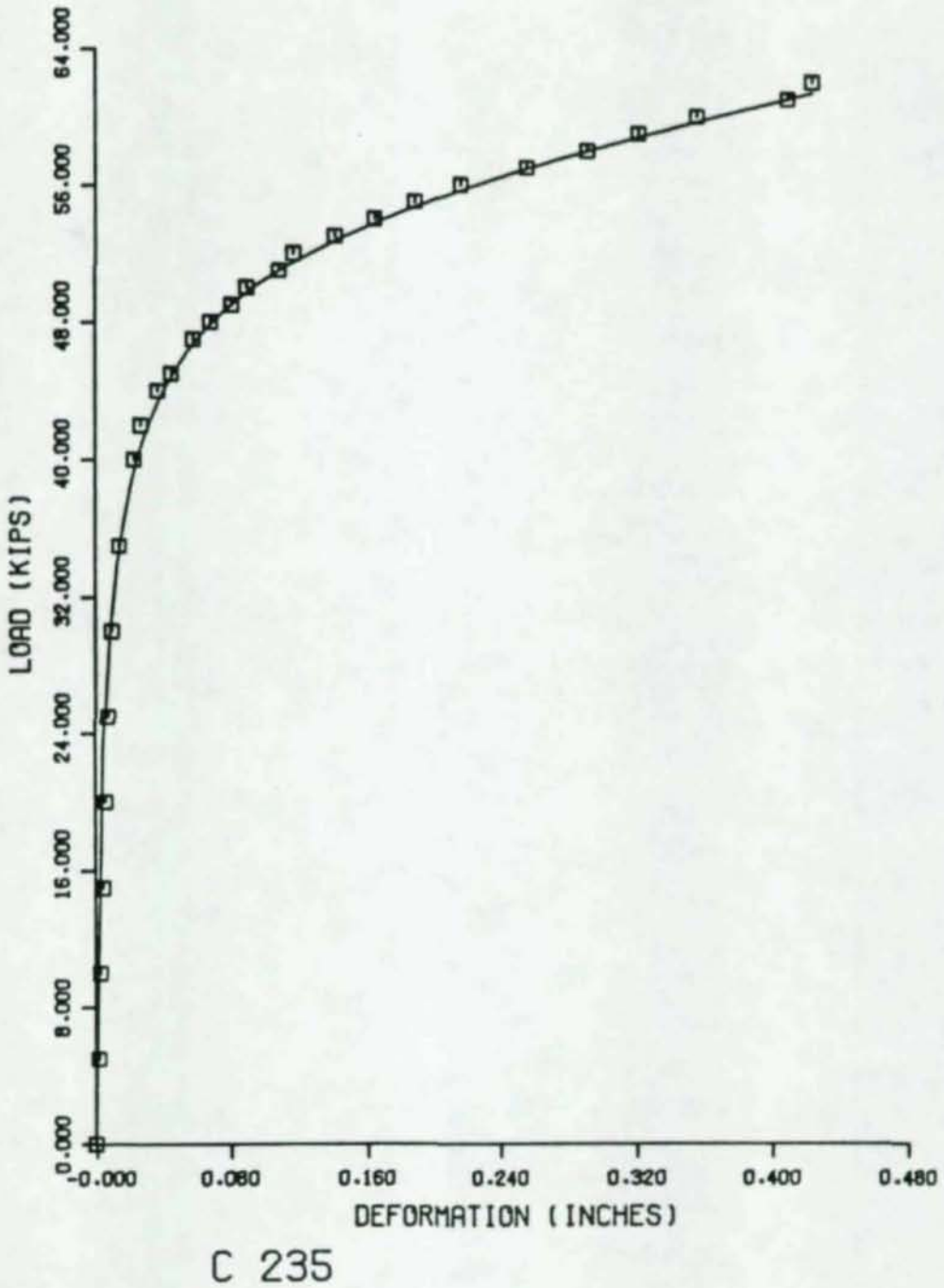

Figure A-3

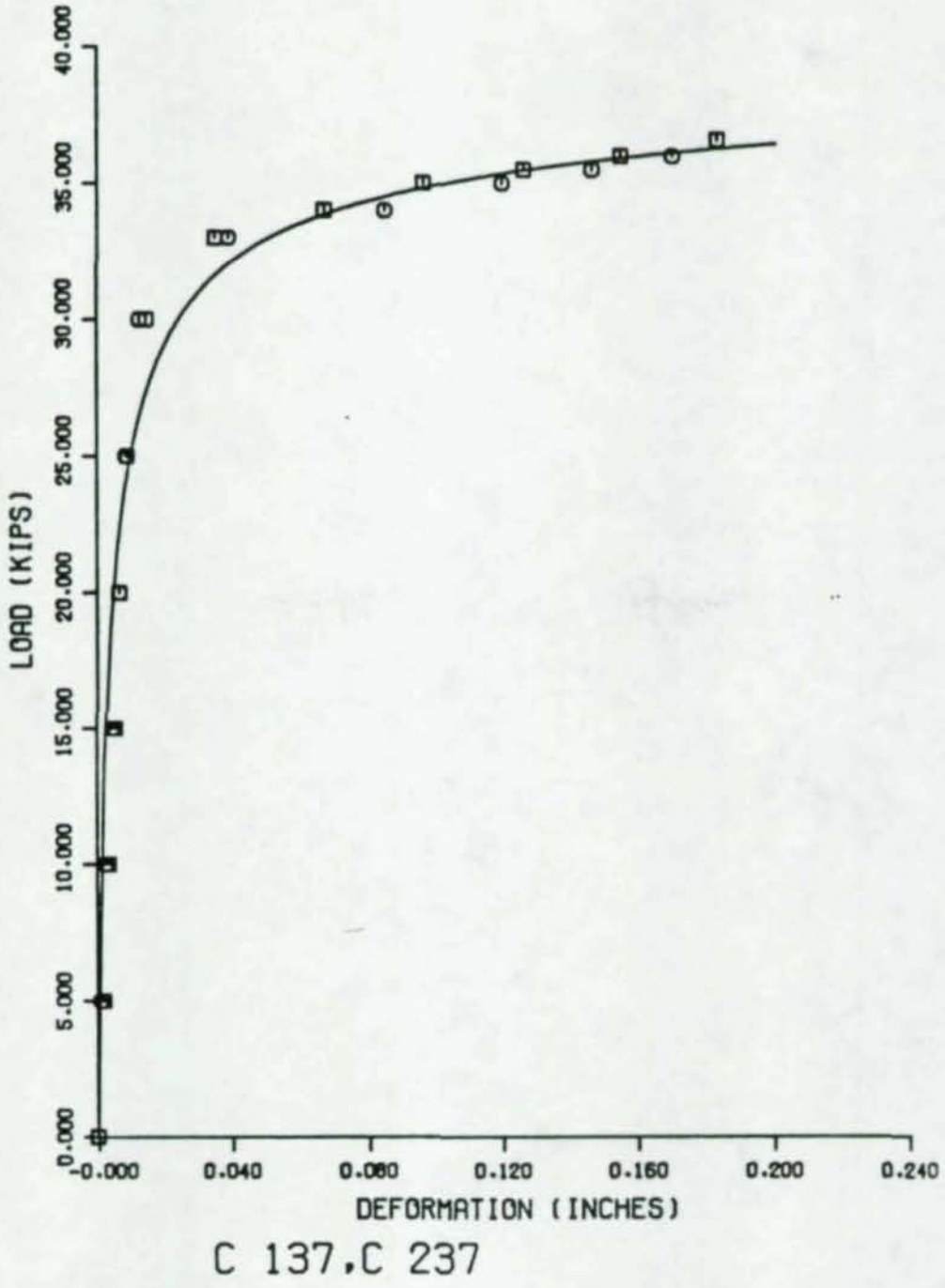
LOAD (KIPS)
0.000
5.000
10.000
15.000
20.000
25.000
30.000
35.000
40.000
0.000
0.040
0.080
0.120
0.160
0.200
0.240
DEFORMATION (INCHES)
C 137,C 237

Figure A-4

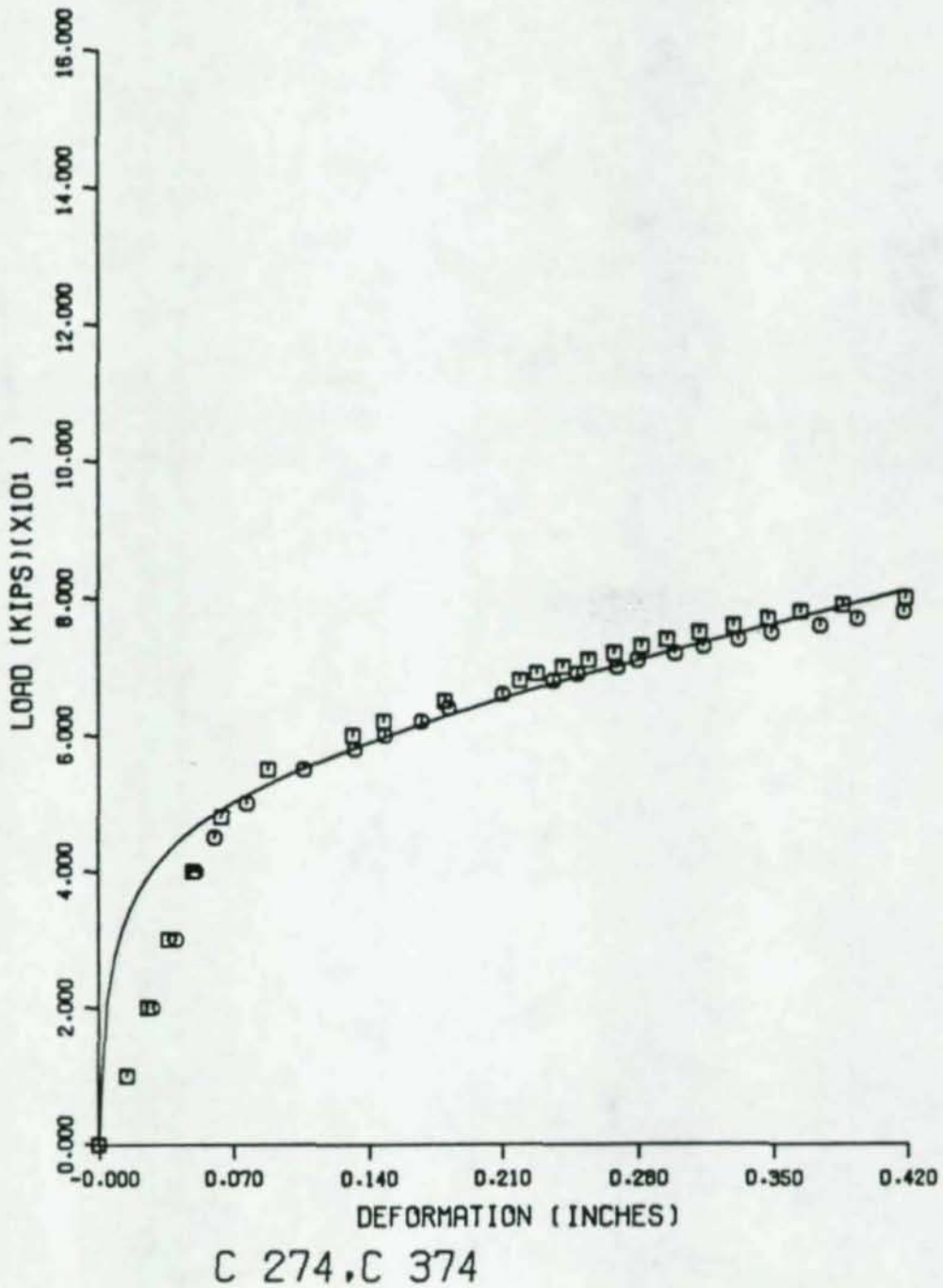
LOAD (KIPS)(X10¹)
16.000
14.000
12.000
10.000
8.000
6.000
4.000
2.000
0.000
-0.000
0.070
0.140
0.210
0.280
0.350
0.420
DEFORMATION (INCHES)
C 274,C 374

Figure A-5

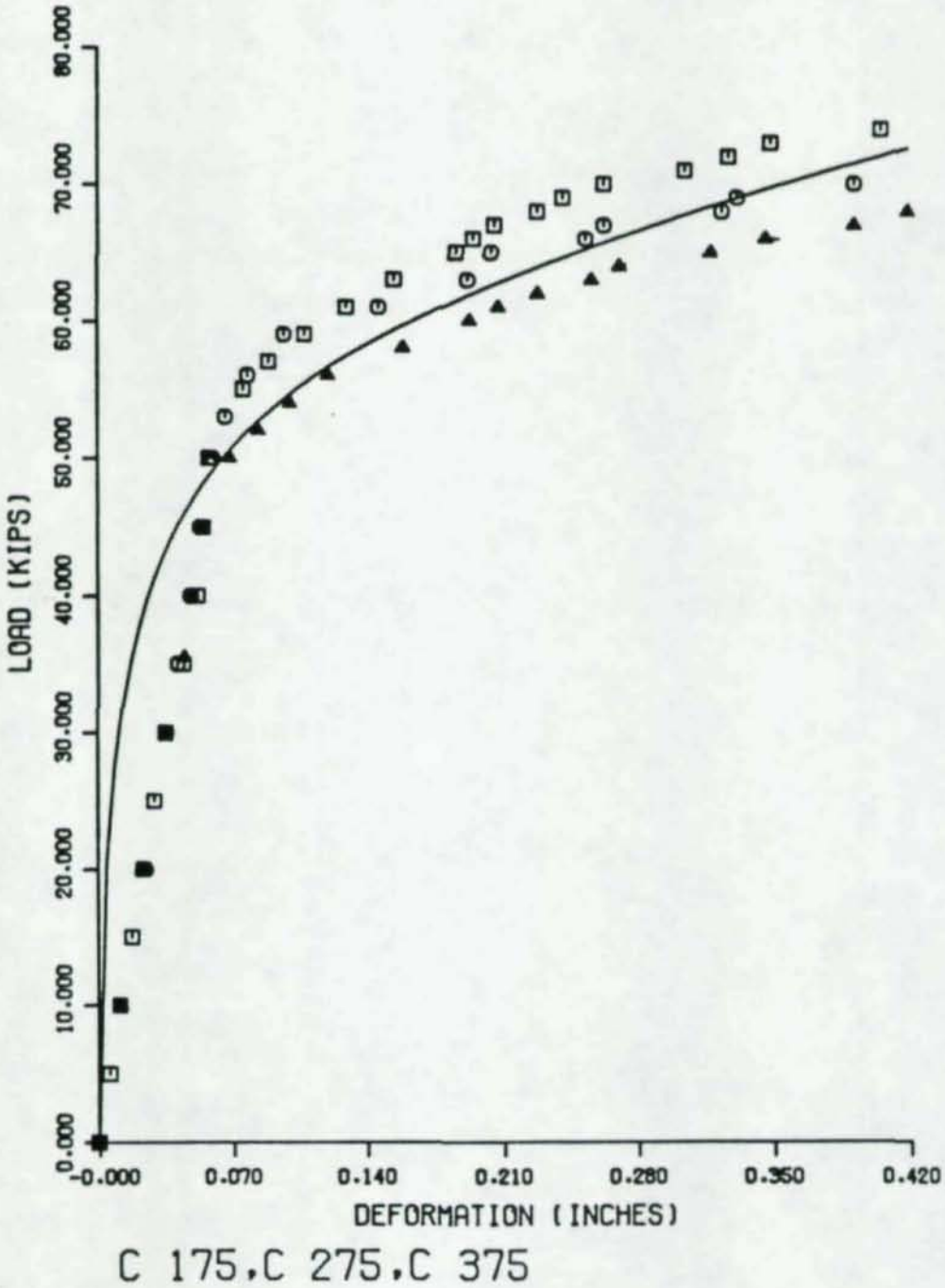

Figure A-6

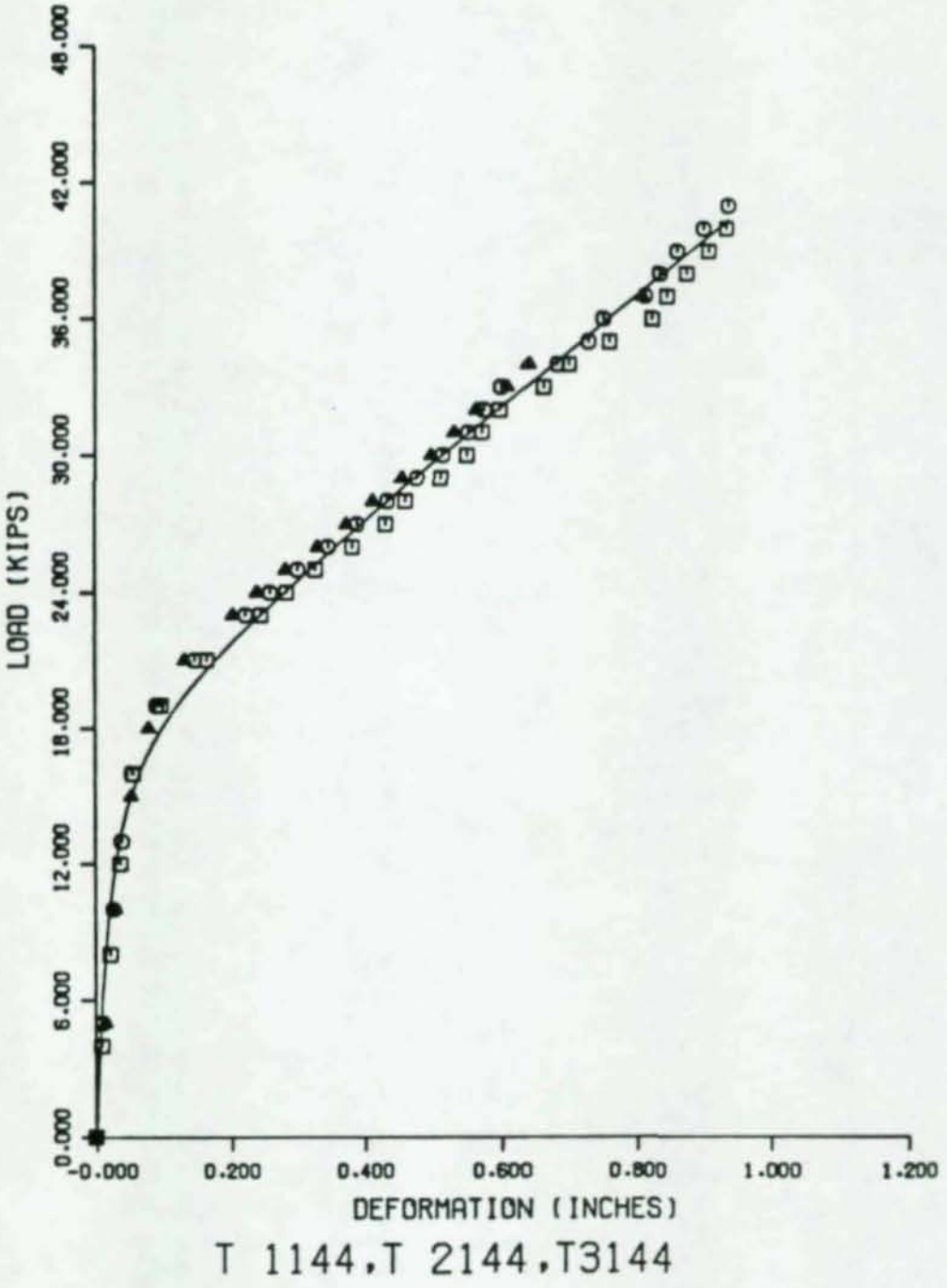

Figure A-7

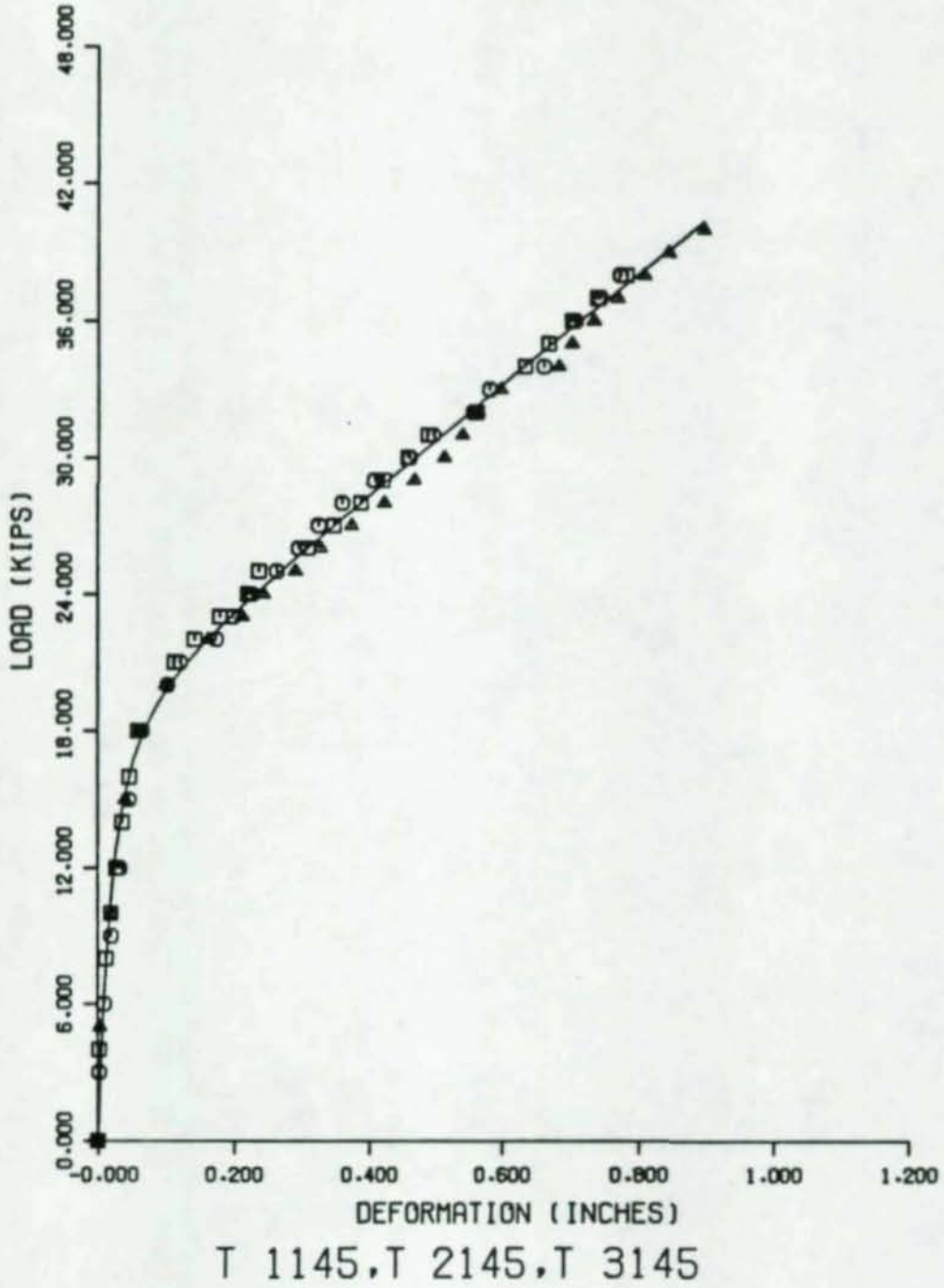

Figure A-8

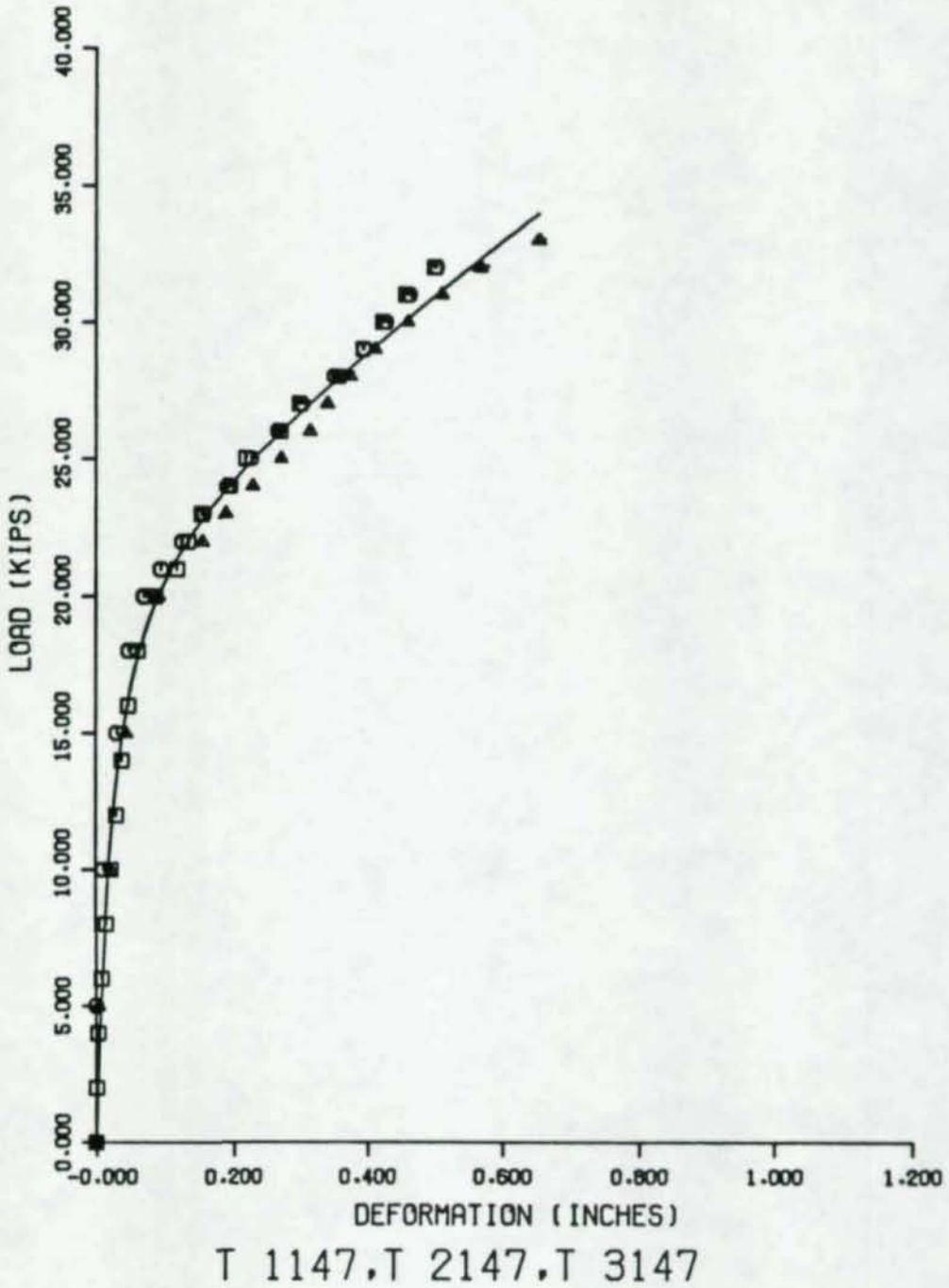

Figure A-9

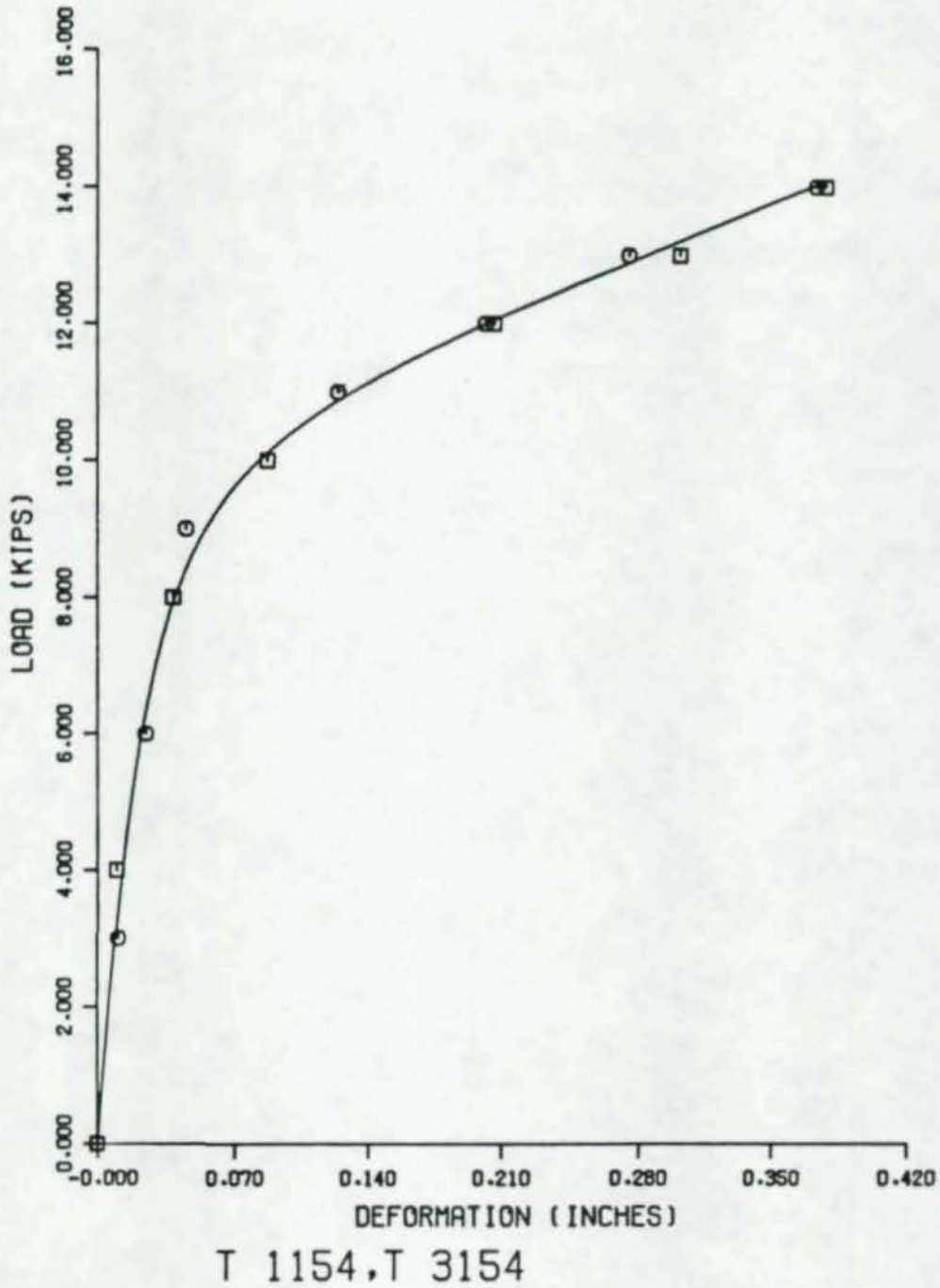

Figure A-10

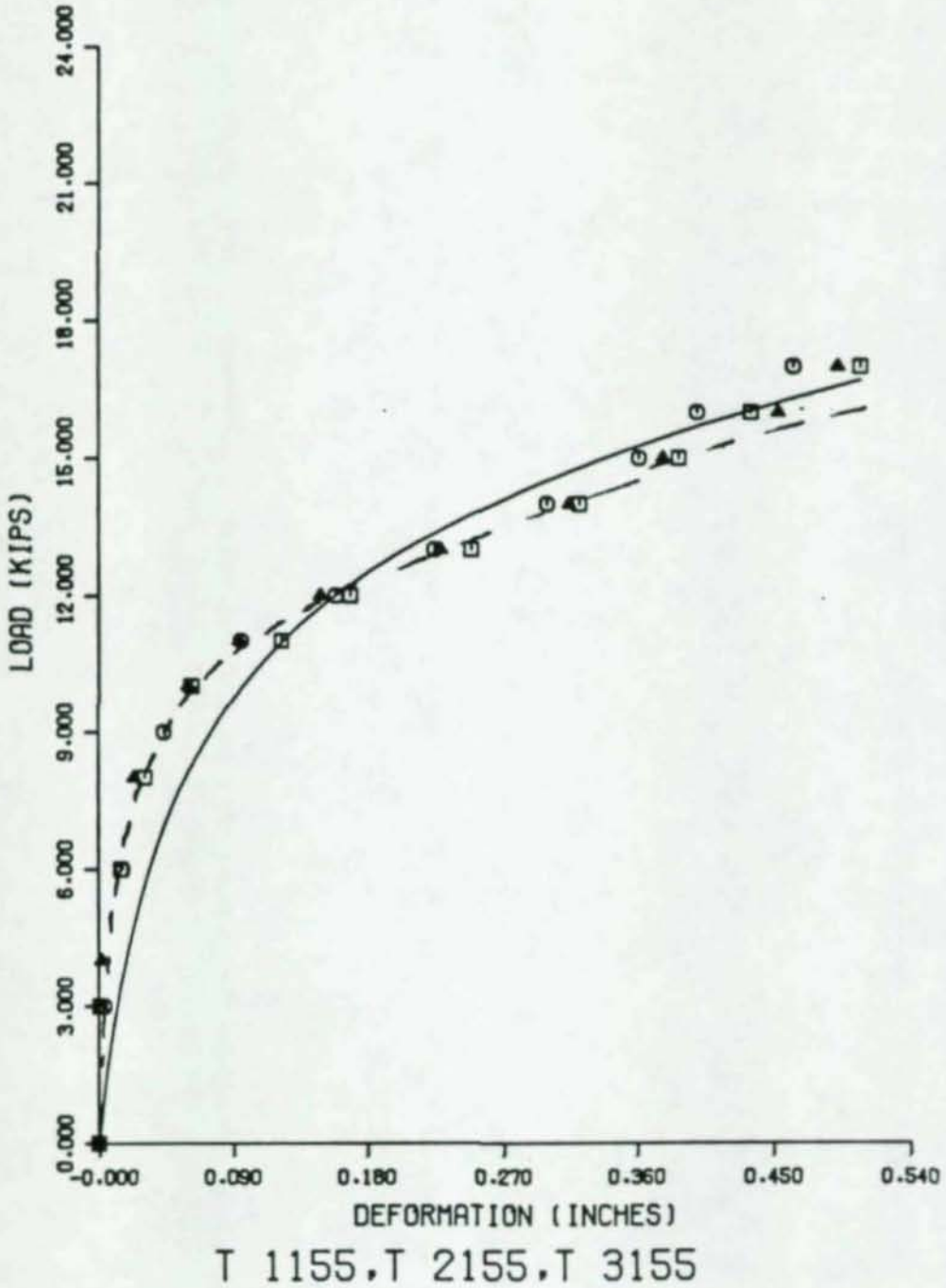
LOAD (KIPS)
0.000
3.000
6.000
9.000
12.000
15.000
18.000
21.000
24.000
-0.000
0.090
0.180
0.270
0.360
0.450
0.540
DEFORMATION (INCHES)
T 1155,T 2155,T 3155

Figure A-11

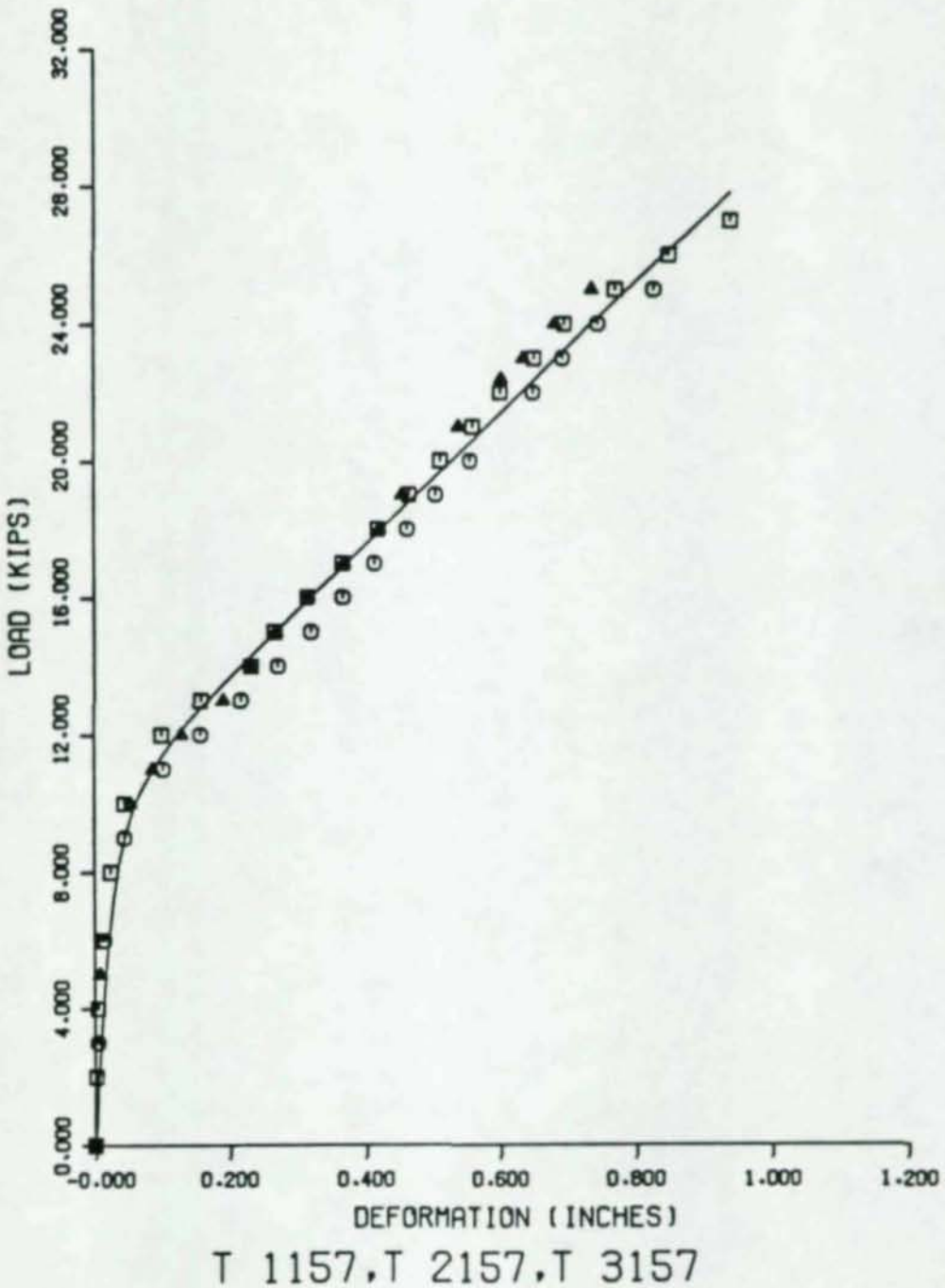
LOAD (KIPS)
0.000
4.000
8.000
12.000
16.000
20.000
24.000
28.000
32.000
-0.000
0.200
0.400
0.600
0.800
1.000
1.200
DEFORMATION (INCHES)
T 1157,T 2157,T 3157

Figure A-12

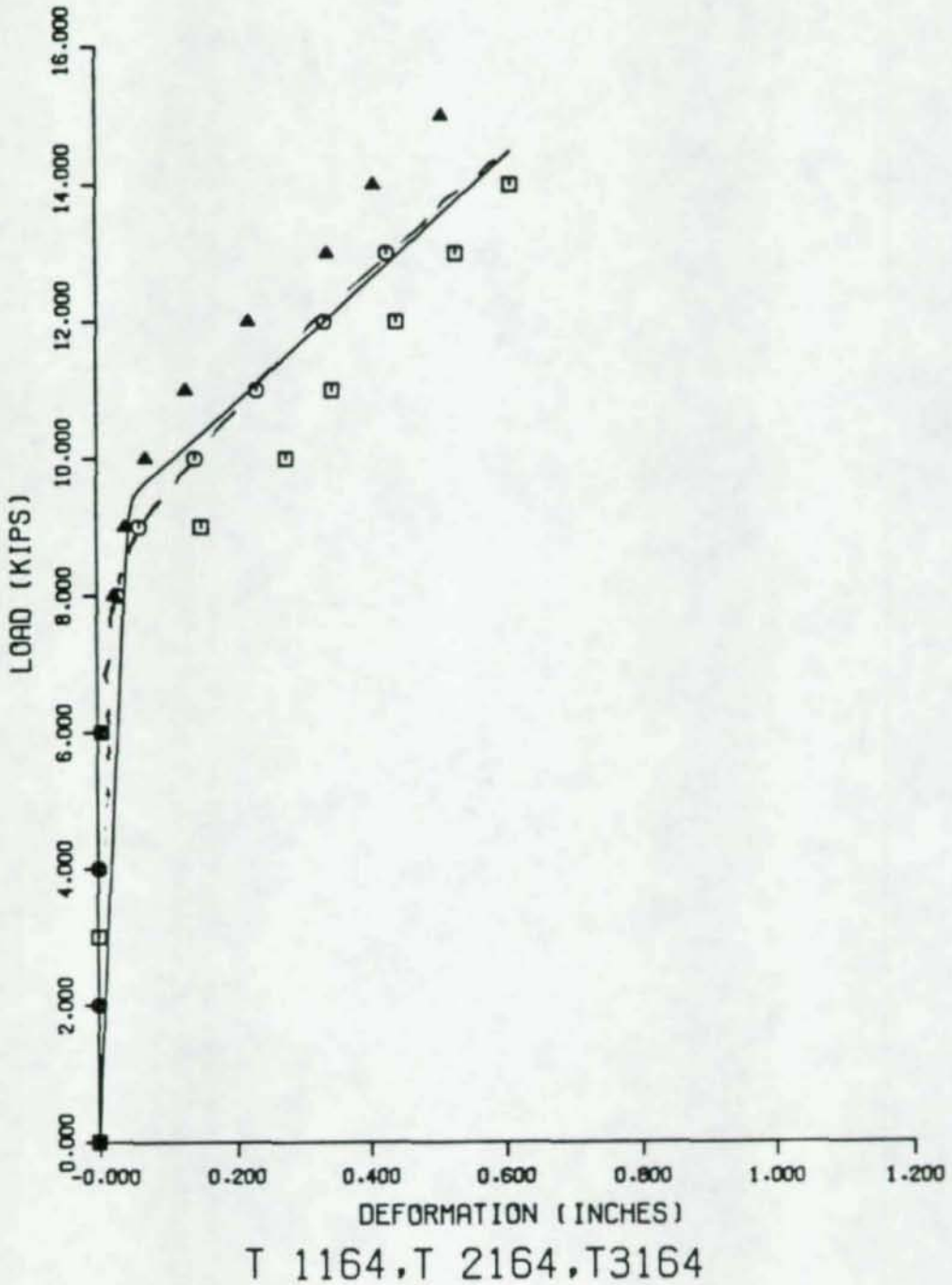
LOAD (KIPS)
0.000
2.000
4.000
6.000
8.000
10.000
12.000
14.000
16.000
-0.000
0.200
0.400
0.600
0.800
1.000
1.200
DEFORMATION (INCHES)
T 1164,T 2164,T3164

Figure A-13

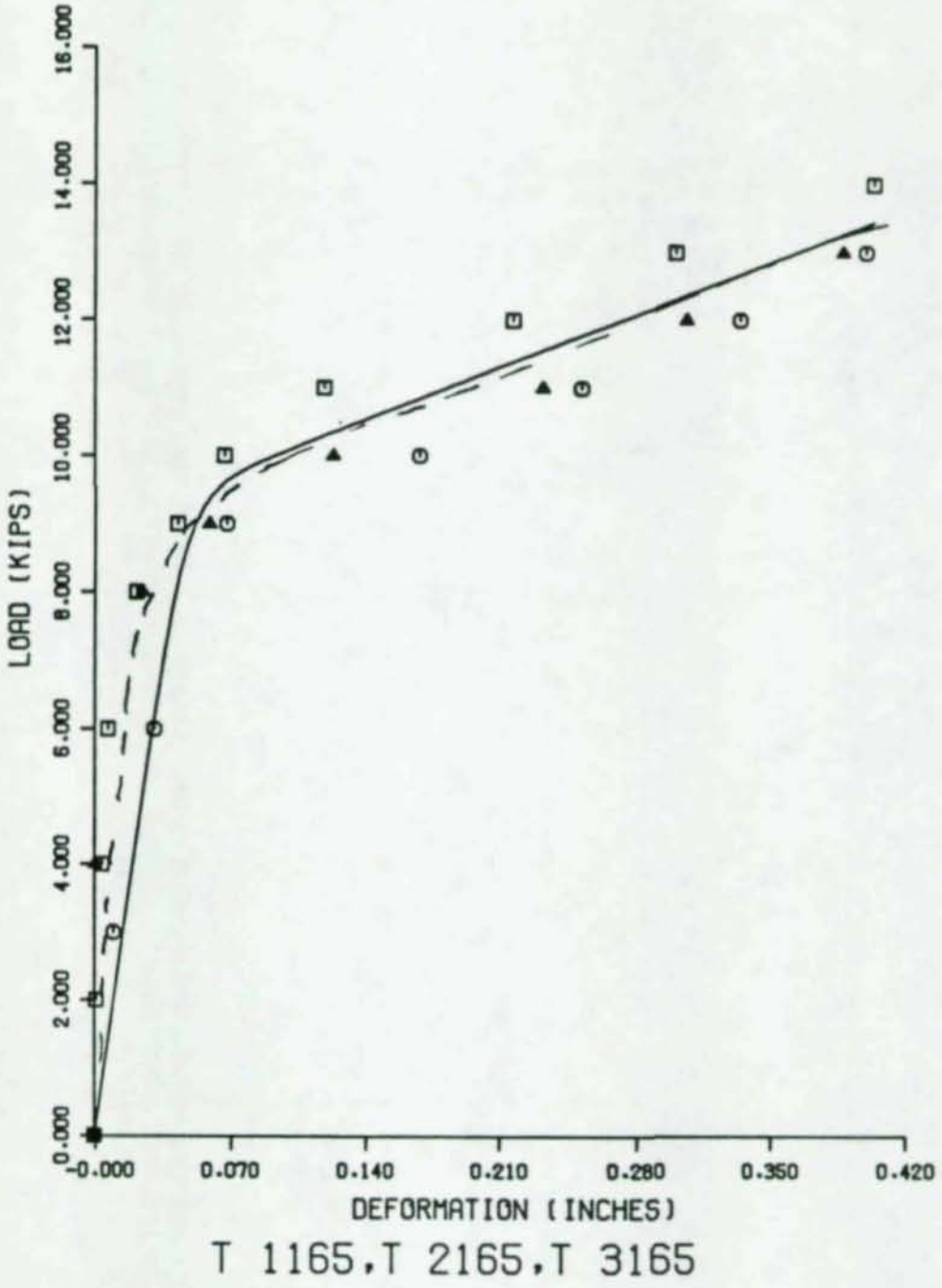
LOAD (KIPS)
0.000
2.000
4.000
6.000
8.000
10.000
12.000
14.000
16.000
-0.000
0.070
0.140
0.210
0.280
0.350
0.420
DEFORMATION (INCHES)
T 1165,T 2165,T 3165

Figure A-14

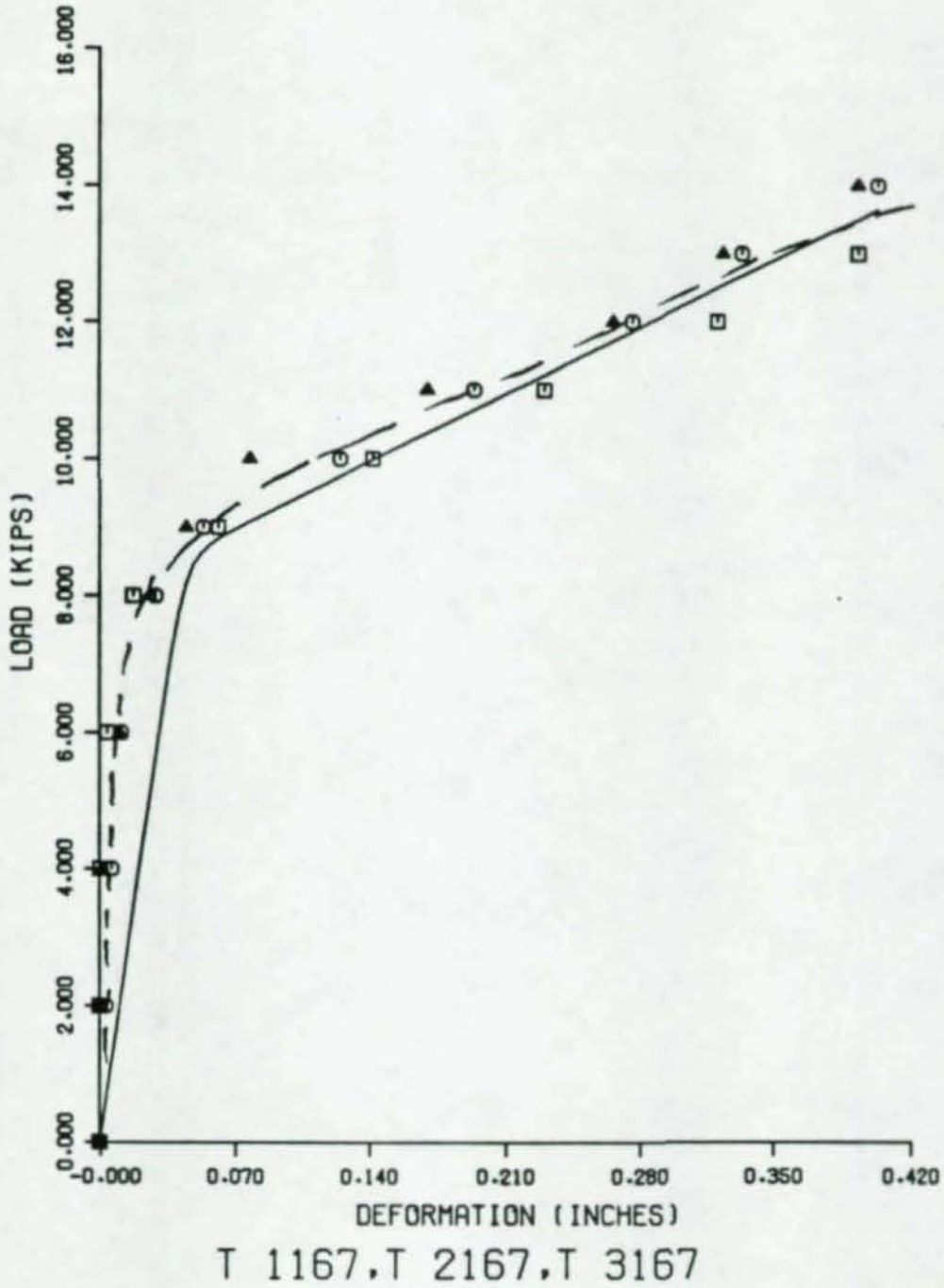
LOAD (KIPS)
0.000
2.000
4.000
6.000
8.000
10.000
12.000
14.000
16.000
-0.000
0.070
0.140
0.210
0.280
0.350
0.420
DEFORMATION (INCHES)
T 1167,T 2167,T 3167

Figure A-15

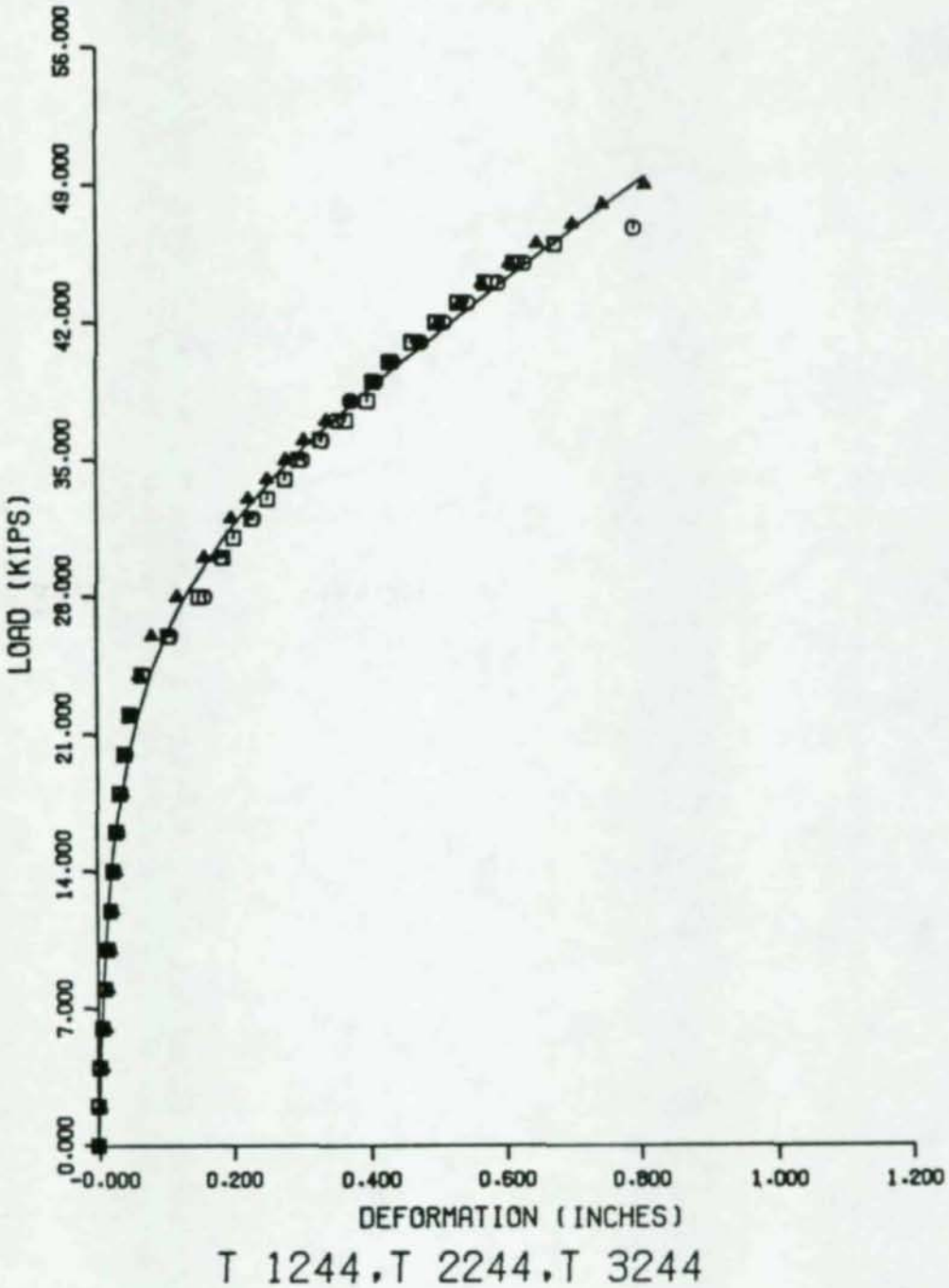

Figure A-16

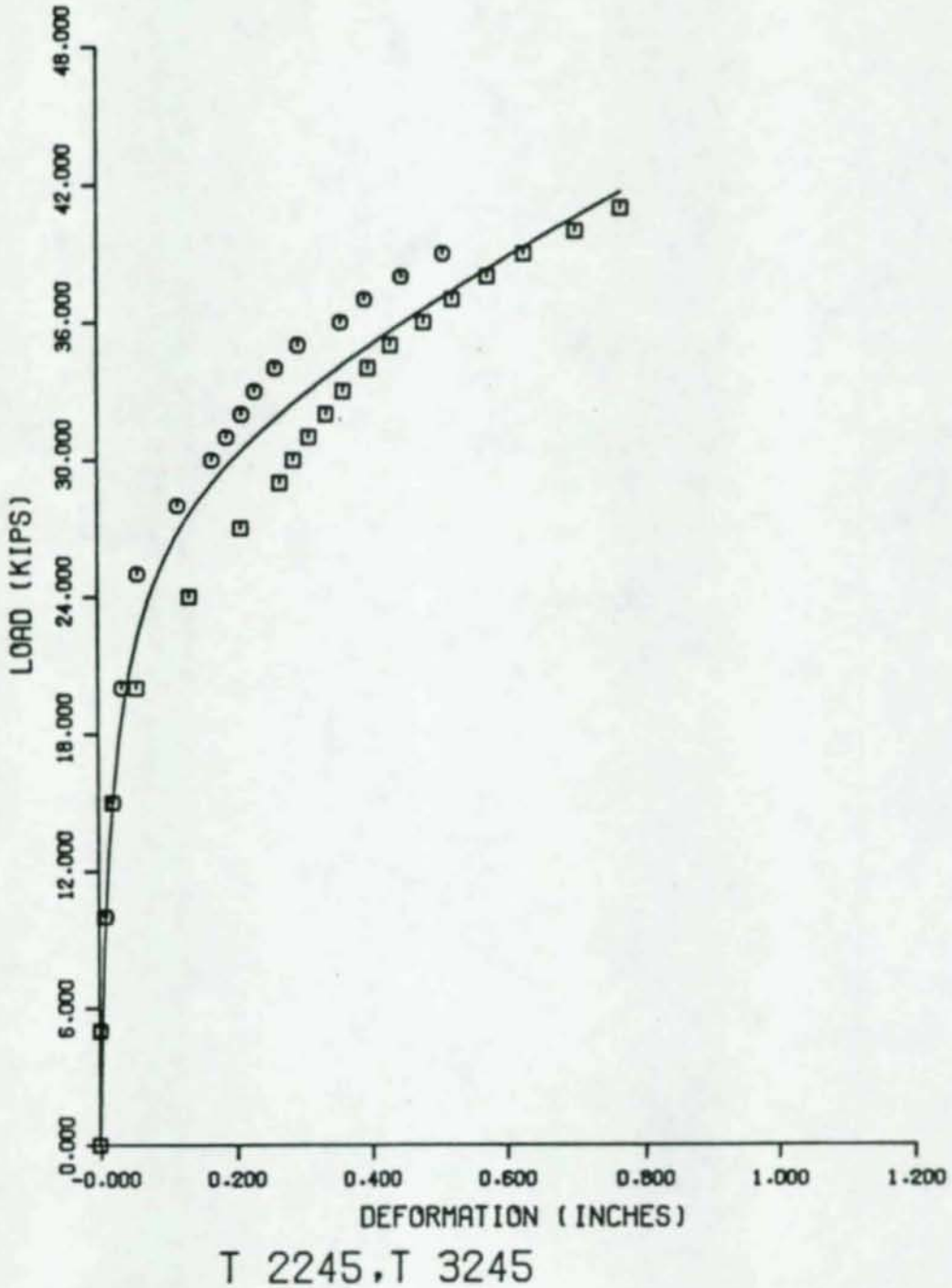

Figure A-17

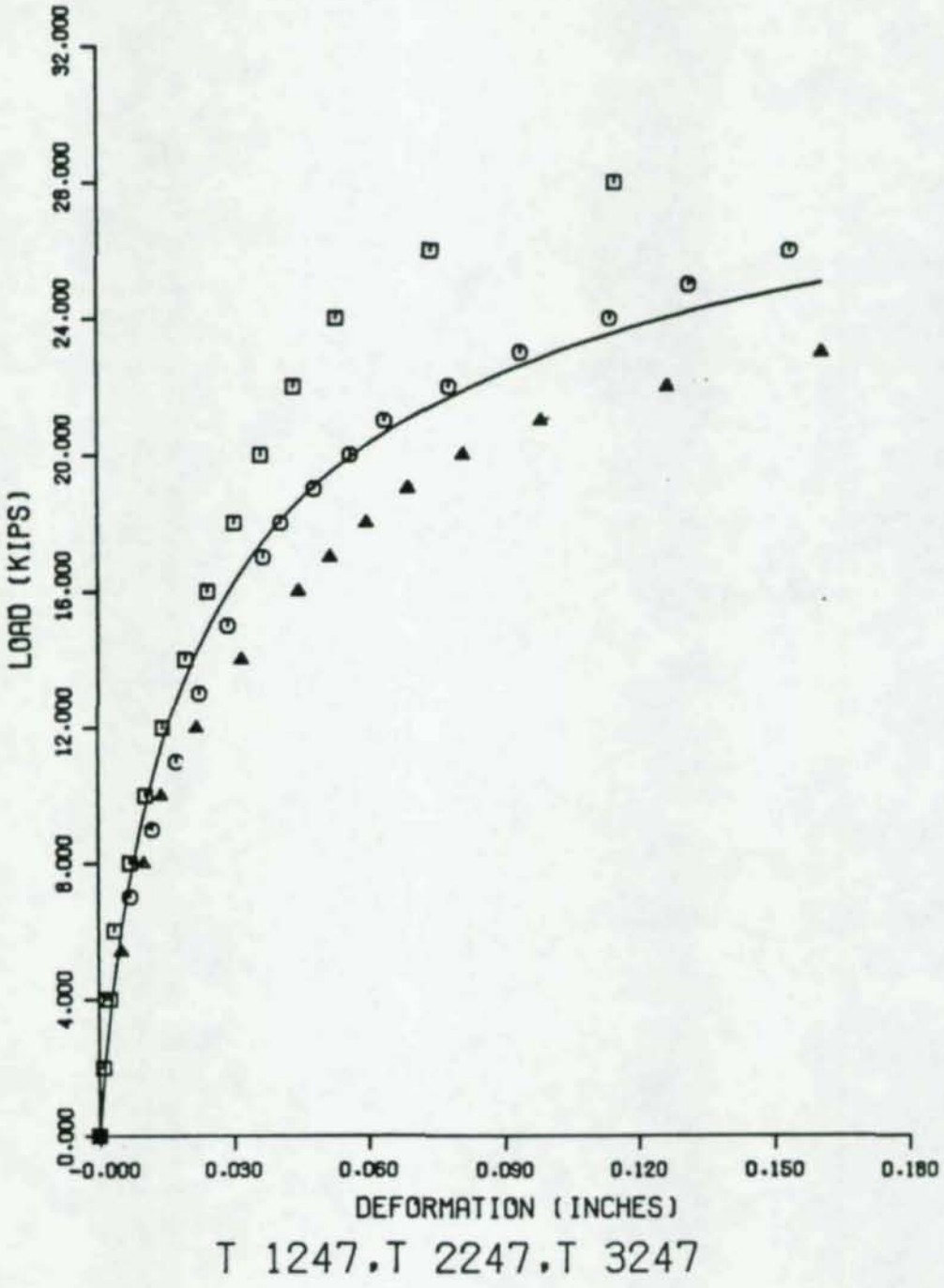
LOAD (KIPS)
0.000
4.000
8.000
12.000
16.000
20.000
24.000
28.000
32.000
-0.000
0.030
0.060
0.090
0.120
0.150
0.180
DEFORMATION (INCHES)
T 1247.T 2247.T 3247

Figure A-18

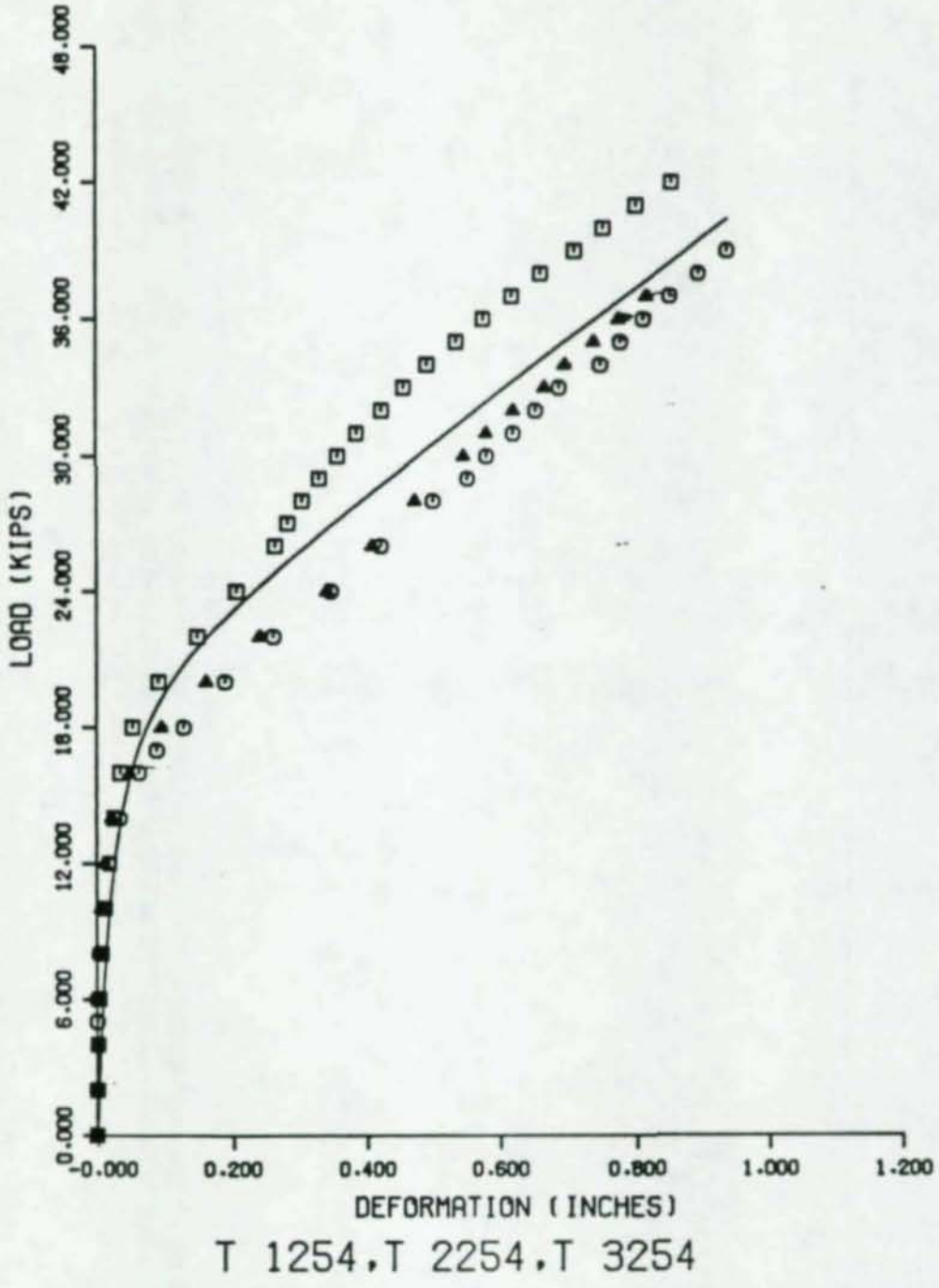

Figure A-19

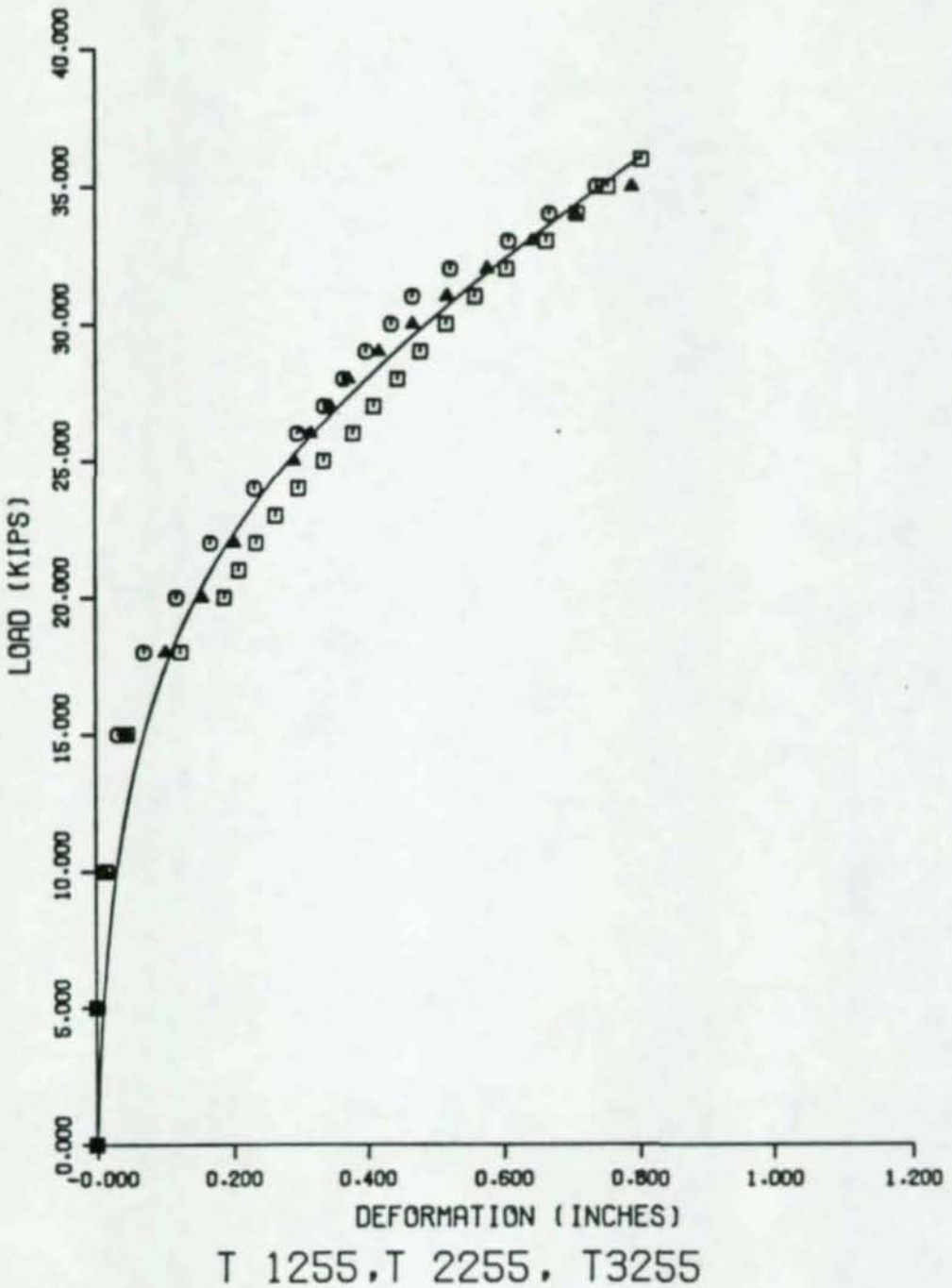

Figure A-20

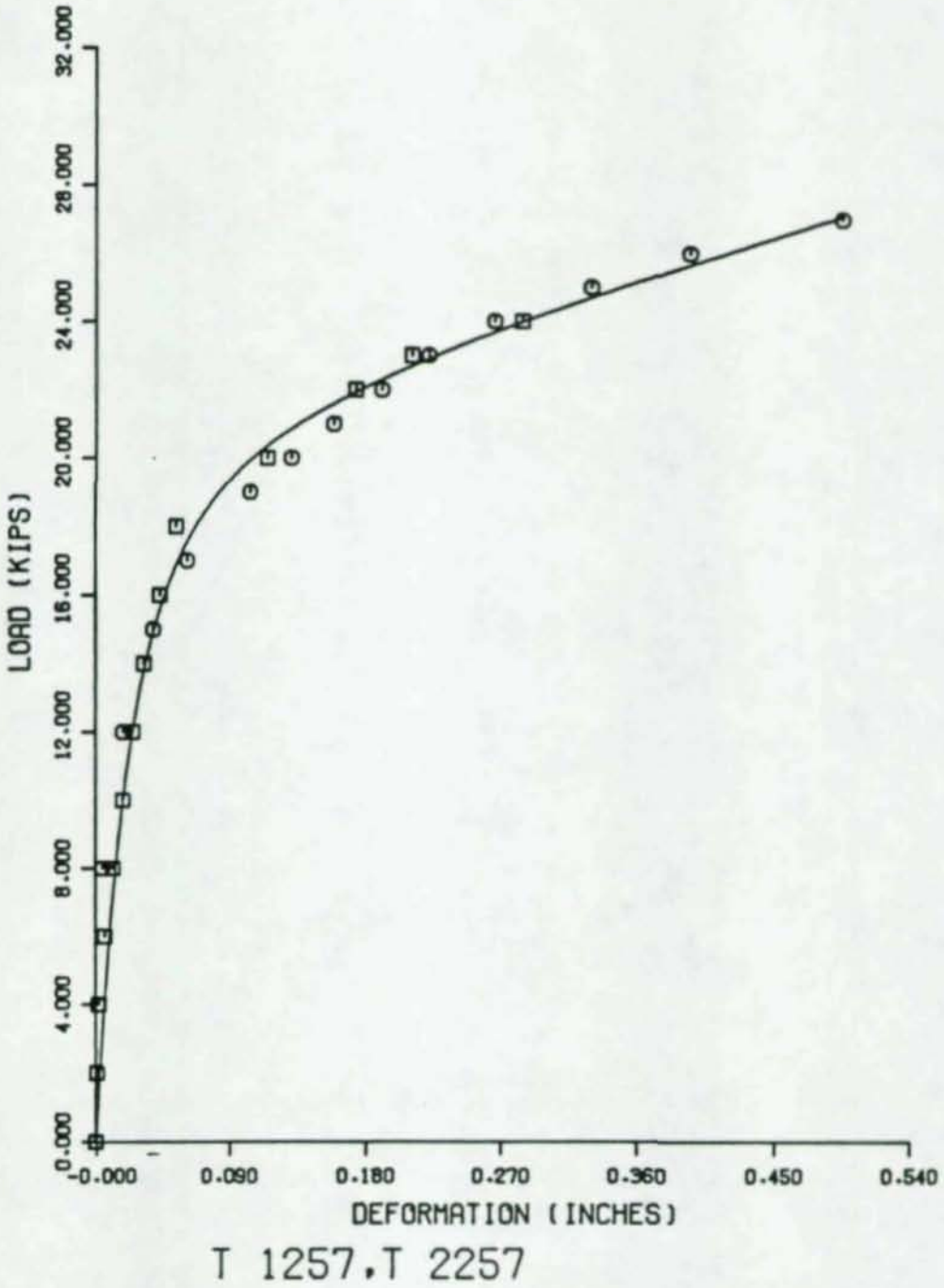

Figure A-21

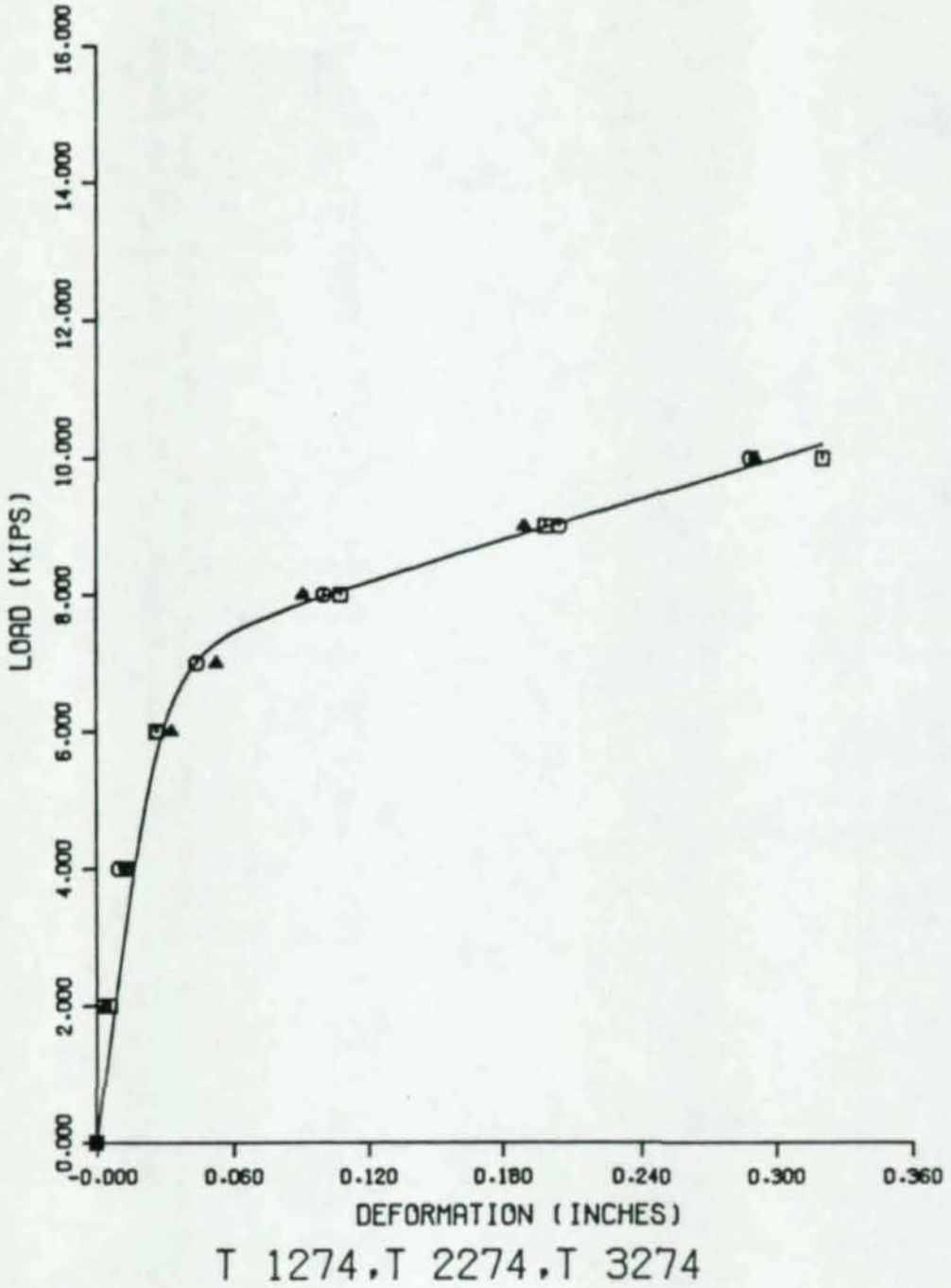

Figure A-22

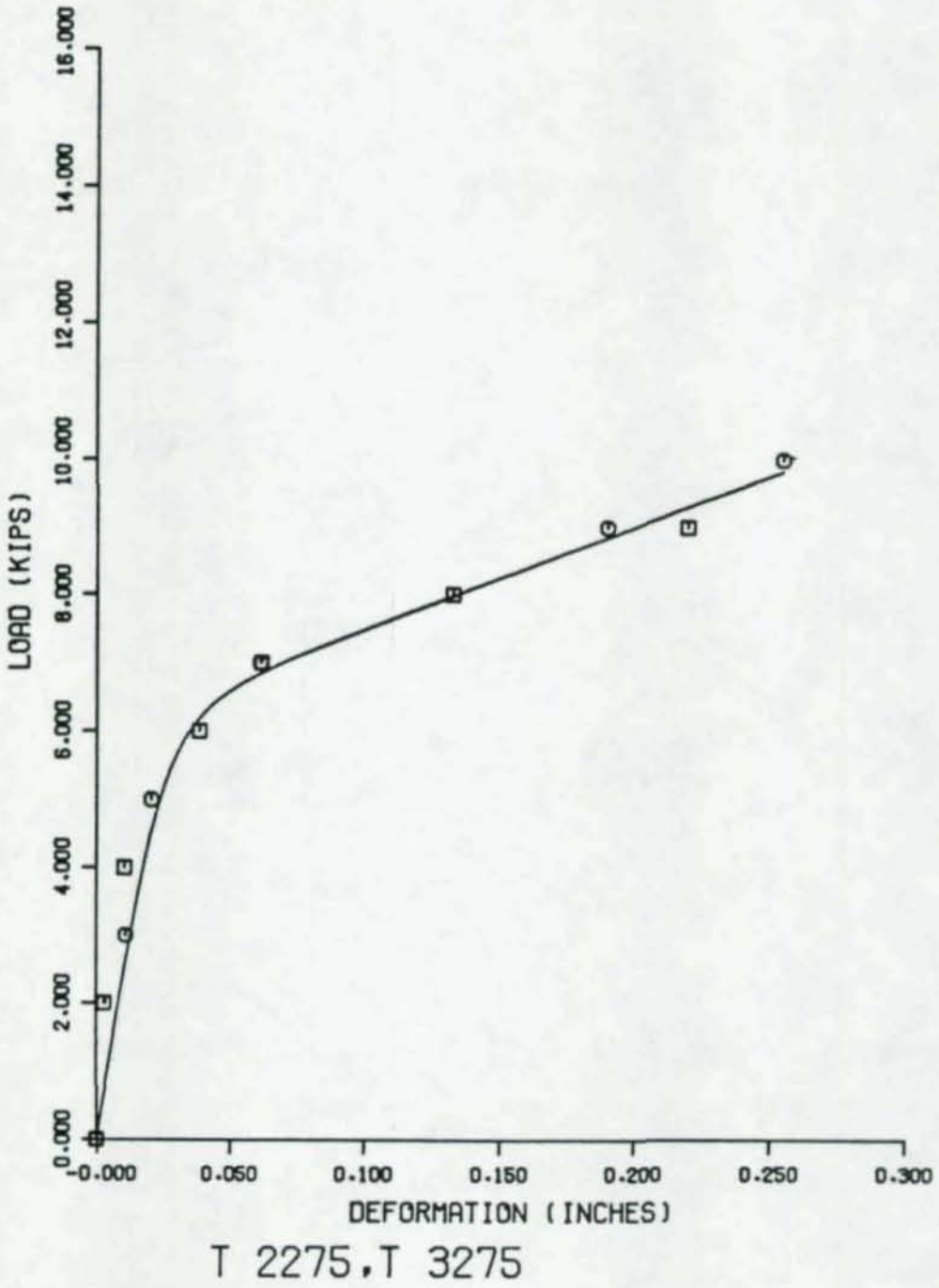

Figure A-23

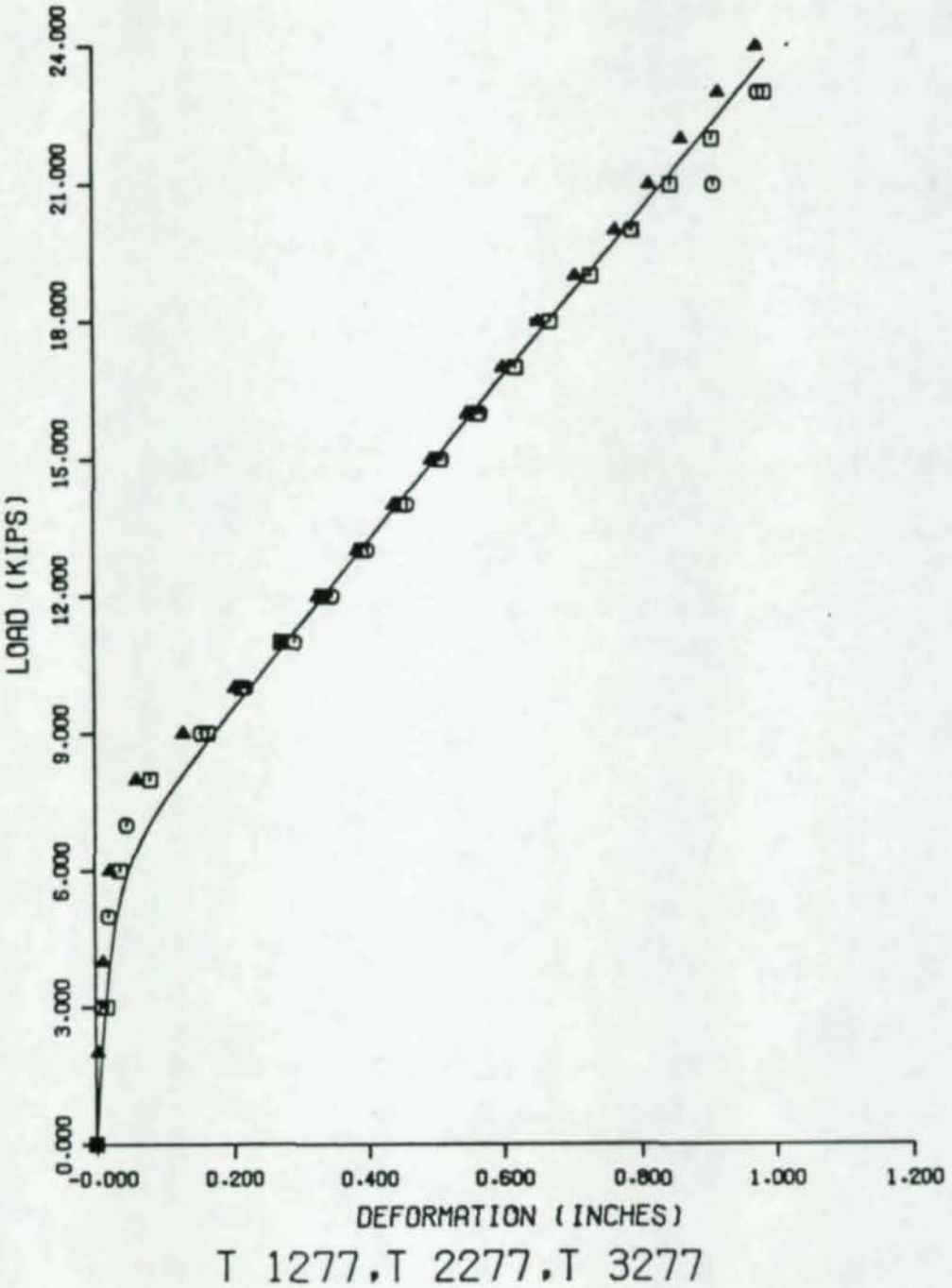

Figure A-24

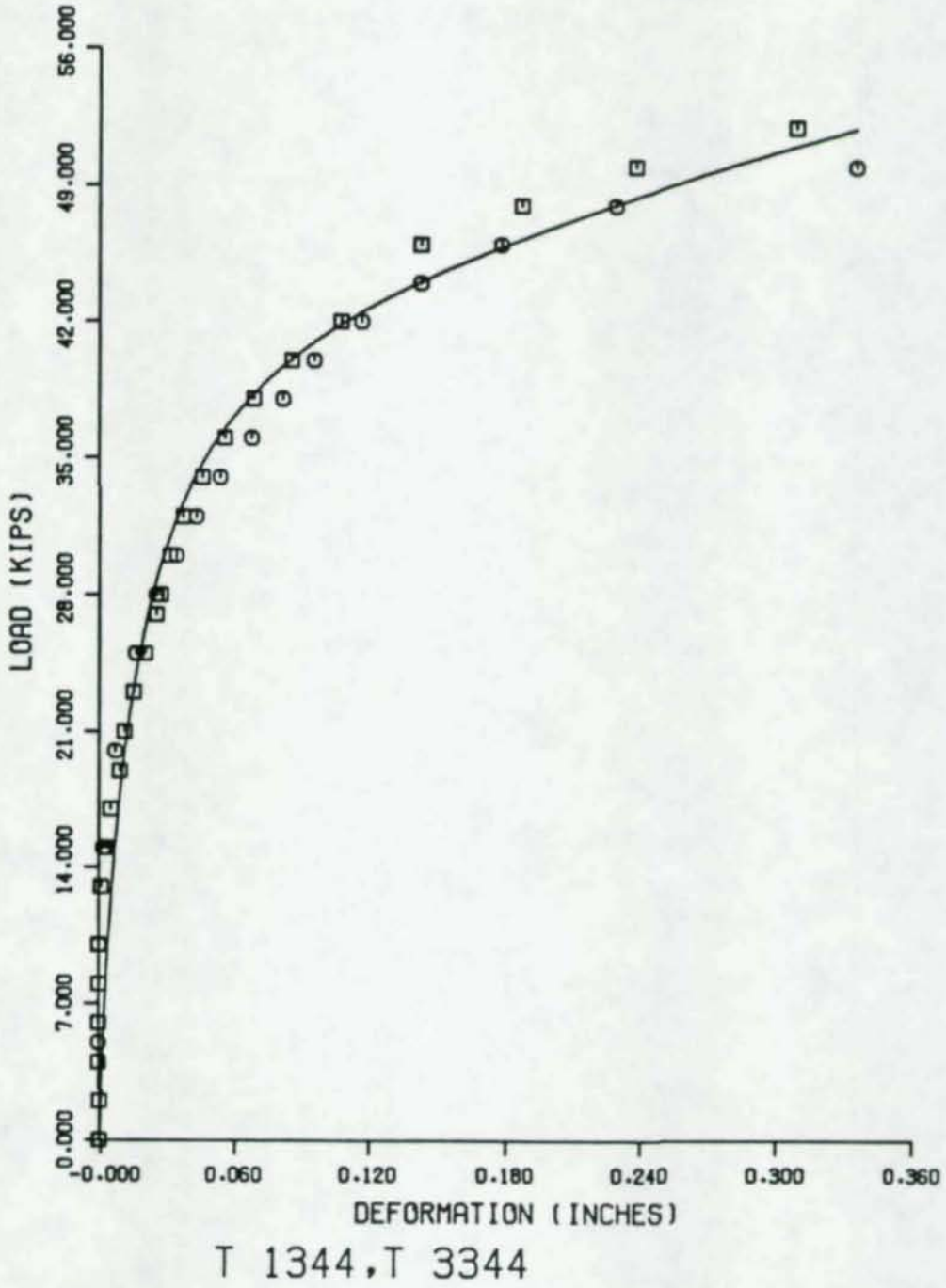

Figure A-25

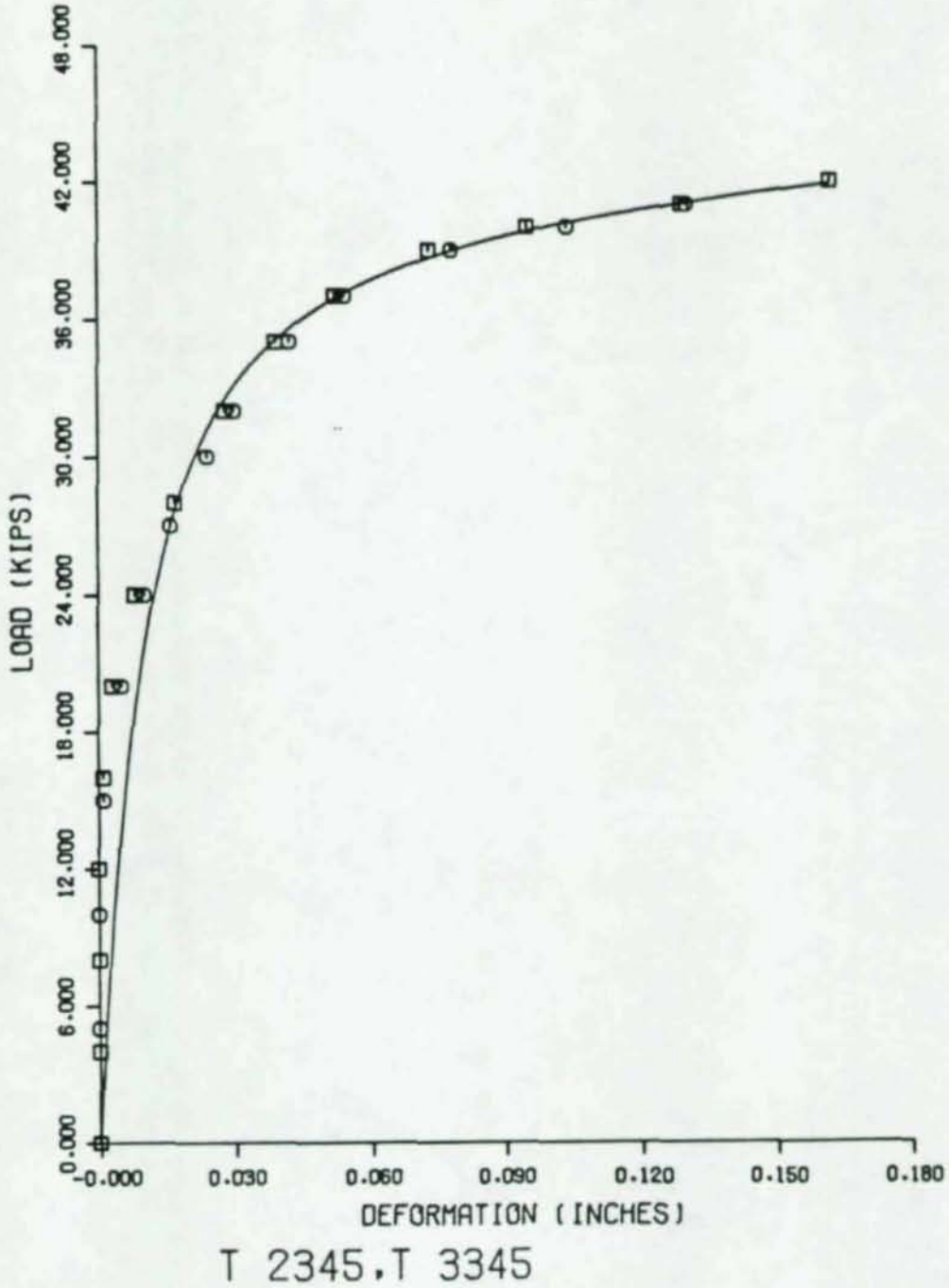

Figure A-26

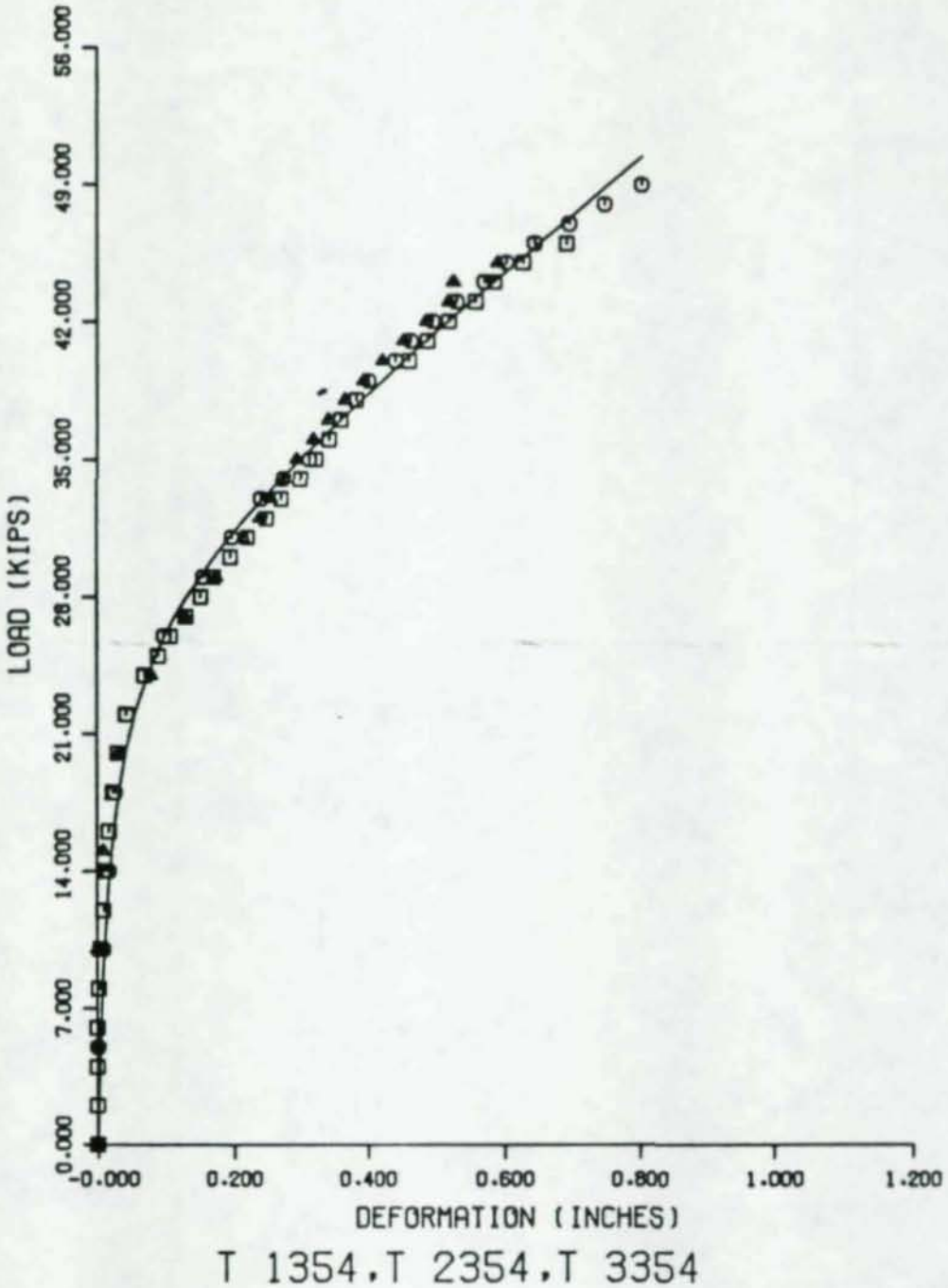

Figure A-27

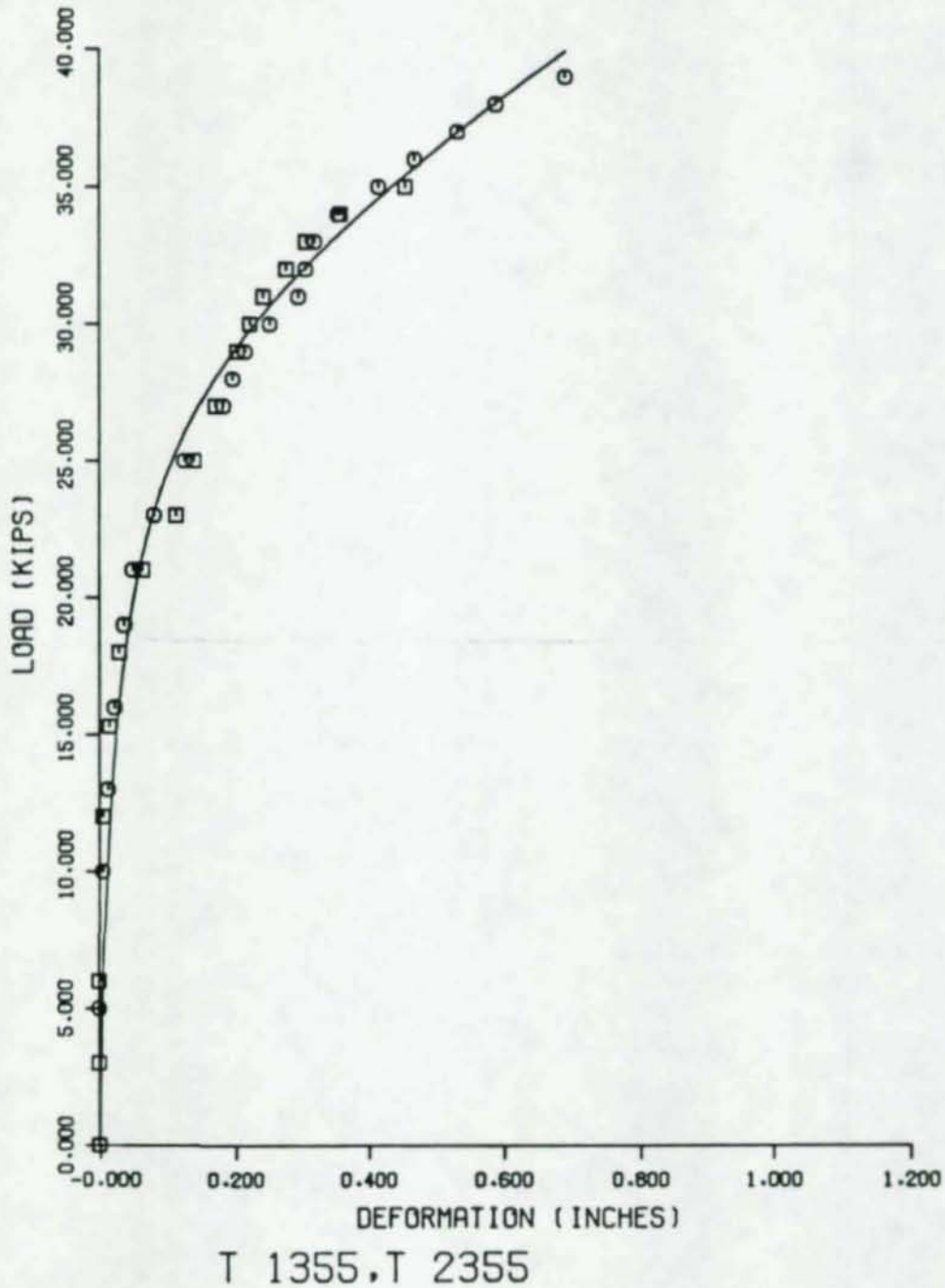

Figure A-28

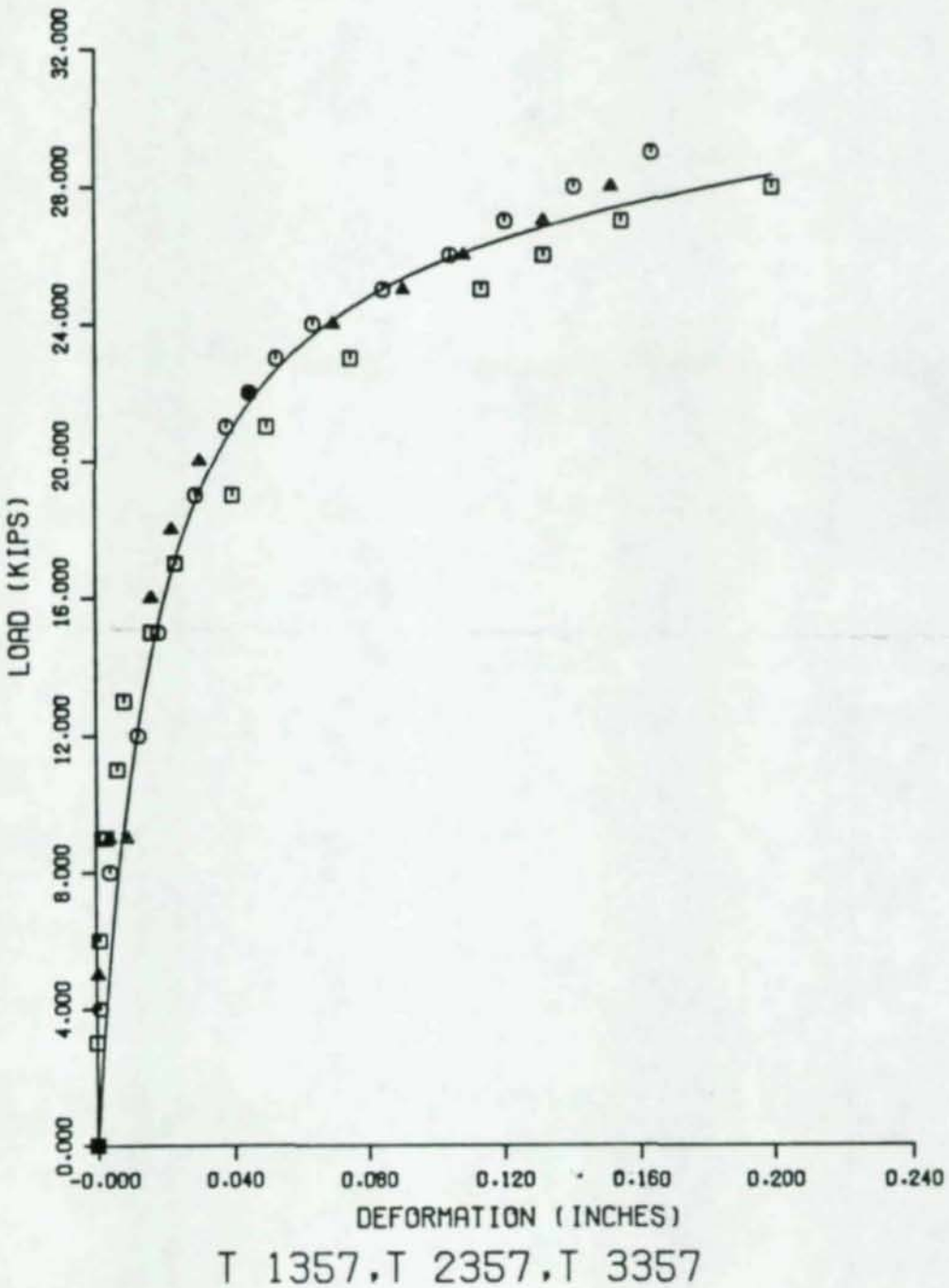

Figure A-29

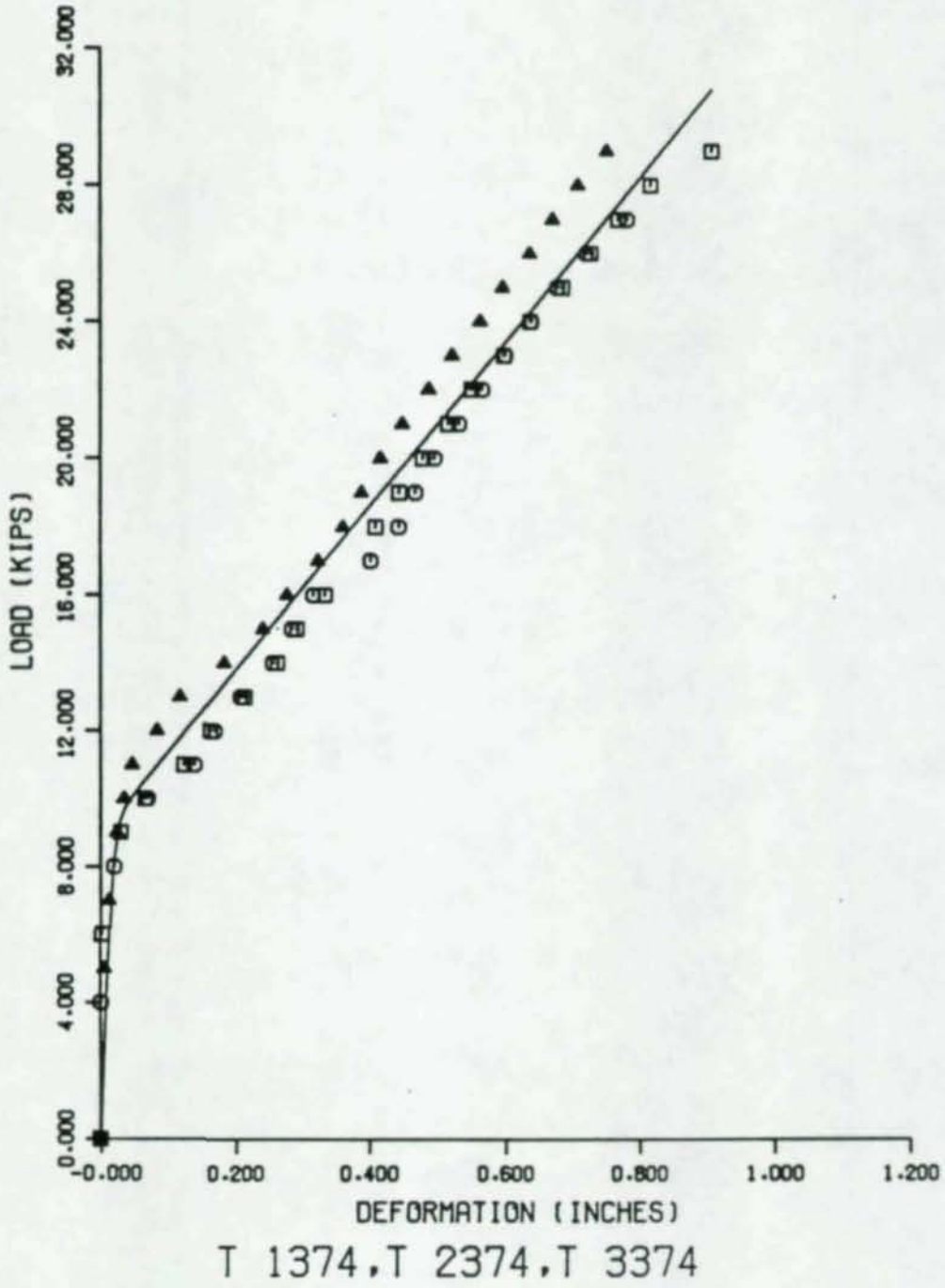

Figure A-30

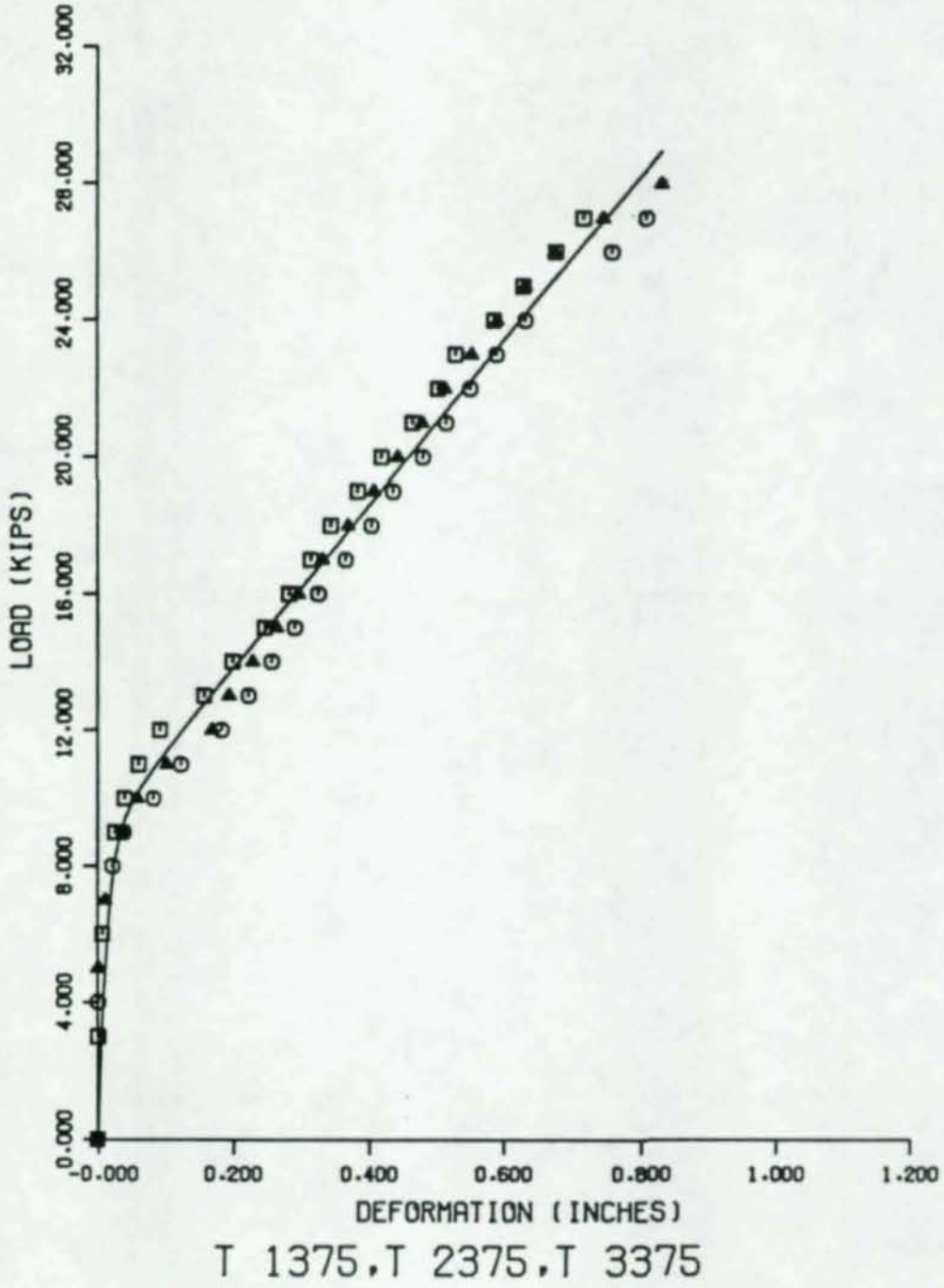
LOAD (KIPS)
0.000
4.000
8.000
12.000
16.000
20.000
24.000
28.000
32.000
-0.000
0.200
0.400
0.600
0.800
1.000
1.200
DEFORMATION (INCHES)
T 1375,T 2375,T 3375

Figure A-31

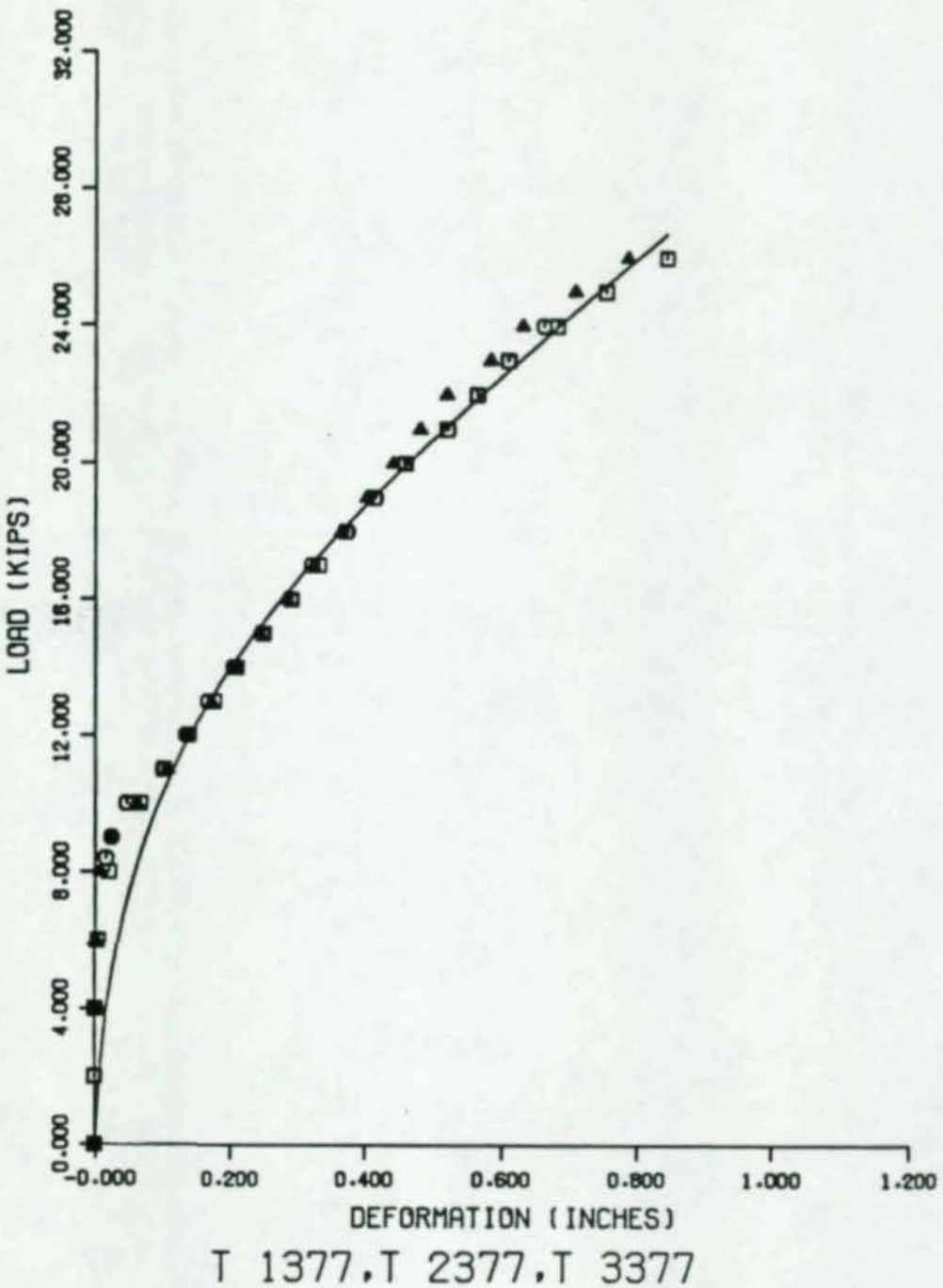
LOAD (KIPS)
0.000
4.000
8.000
12.000
16.000
20.000
24.000
28.000
32.000
-0.000
0.200
0.400
0.600
0.800
1.000
1.200
DEFORMATION (INCHES)
T 1377,T 2377,T 3377

Figure A-32

APPENDIX B

VARIATION IN LOAD-DEFORMATION CURVES WITH RESPECT TO A CHANGE IN THE LOAD-BEARING PLATE THICKNESS

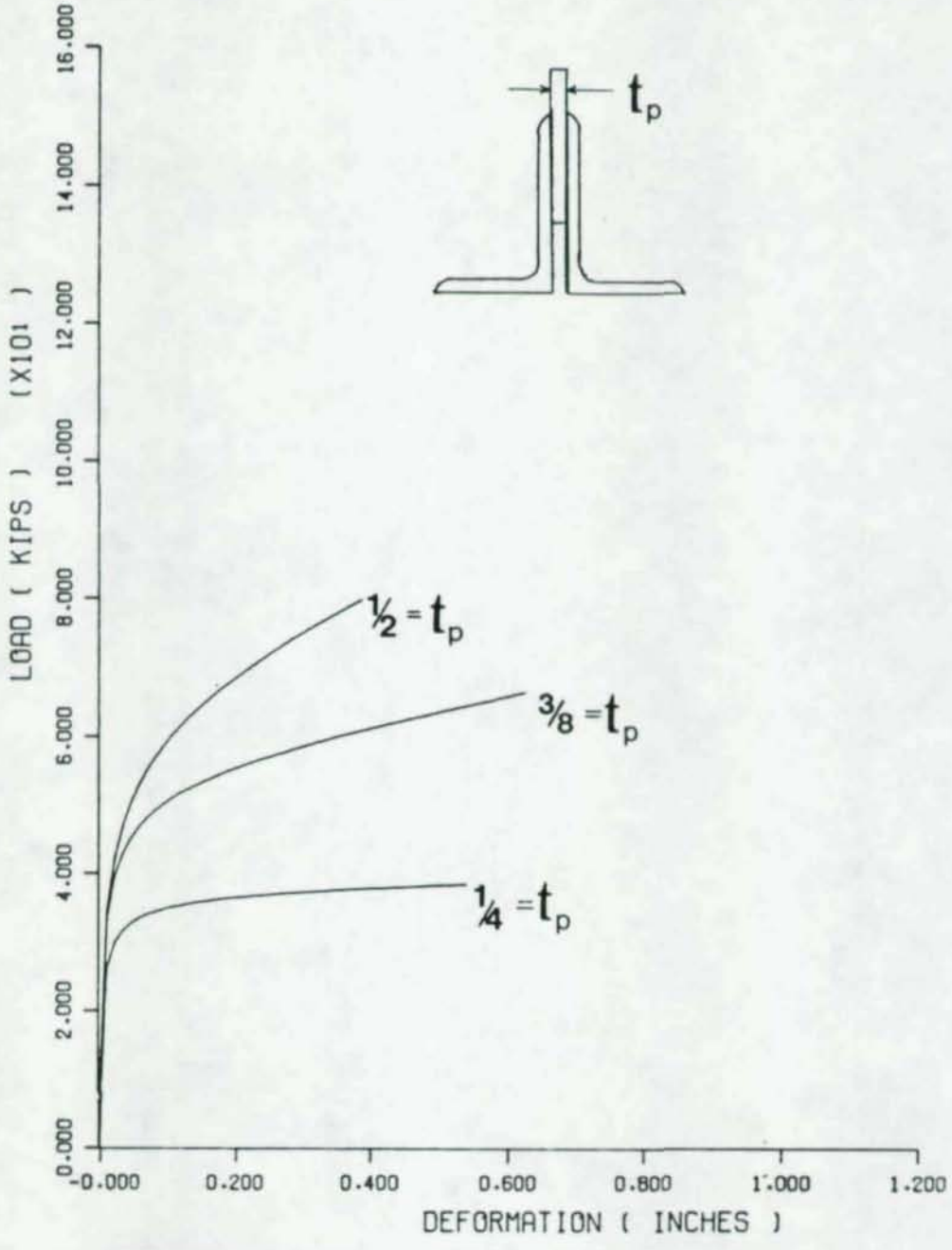

COMPRESSION TESTS: 3/4 INCH BOLTS

Figure B-1

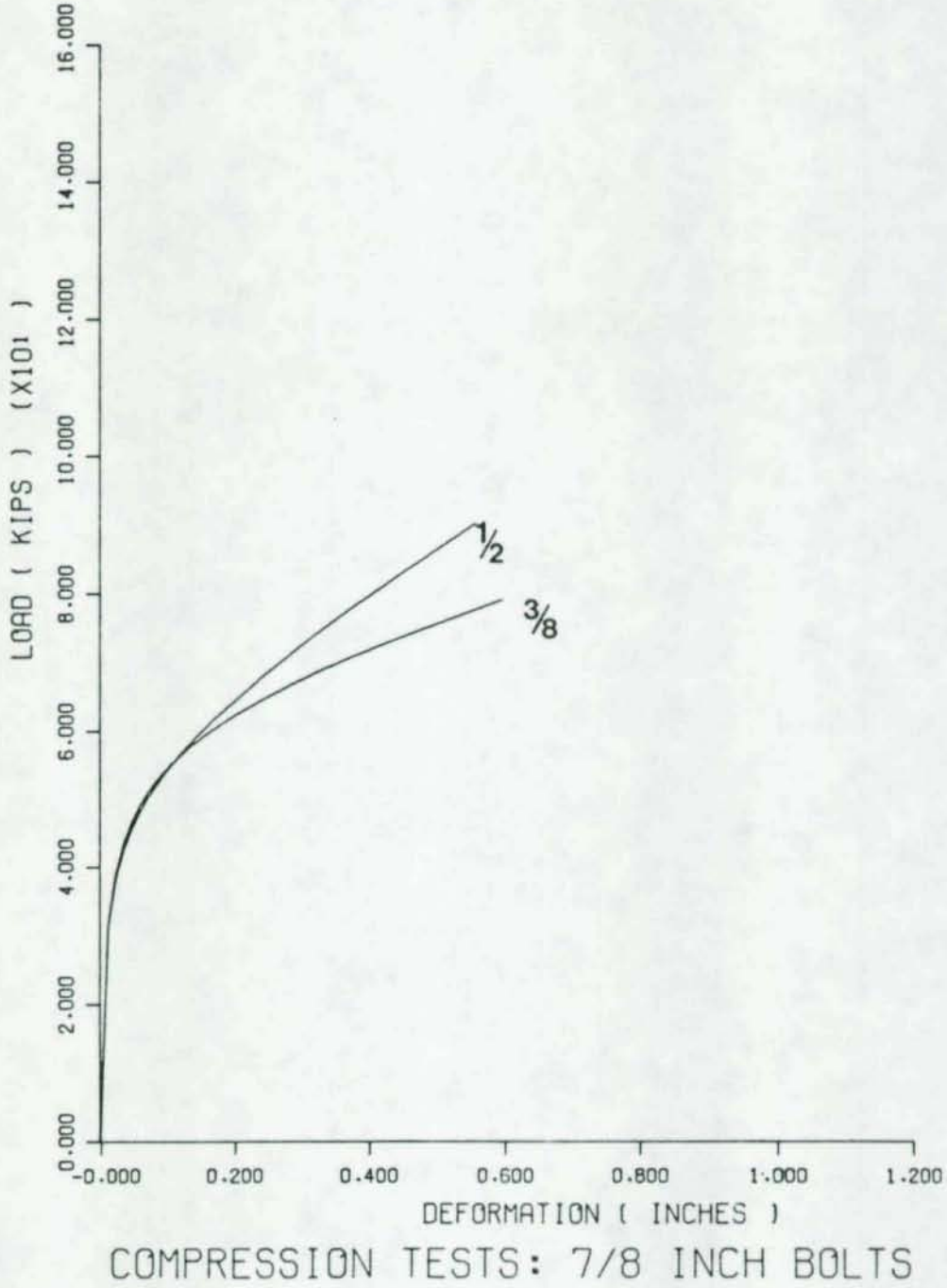

Figure B-2

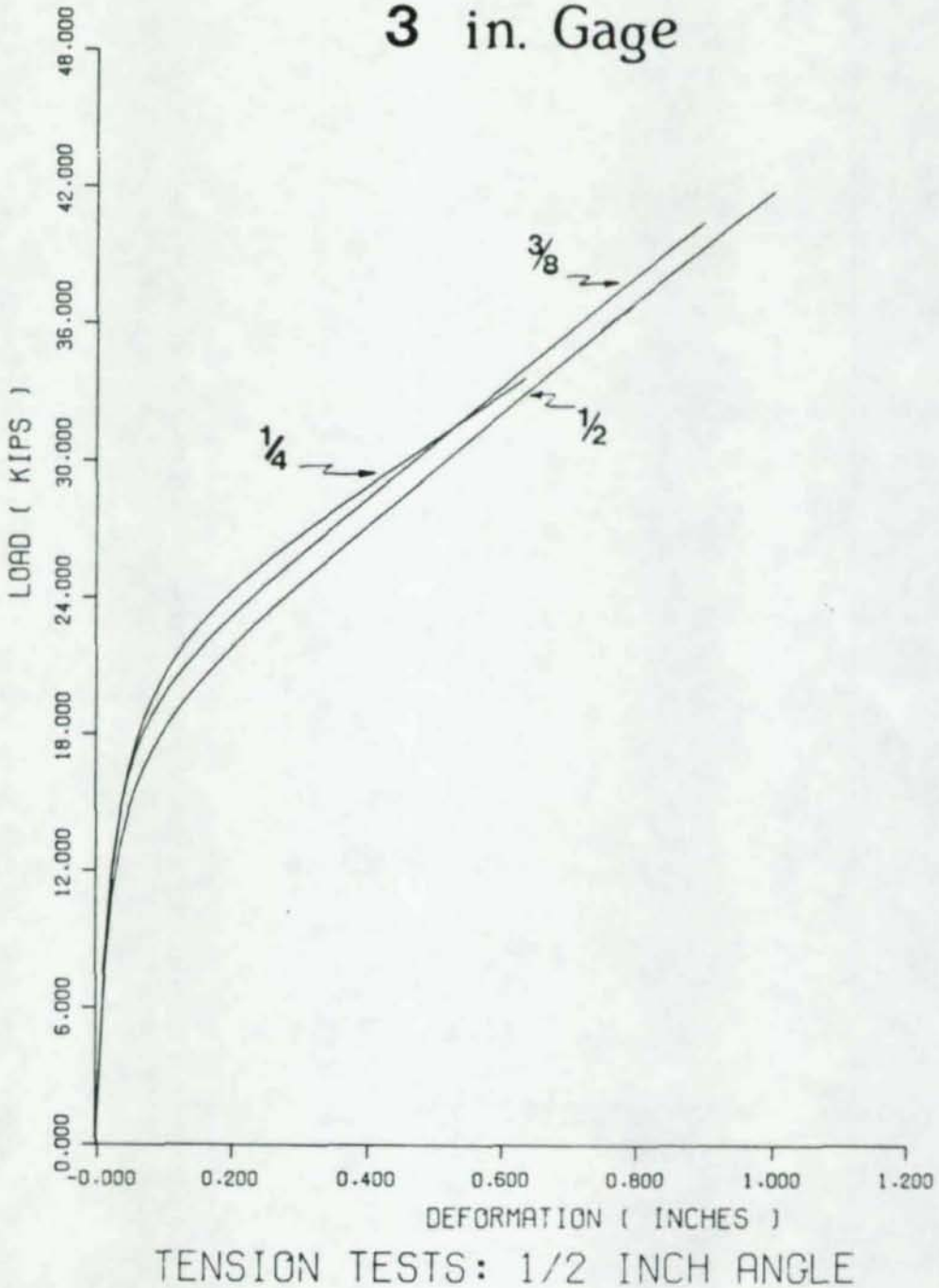

Figure B-3

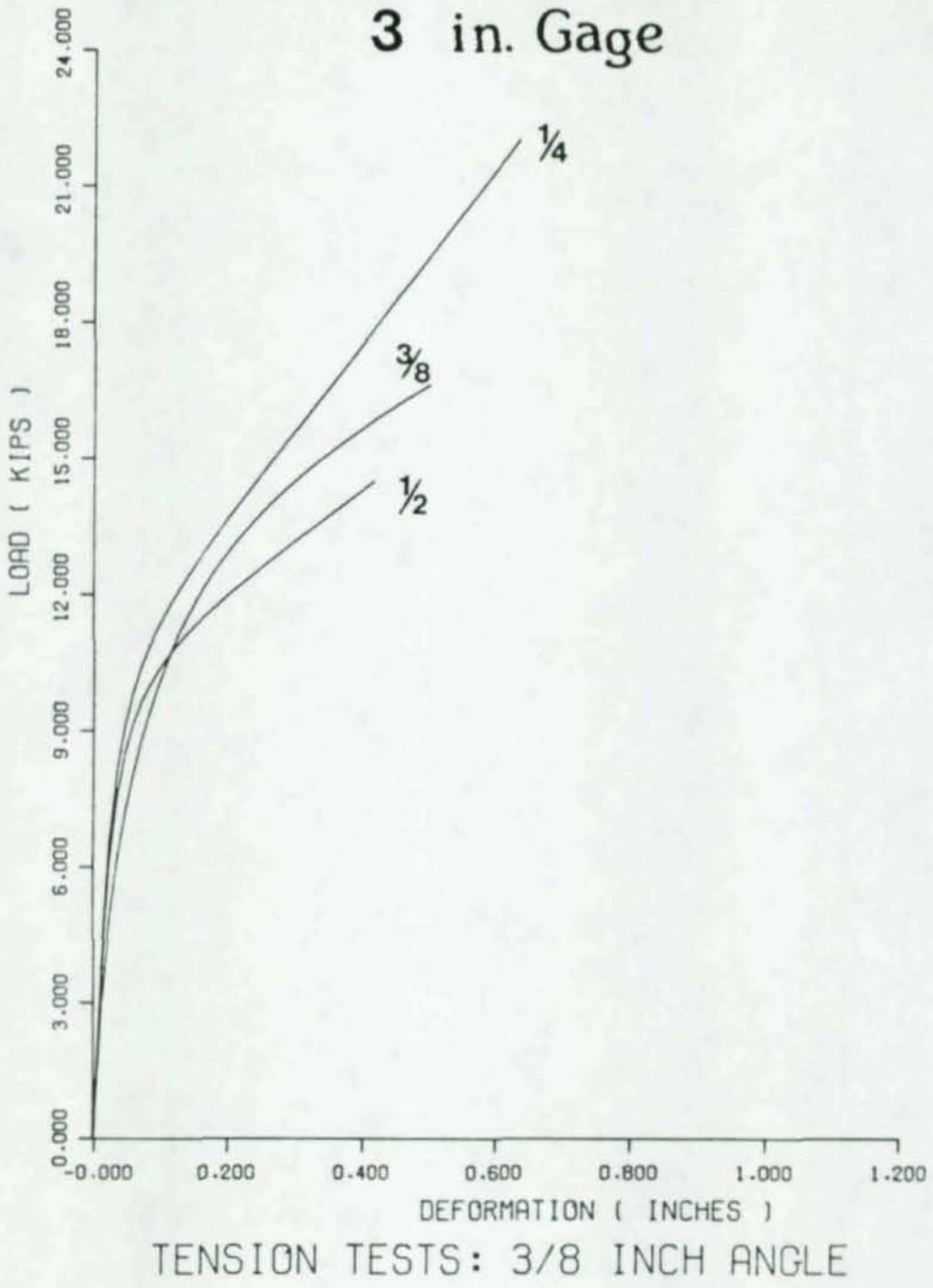
3 in. Gage
1/4
3/8
1/2
LOAD (KIPS)
0.000
3.000
6.000
9.000
12.000
15.000
18.000
21.000
24.000
0.000
0.200
0.400
0.600
0.800
1.000
1.200
DEFORMATION (INCHES)
TENSION TESTS: 3/8 INCH ANGLE

Figure B-4

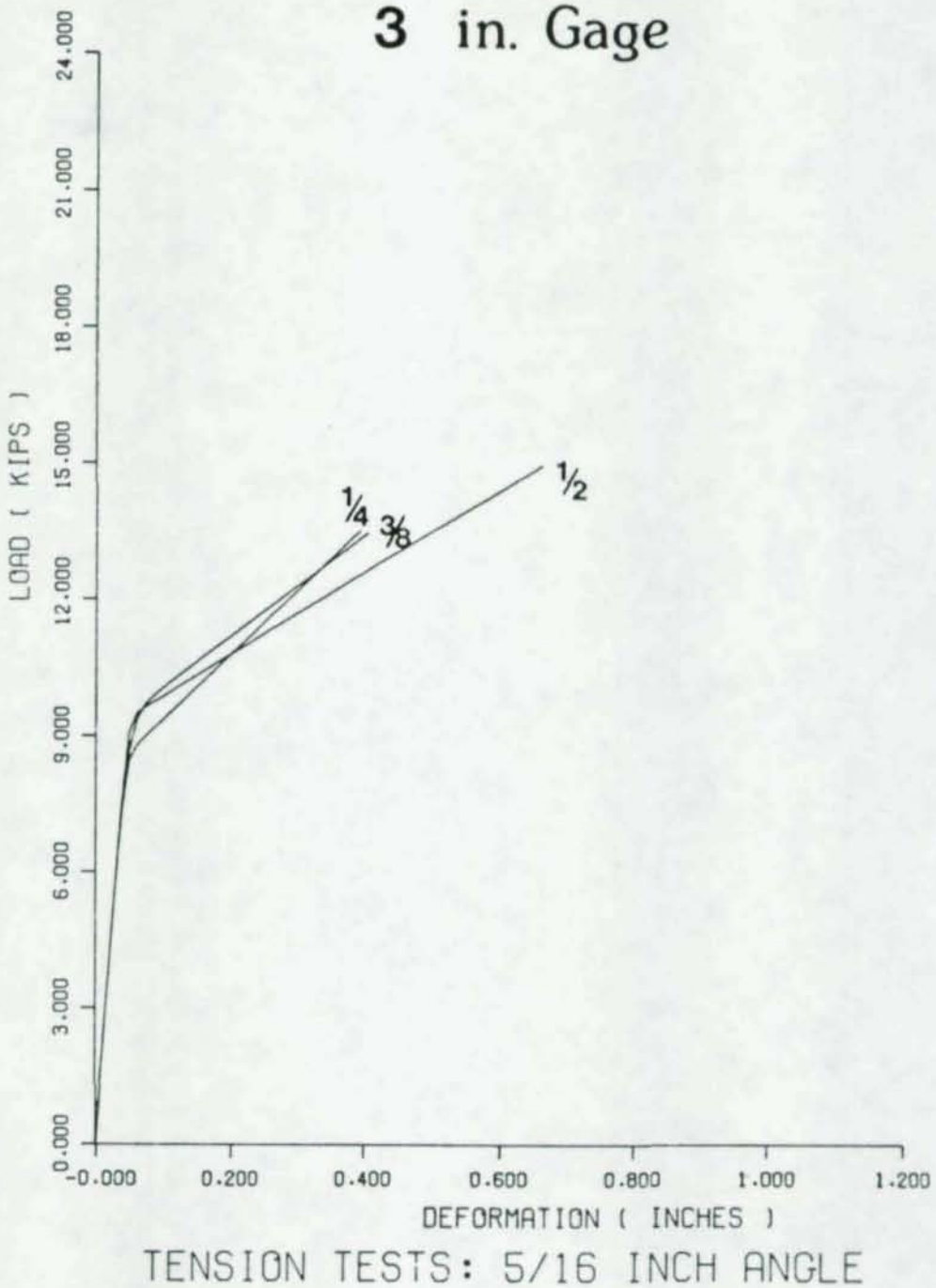

Figure B-5

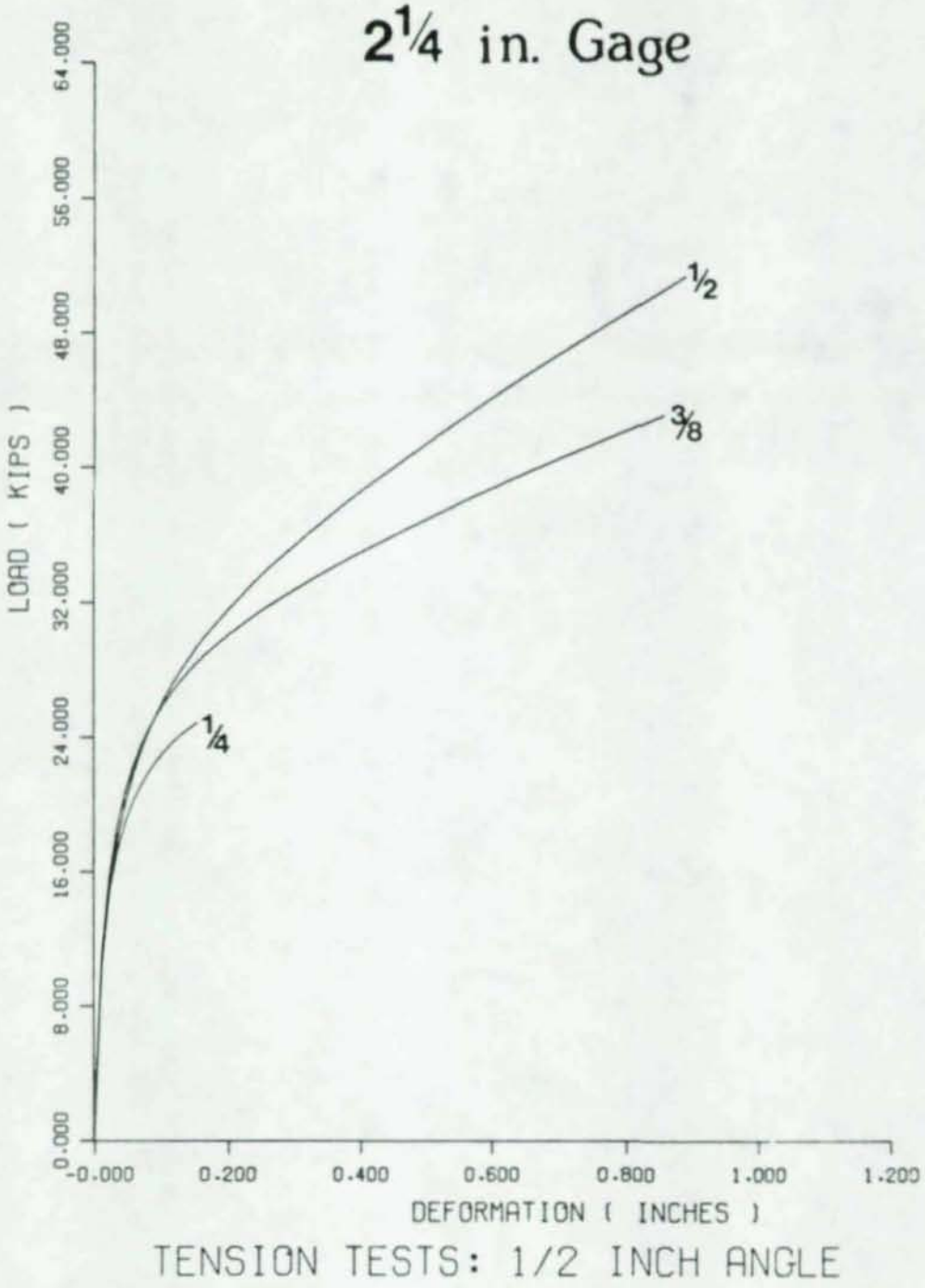
2¼ in. Gage
LOAD (KIPS)
0.000
8.000
16.000
24.000
32.000
40.000
48.000
56.000
64.000
0.000
0.200
0.400
0.600
0.800
1.000
1.200
DEFORMATION (INCHES)
½
⅜
¼
TENSION TESTS: 1/2 INCH ANGLE

Figure B-6

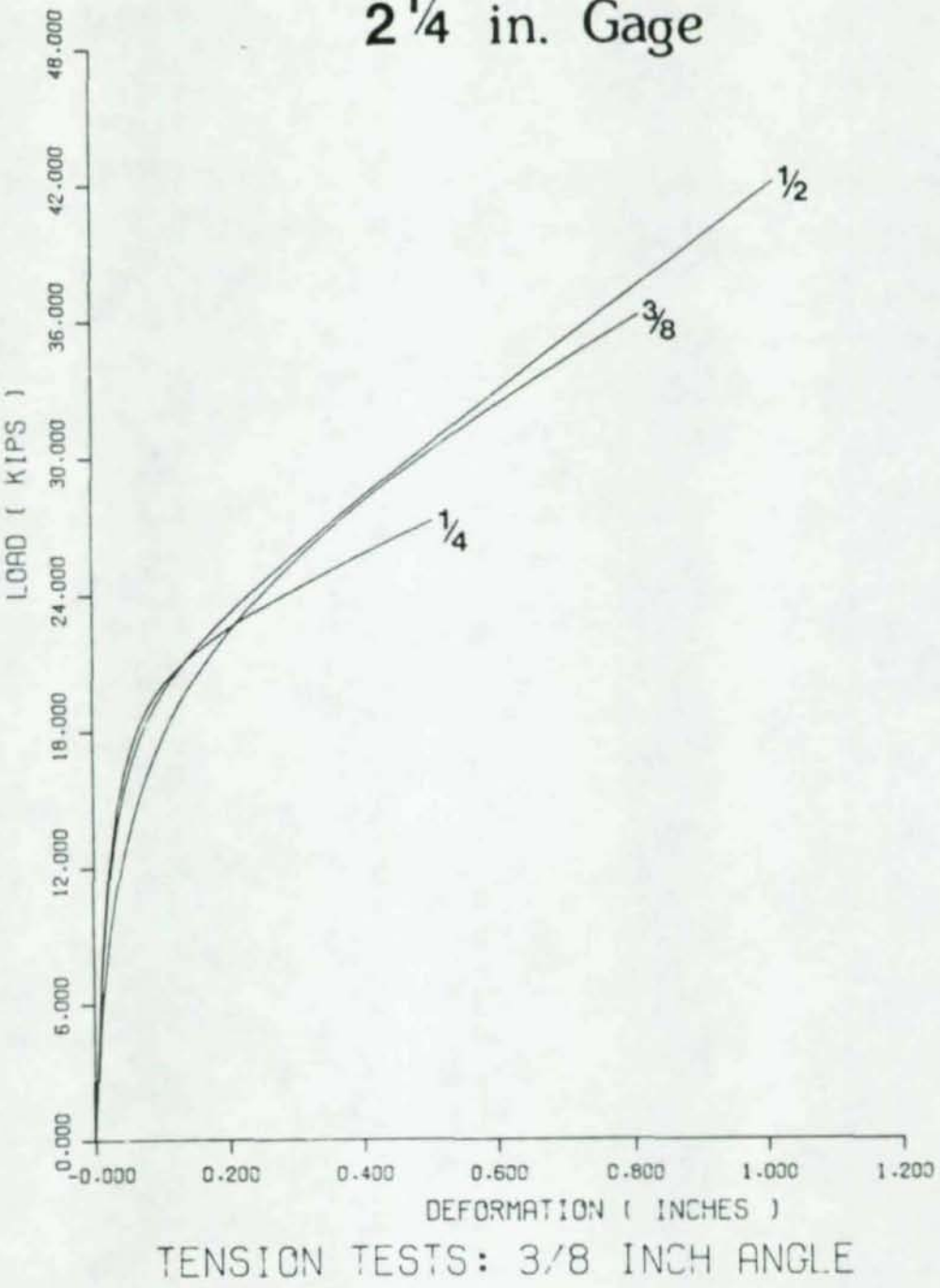

Figure B-7

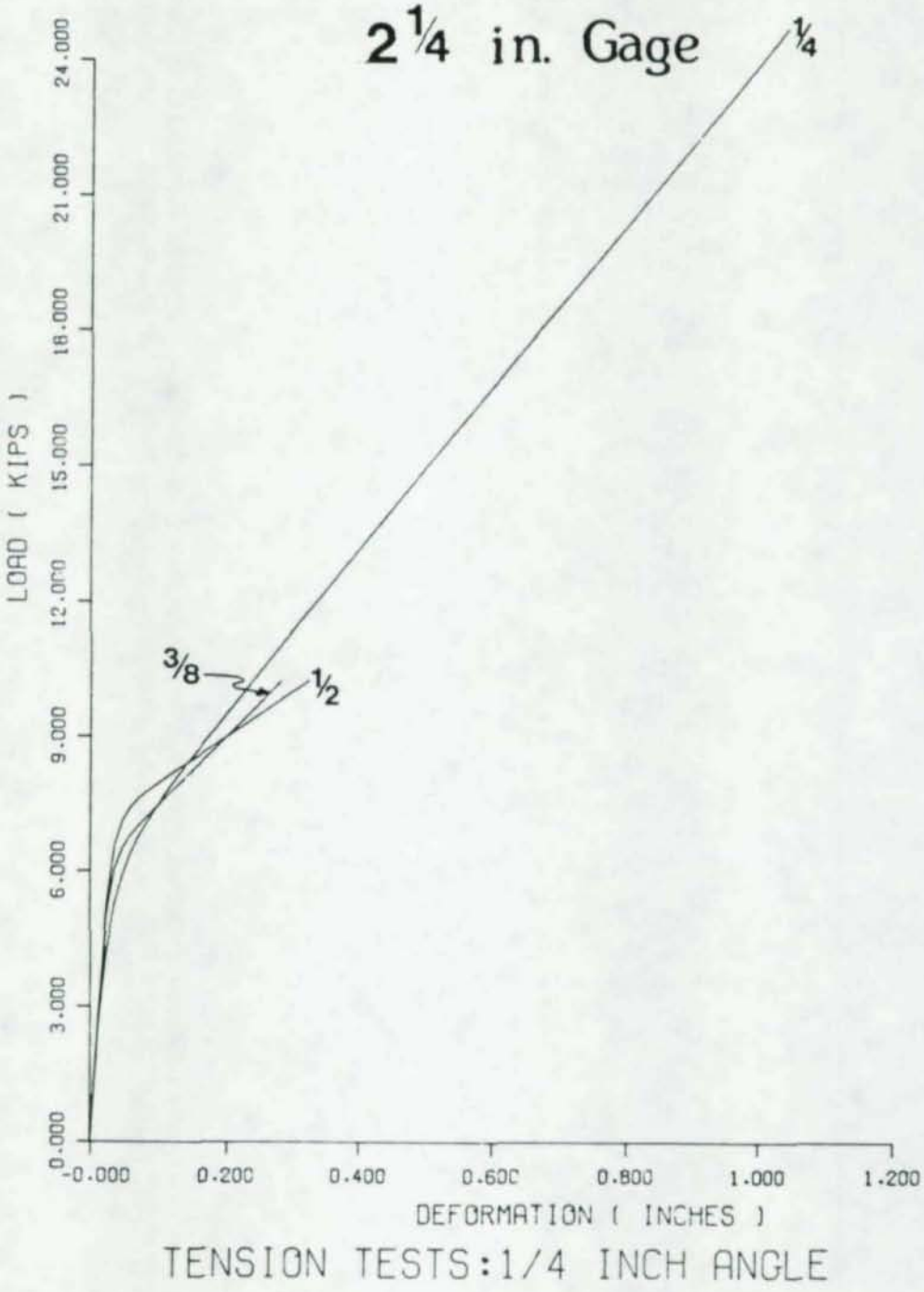
2 1/4 in. Gage
1/4
3/8
1/2
LOAD (KIPS)
0.000
3.000
6.000
9.000
12.000
15.000
18.000
21.000
24.000
-0.000
0.200
0.400
0.600
0.800
1.000
1.200
DEFORMATION (INCHES)
TENSION TESTS:1/4 INCH ANGLE

Figure B-8

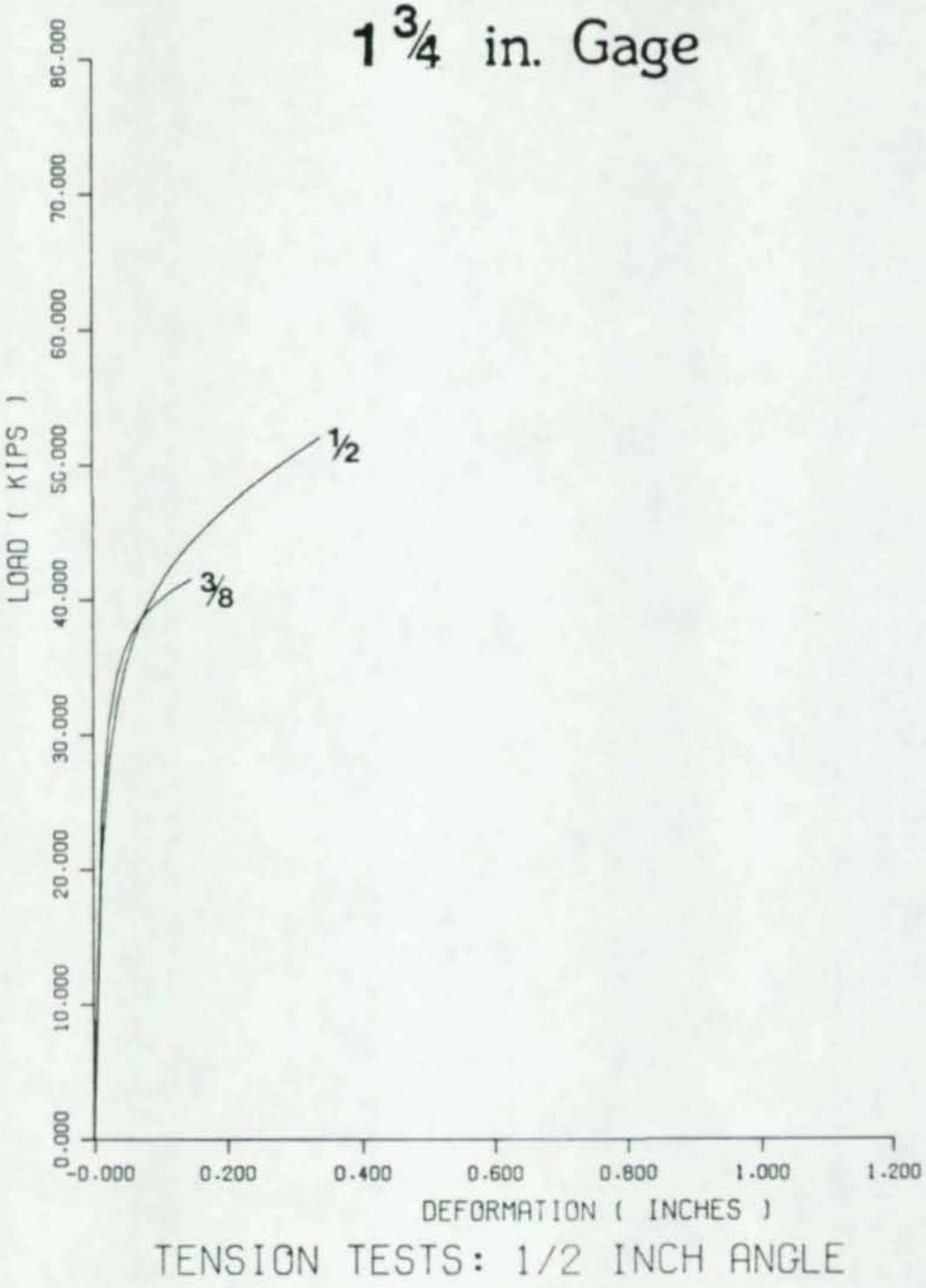

Figure B-9

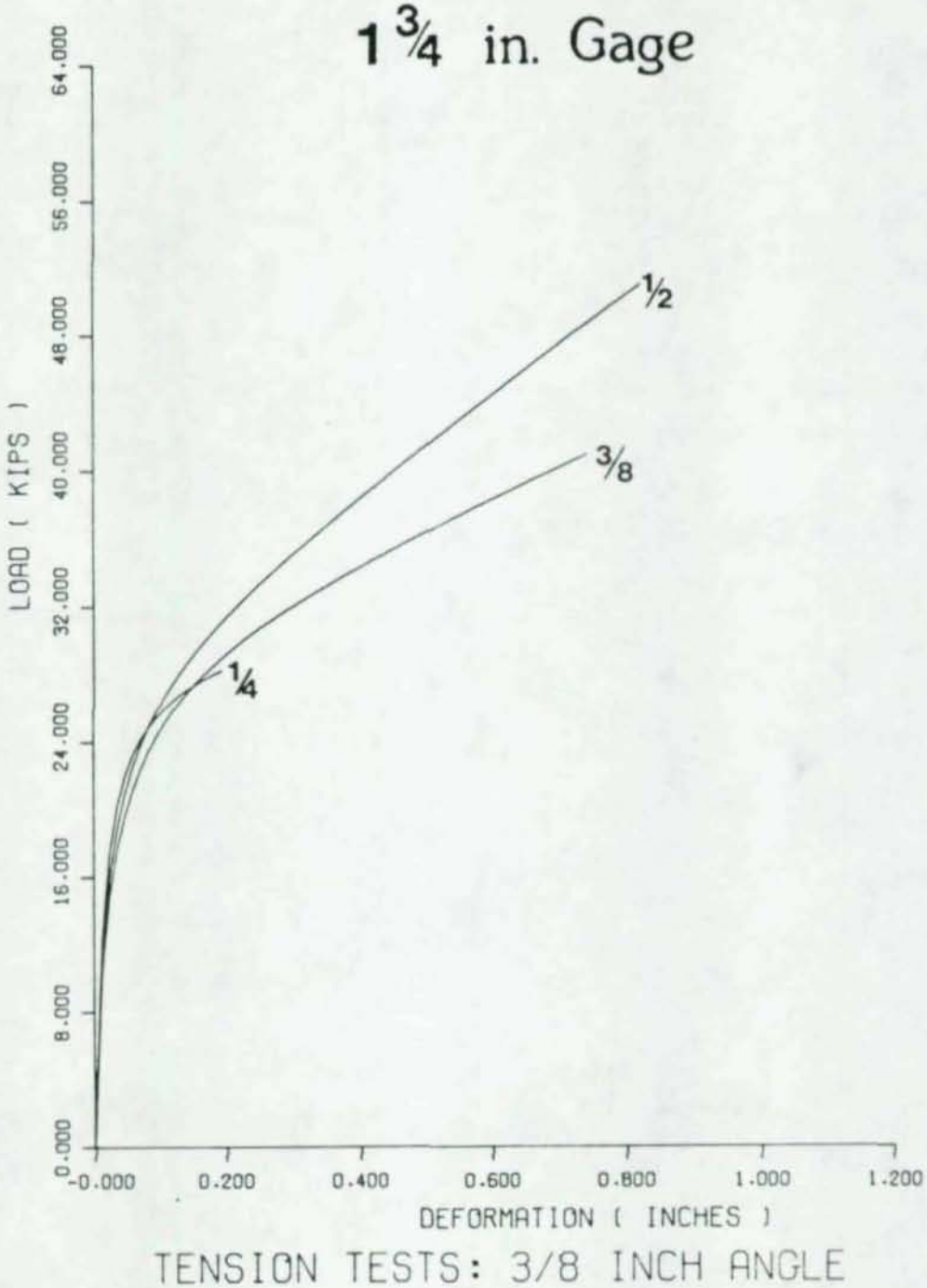

TENSION TESTS: 3/8 INCH ANGLE

Figure B-10

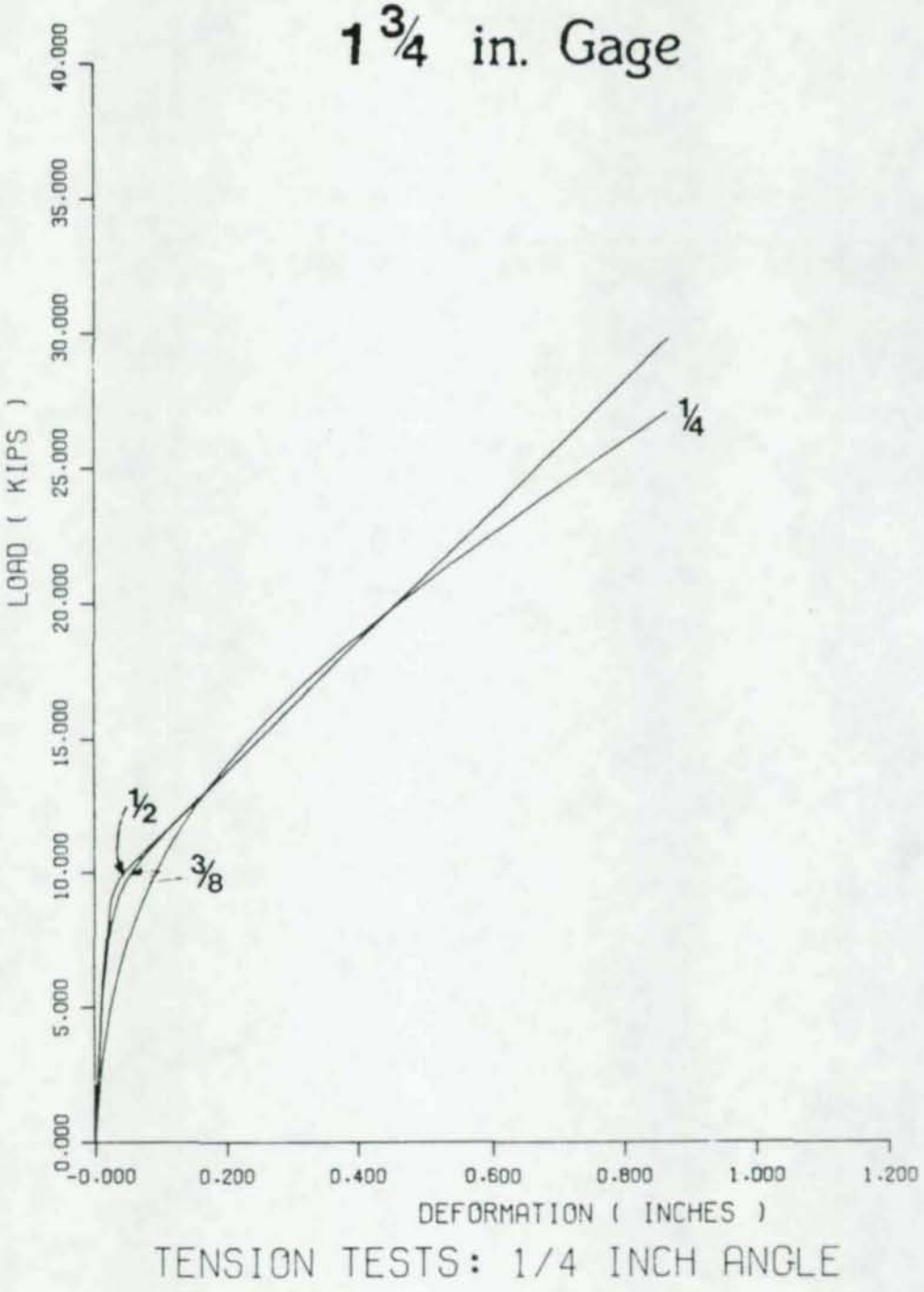
1 3/4 in. Gage
LOAD (KIPS)
0.000
5.000
10.000
15.000
20.000
25.000
30.000
35.000
40.000
-0.000
0.200
0.400
0.600
0.800
1.000
1.200
DEFORMATION (INCHES)
1/4
1/2
3/8
TENSION TESTS: 1/4 INCH ANGLE

Figure B-11

APPENDIX C

VARIATION IN LOAD-DEFORMATION CURVES WITH RESPECT TO A CHANGE IN ANGLE THICKNESS

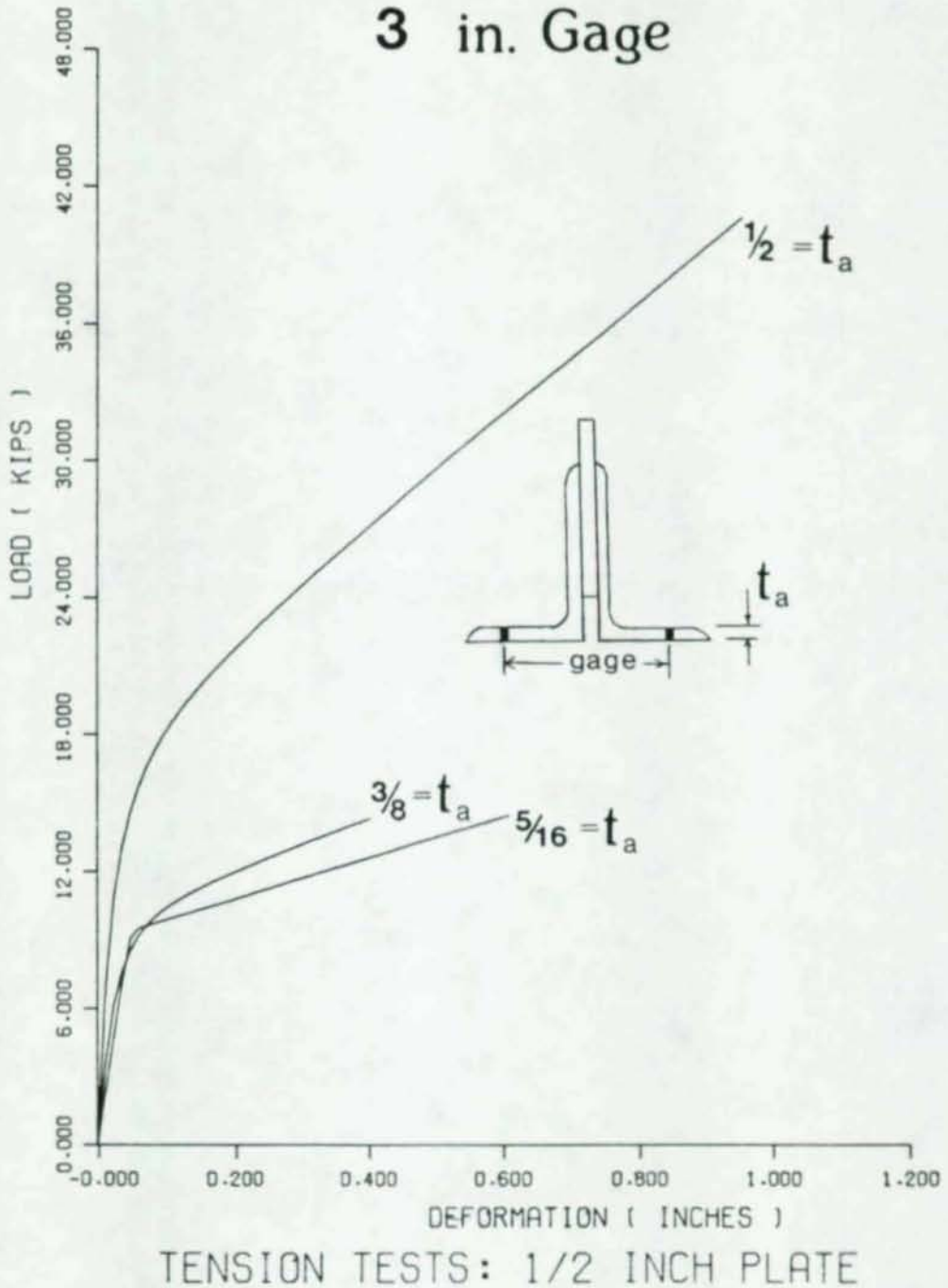
3 in. Gage
LOAD (KIPS)
0.000
6.000
12.000
18.000
24.000
30.000
36.000
42.000
48.000
-0.000
0.200
0.400
0.600
0.800
1.000
1.200
DEFORMATION (INCHES)
½ = t_a
3/8 = t_a
5/16 = t_a
t_a
gage
TENSION TESTS: 1/2 INCH PLATE

Figure C-1

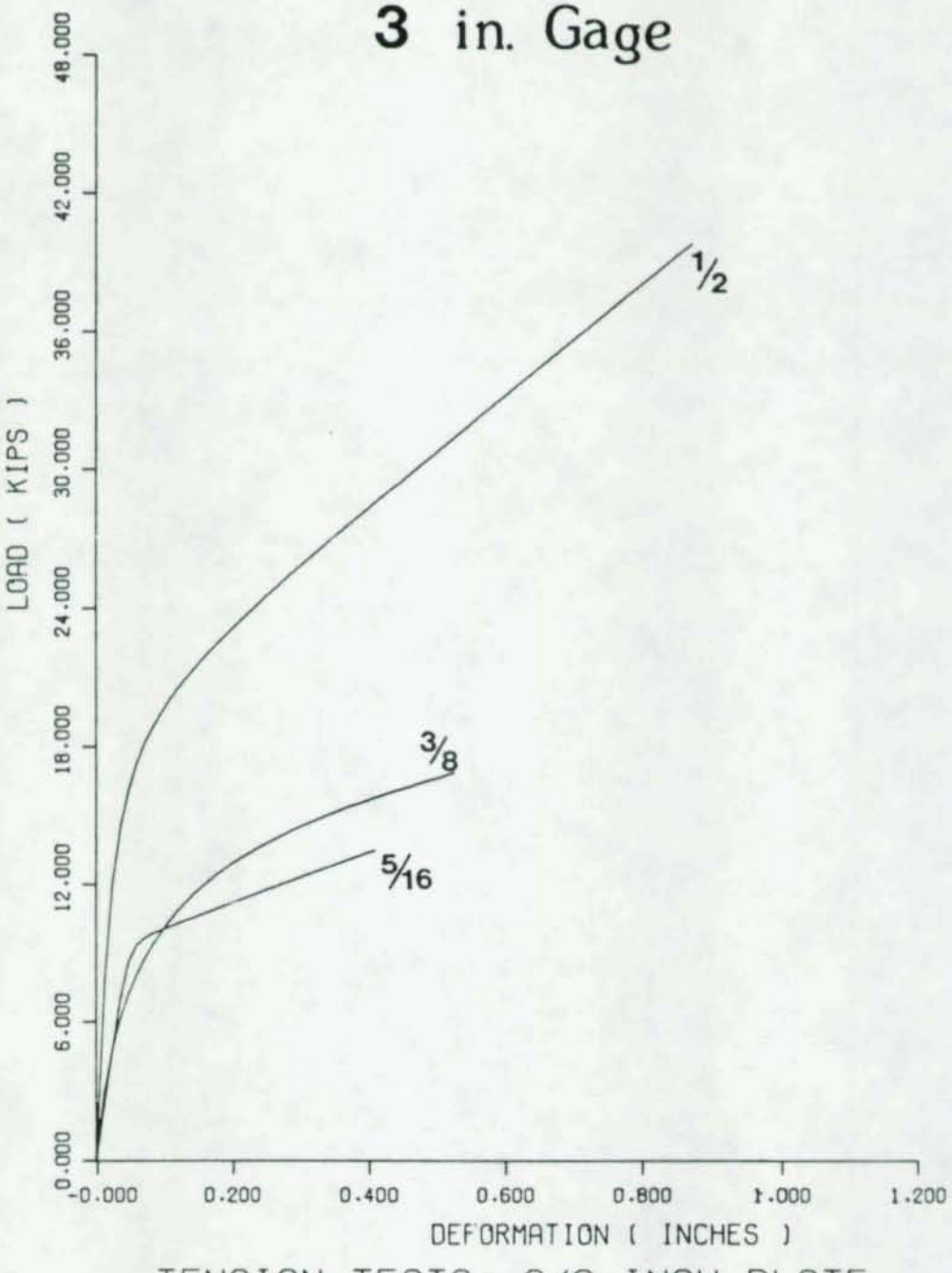

Figure C-2

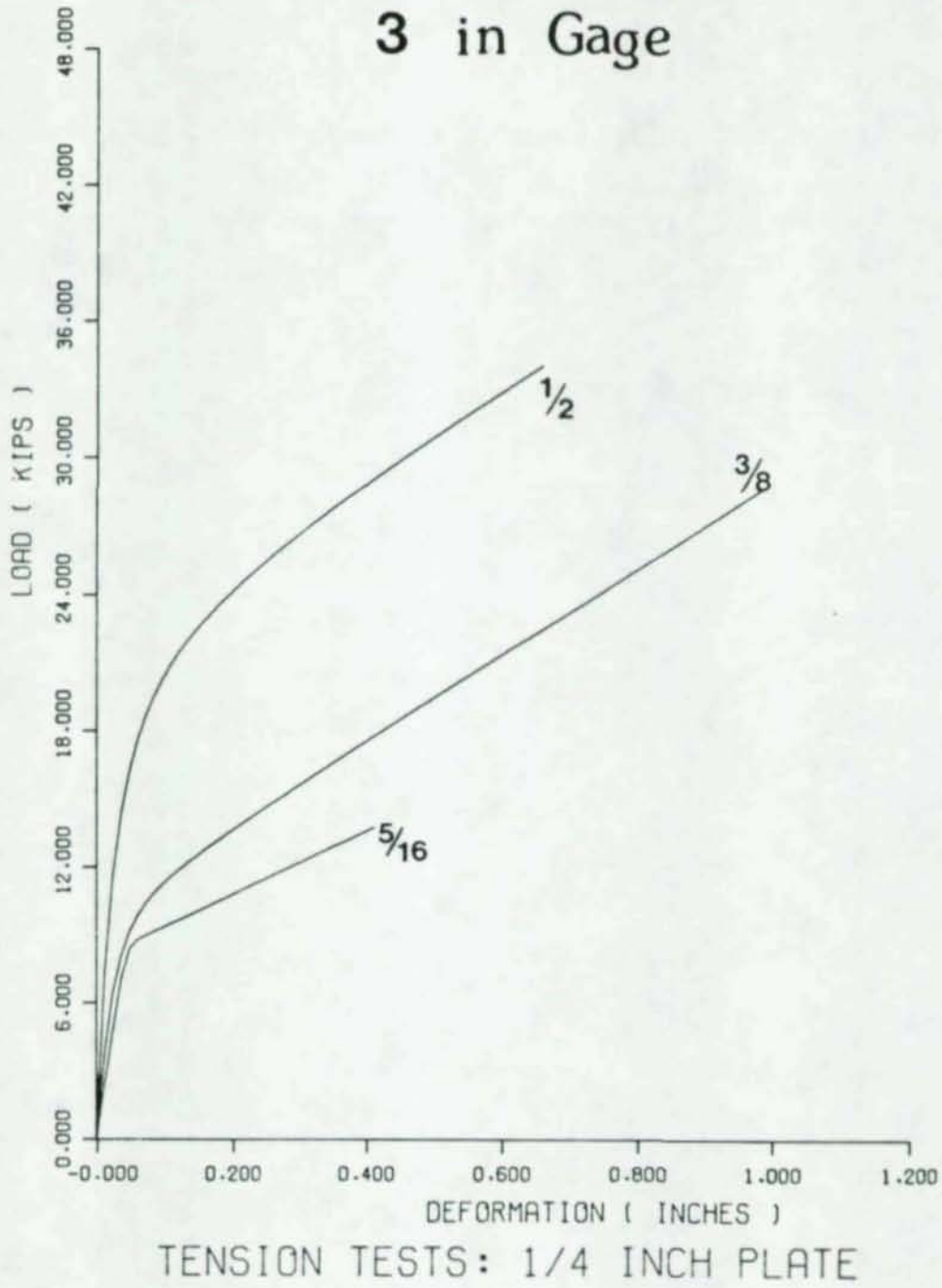
3 in Gage
LOAD (KIPS)
0.000
6.000
12.000
18.000
24.000
30.000
36.000
42.000
48.000
1/2
3/8
5/16
-0.000
0.200
0.400
0.600
0.800
1.000
1.200
DEFORMATION (INCHES)
TENSION TESTS: 1/4 INCH PLATE

Figure C-3

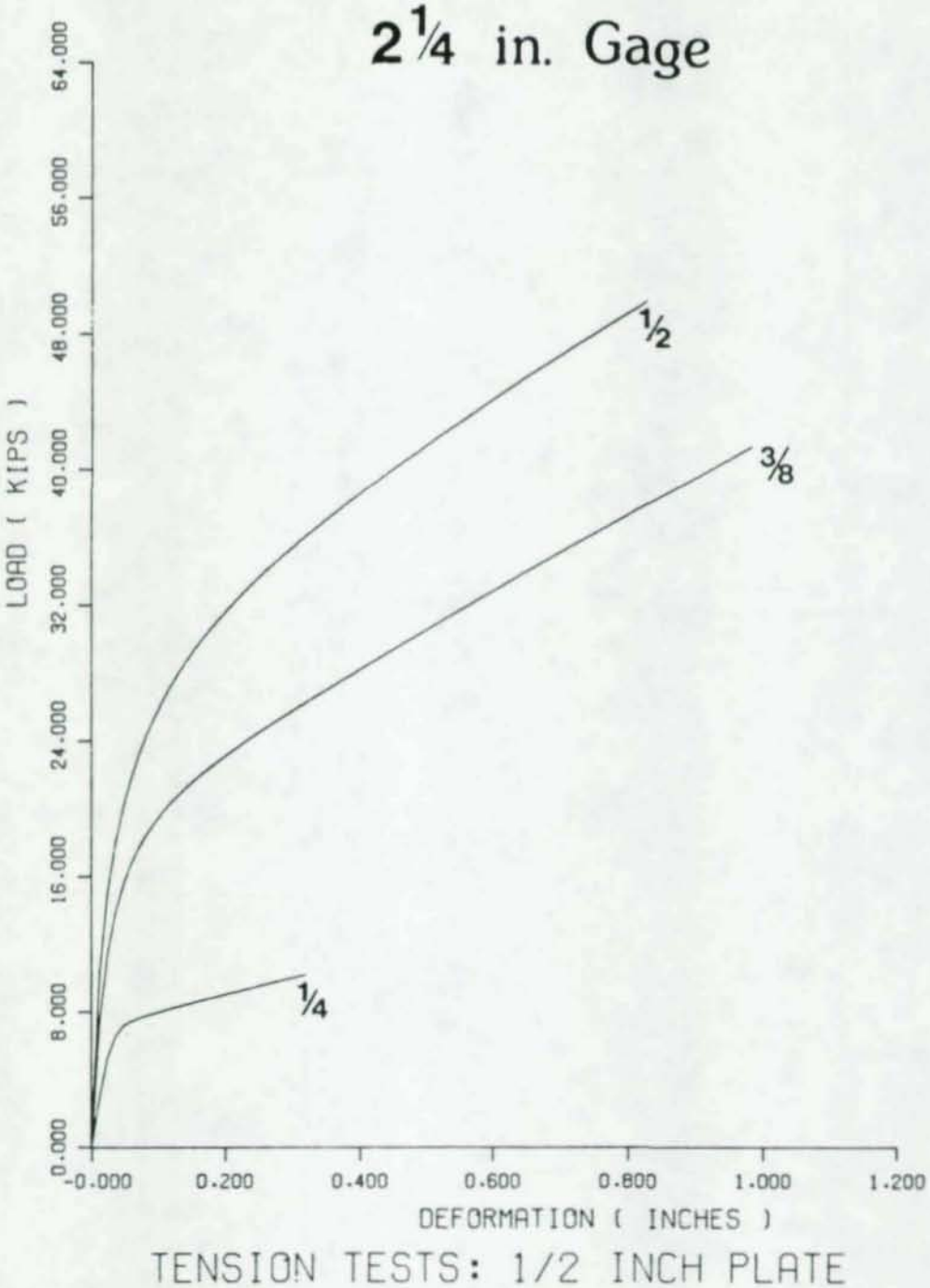

Figure C-4

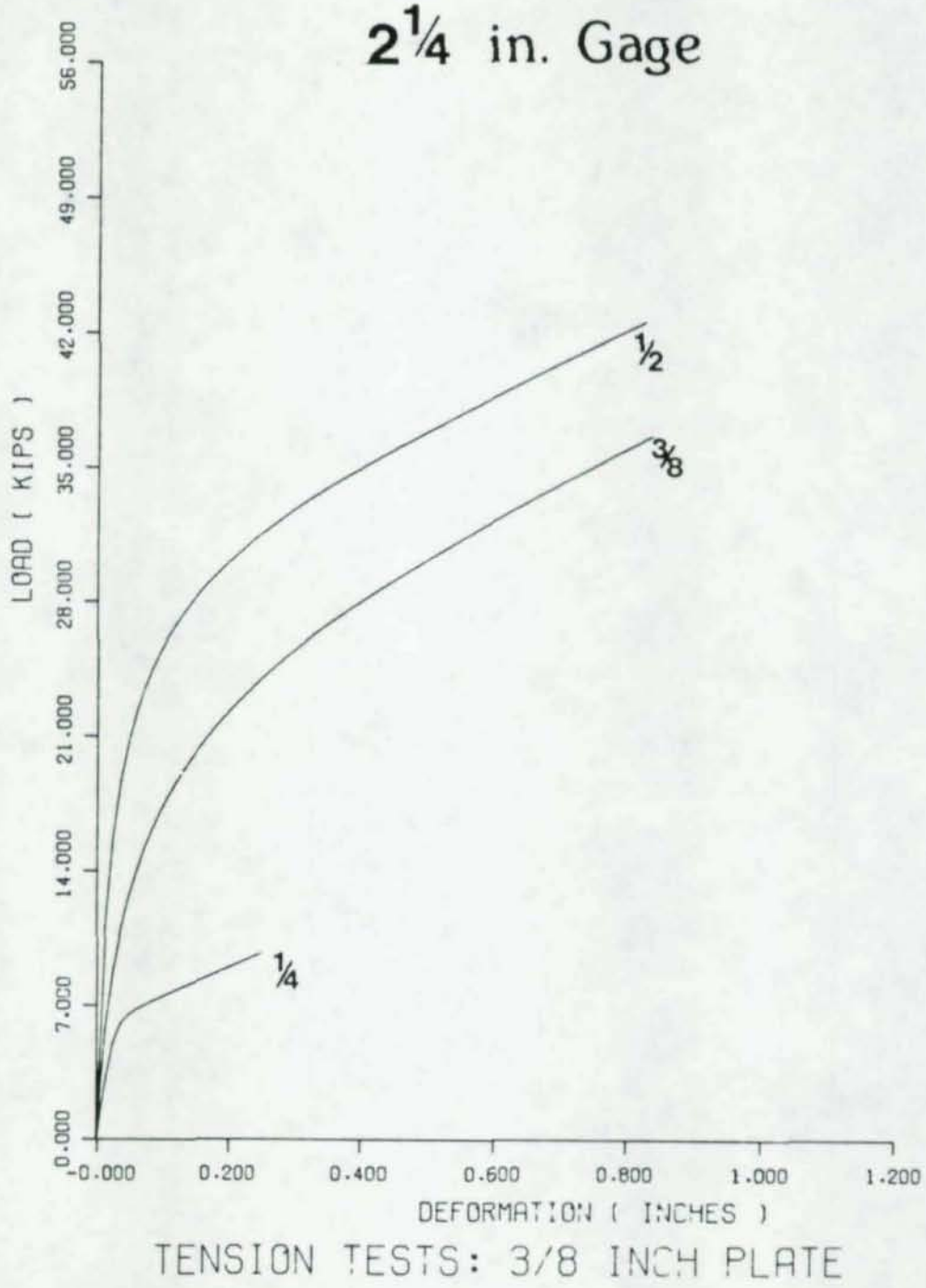

Figure C-5

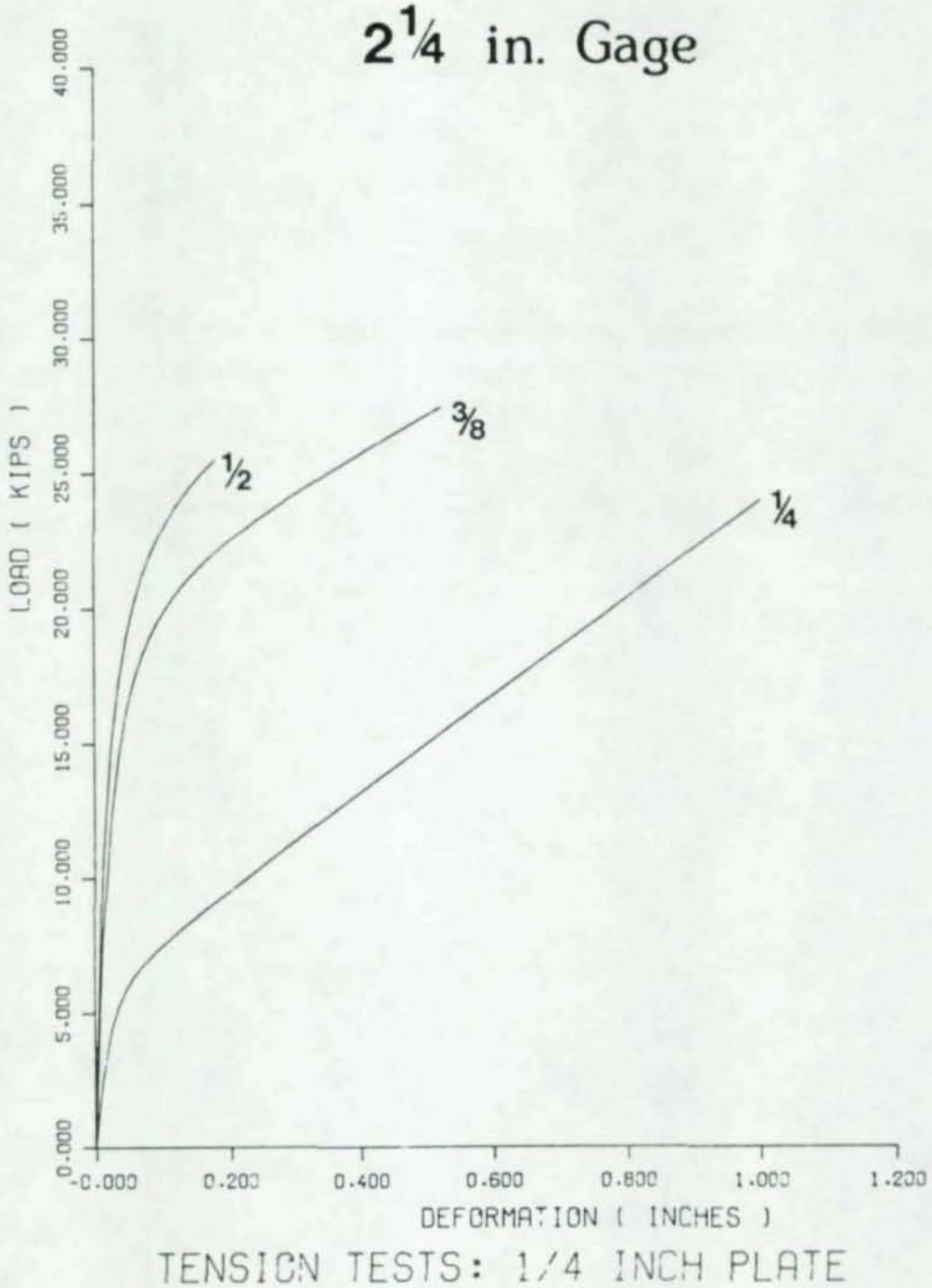

Figure C-6

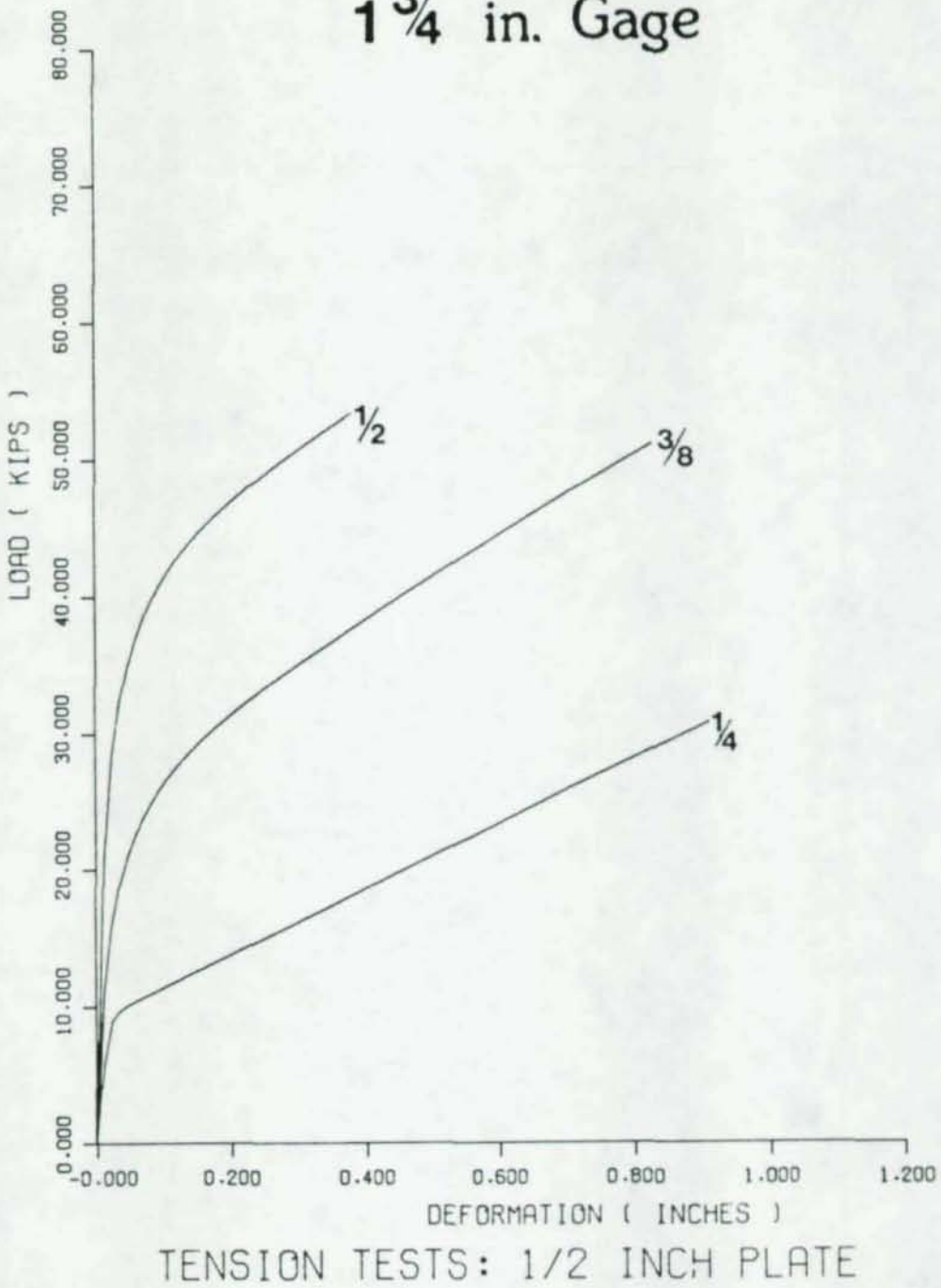
1 3/4 in. Gage
LOAD (KIPS)
0.000
10.000
20.000
30.000
40.000
50.000
60.000
70.000
80.000
1/2
3/8
1/4
-0.000
0.200
0.400
0.600
0.800
1.000
1.200
DEFORMATION (INCHES)
TENSION TESTS: 1/2 INCH PLATE

Figure C-7

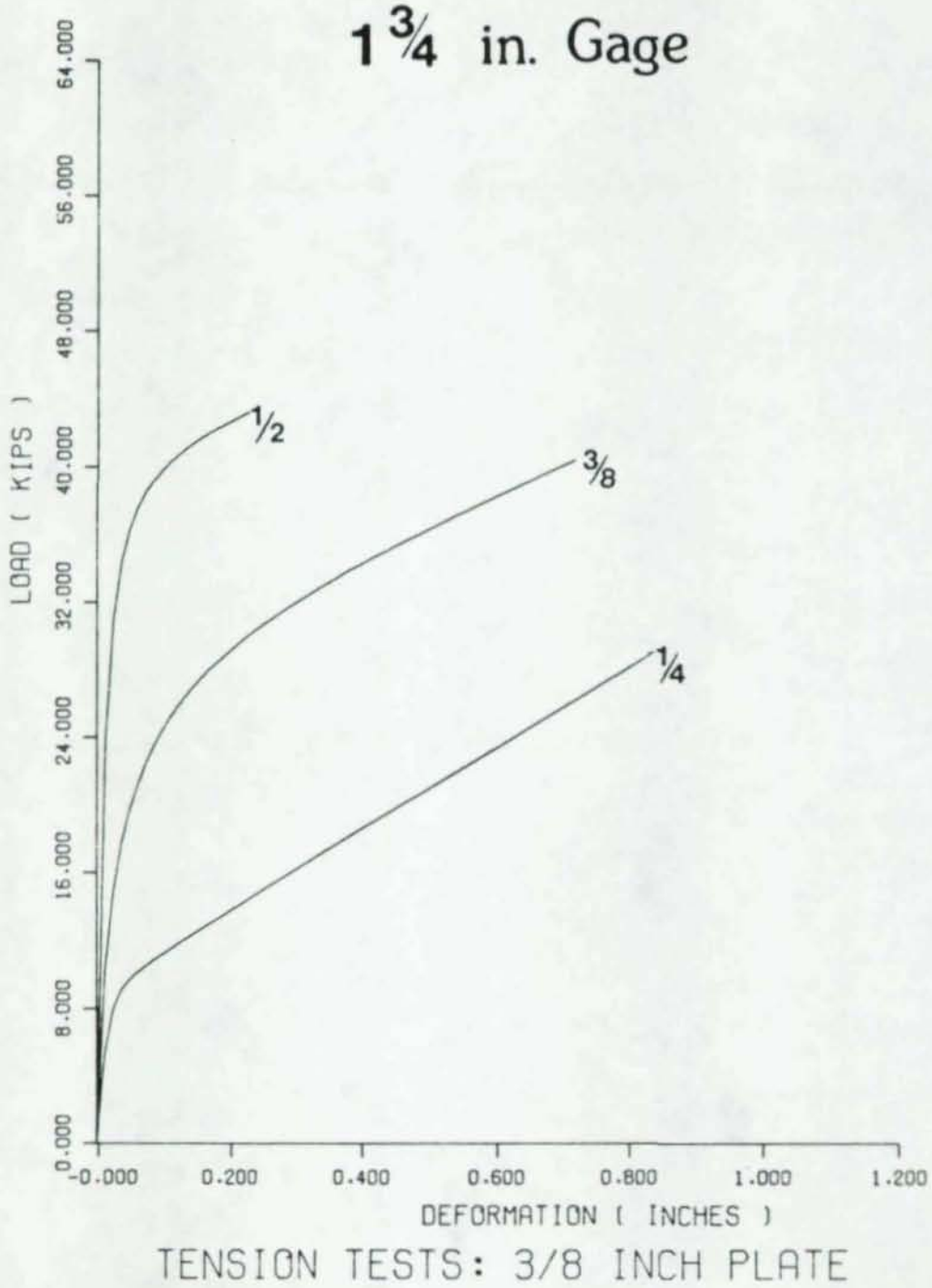
1 3/4 in. Gage
LOAD (KIPS)
0.000
8.000
16.000
24.000
32.000
40.000
48.000
56.000
64.000
1/2
3/8
1/4
-0.000
0.200
0.400
0.600
0.800
1.000
1.200
DEFORMATION (INCHES)
TENSION TESTS: 3/8 INCH PLATE

Figure C-8

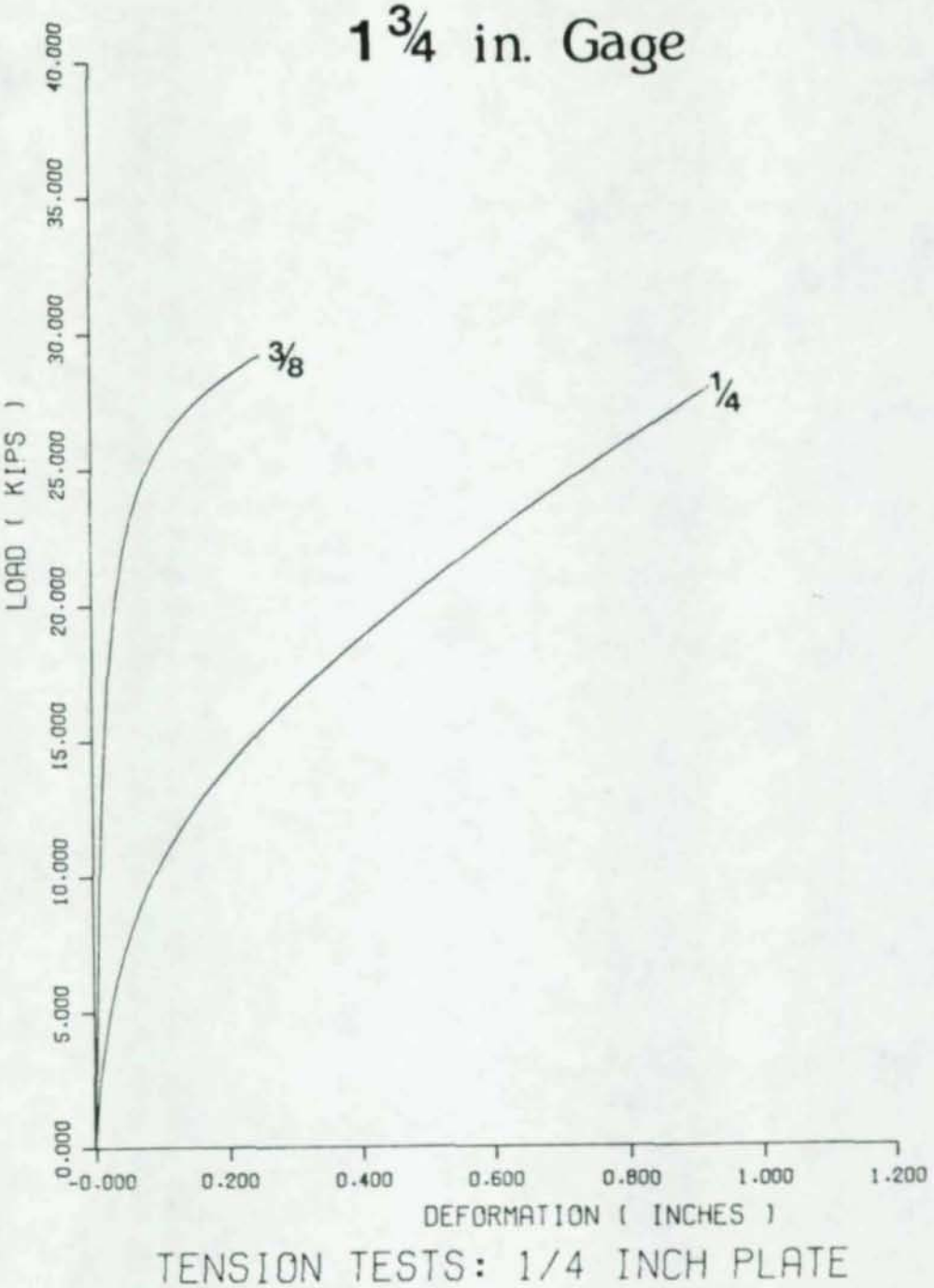
1 3/4 in. Gage
LOAD (KIPS)
0.000
5.000
10.000
15.000
20.000
25.000
30.000
35.000
40.000
3/8
1/4
0.000
0.200
0.400
0.600
0.800
1.000
1.200
DEFORMATION (INCHES)
TENSION TESTS: 1/4 INCH PLATE

Figure C-9

APPENDIX D

VARIATION IN LOAD-DEFORMATION CURVES WITH RESPECT TO A CHANGE IN GAGE LENGTH

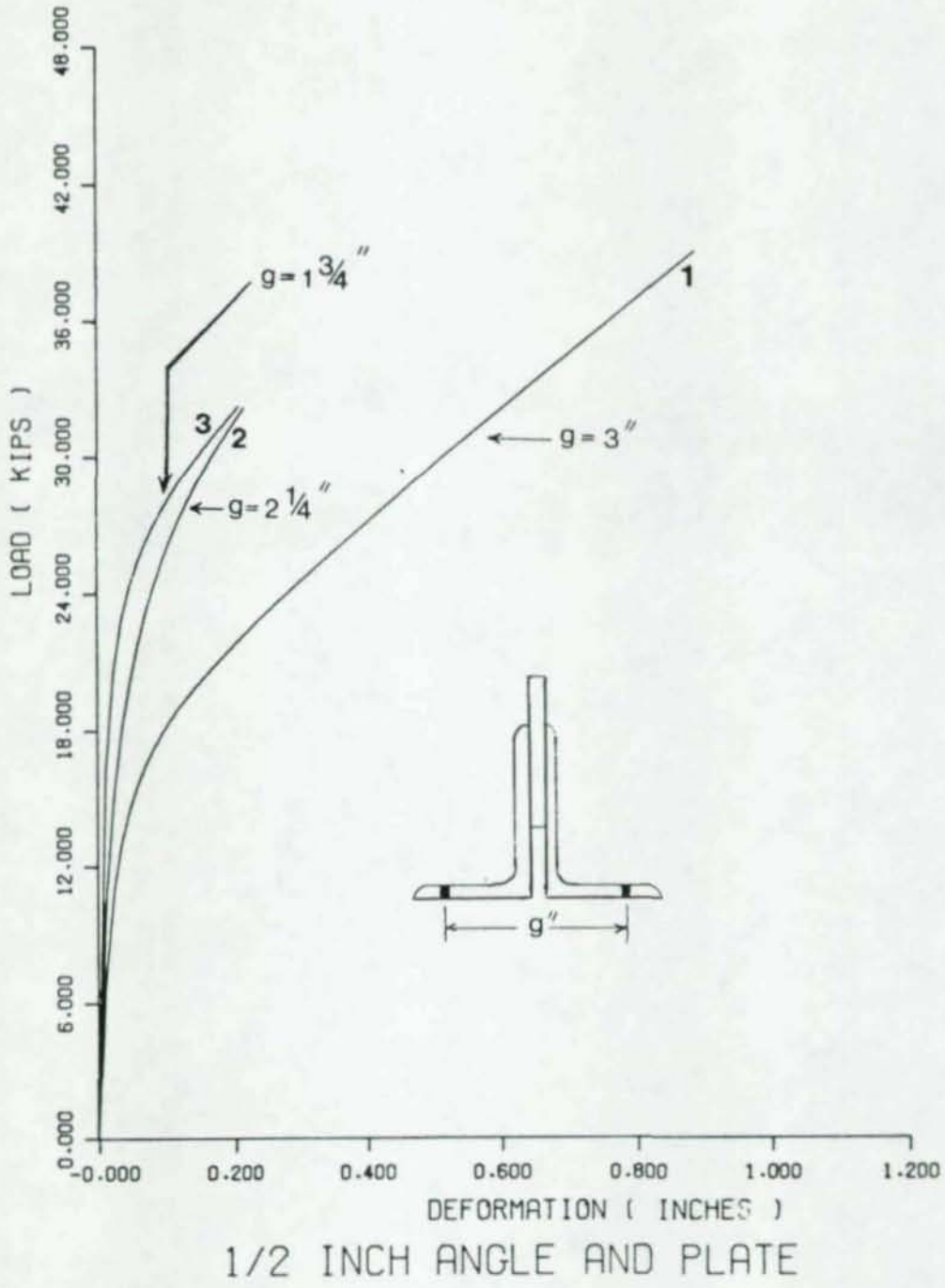
LOAD (KIPS)
48.000
42.000
36.000
30.000
24.000
18.000
12.000
6.000
0.000
-0.000
0.200
0.400
0.600
0.800
1.000
1.200
DEFORMATION (INCHES)
g= 1 3/4 "
g= 2 1/4 "
g= 3 "
1
2
3
g"
1/2 INCH ANGLE AND PLATE

Figure D-1

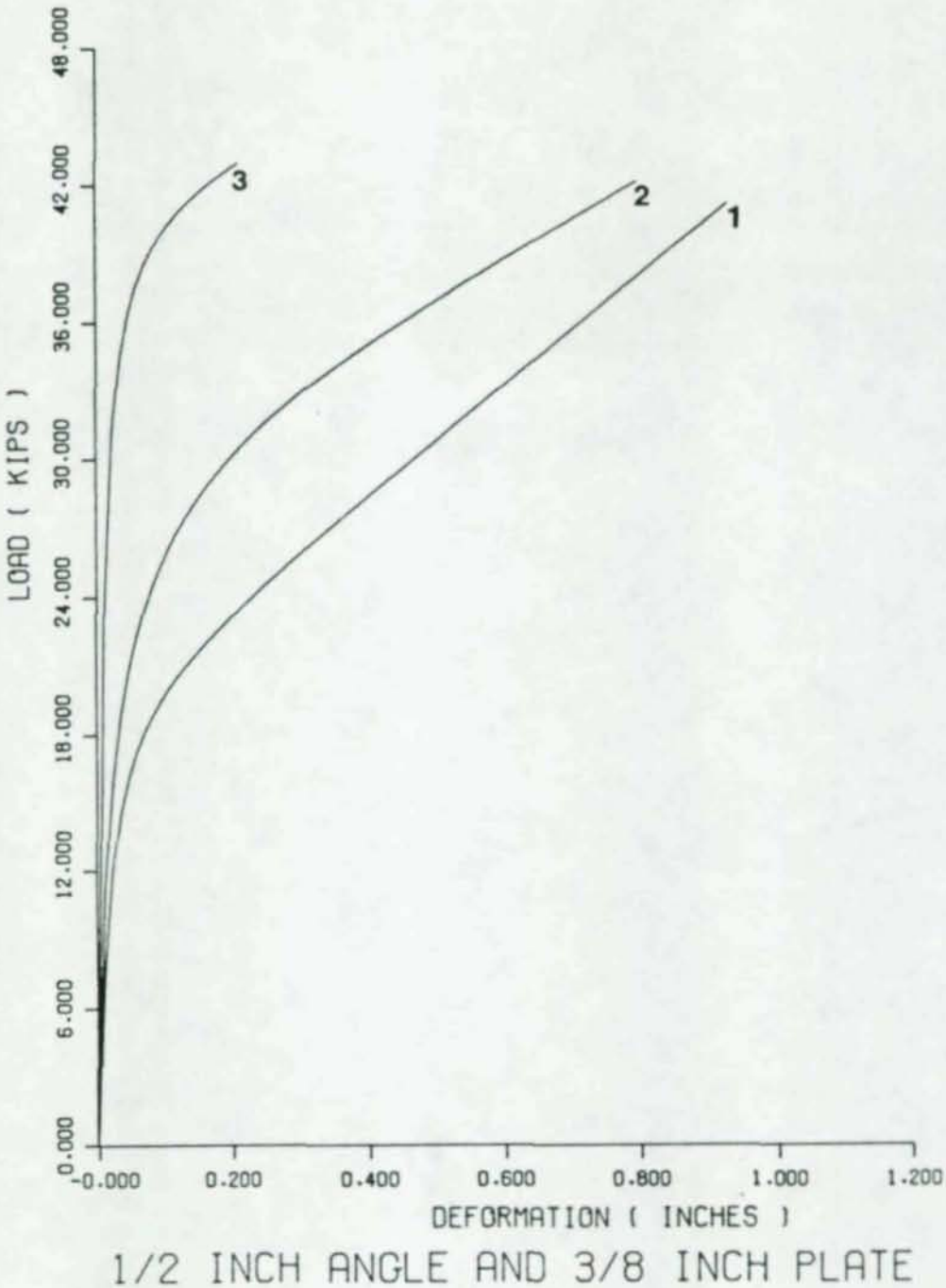
LOAD (KIPS)
0.000
6.000
12.000
18.000
24.000
30.000
36.000
42.000
48.000
-0.000
0.200
0.400
0.600
0.800
1.000
1.200
DEFORMATION (INCHES)
1
2
3
1/2 INCH ANGLE AND 3/8 INCH PLATE

Figure D-2

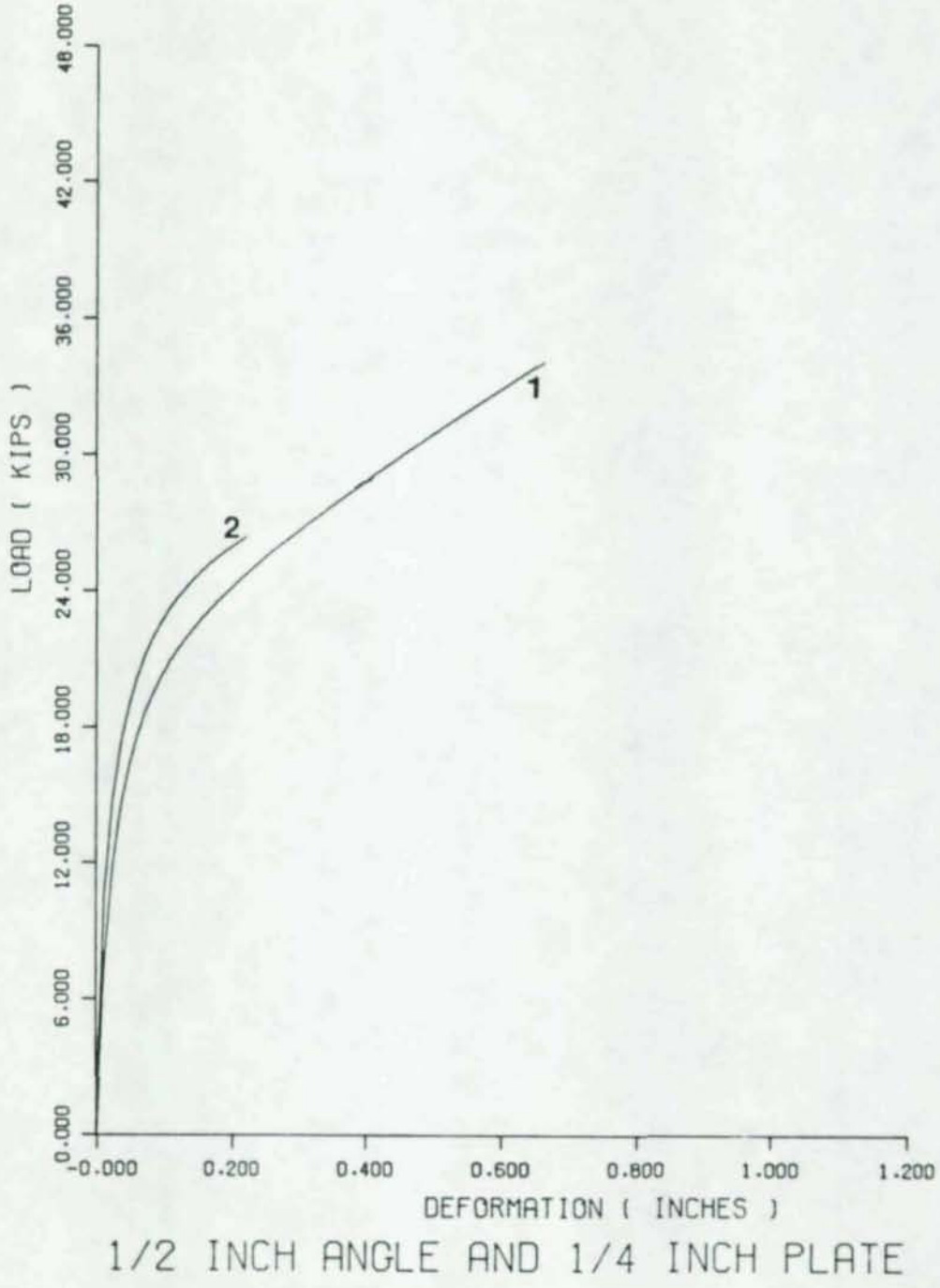
LOAD (KIPS)
0.000
6.000
12.000
18.000
24.000
30.000
36.000
42.000
48.000
0.000
0.200
0.400
0.600
0.800
1.000
1.200
DEFORMATION (INCHES)
1
2
1/2 INCH ANGLE AND 1/4 INCH PLATE

Figure D-3

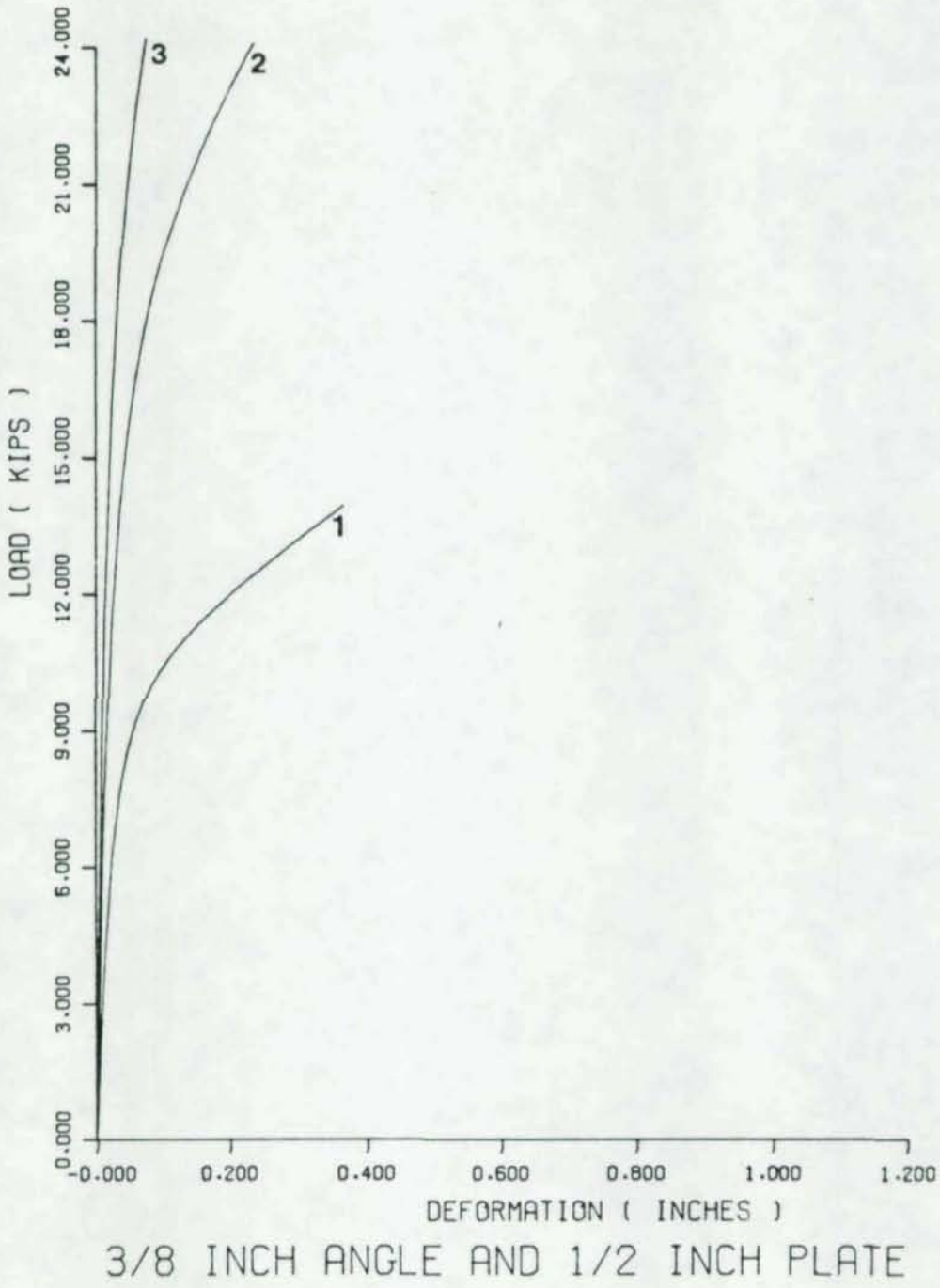
LOAD (KIPS)
0.000
3.000
6.000
9.000
12.000
15.000
18.000
21.000
24.000
-0.000
0.200
0.400
0.600
0.800
1.000
1.200
DEFORMATION (INCHES)
1
2
3
3/8 INCH ANGLE AND 1/2 INCH PLATE

Figure D-4

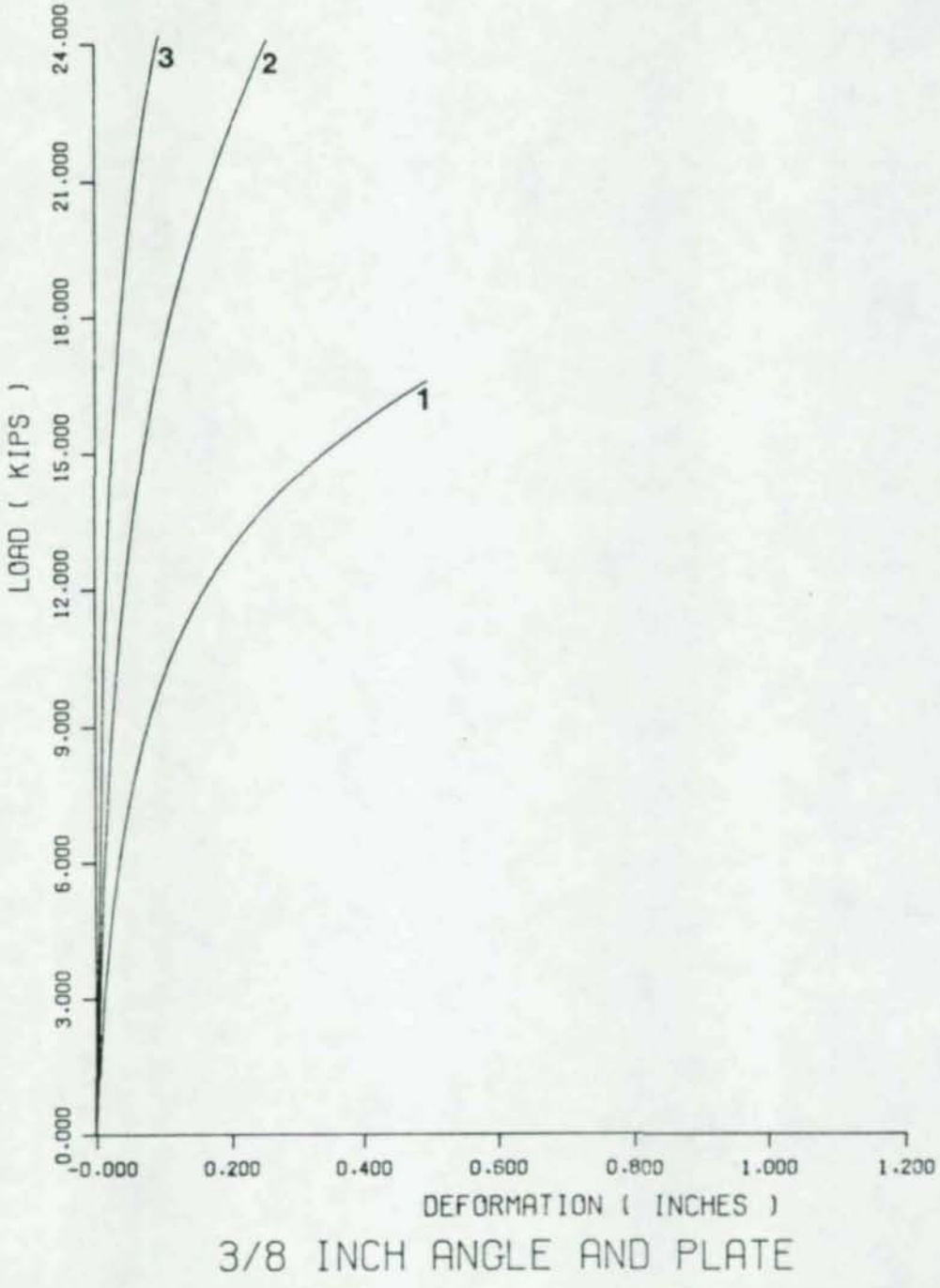
LOAD (KIPS)
0.000
3.000
6.000
9.000
12.000
15.000
18.000
21.000
24.000
-0.000
0.200
0.400
0.600
0.800
1.000
1.200
DEFORMATION (INCHES)
1
2
3
3/8 INCH ANGLE AND PLATE

Figure D-5

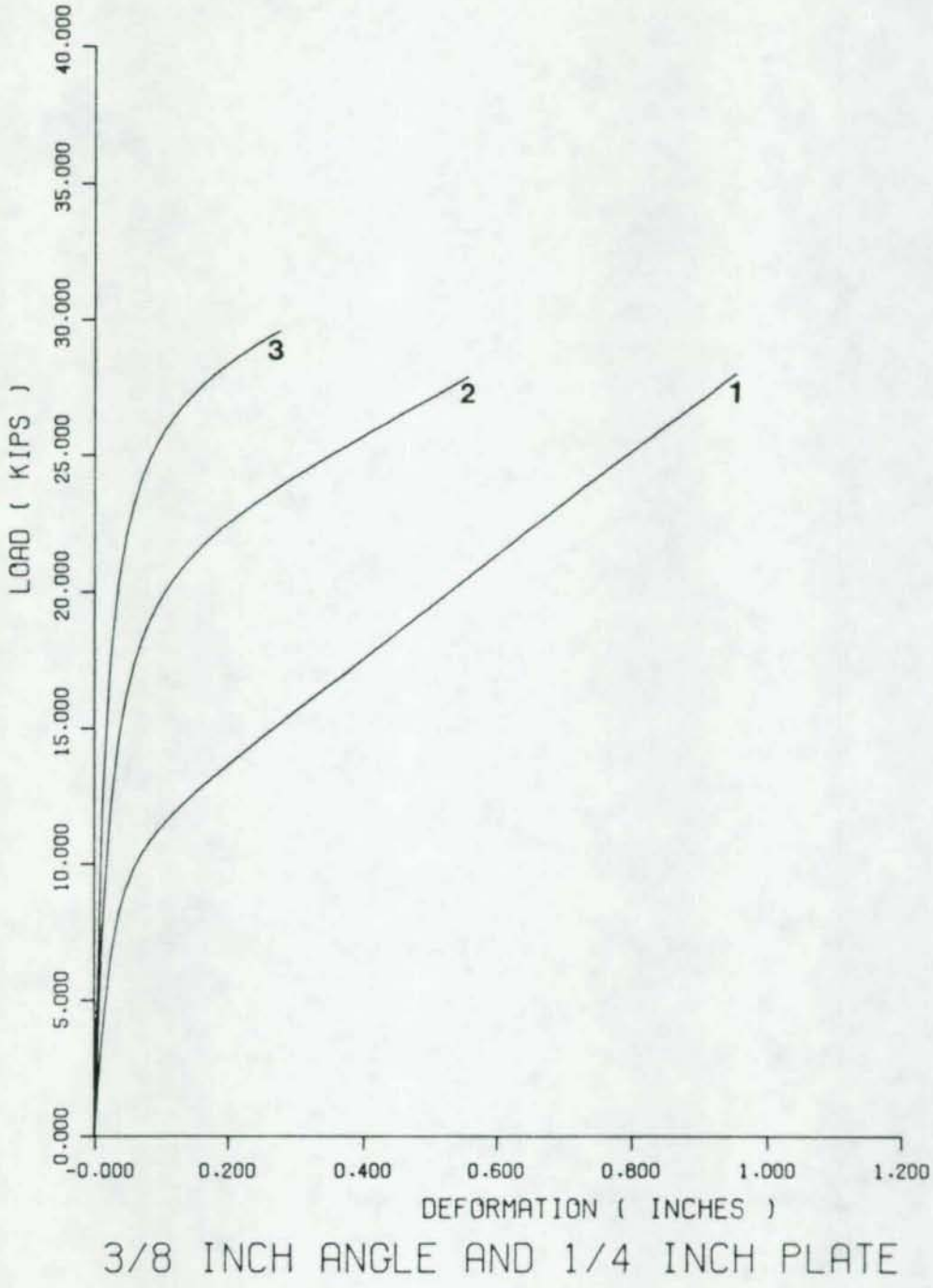
LOAD (KIPS)
0.000
5.000
10.000
15.000
20.000
25.000
30.000
35.000
40.000
-0.000
0.200
0.400
0.600
0.800
1.000
1.200
DEFORMATION (INCHES)
1
2
3
3/8 INCH ANGLE AND 1/4 INCH PLATE

Figure D-6

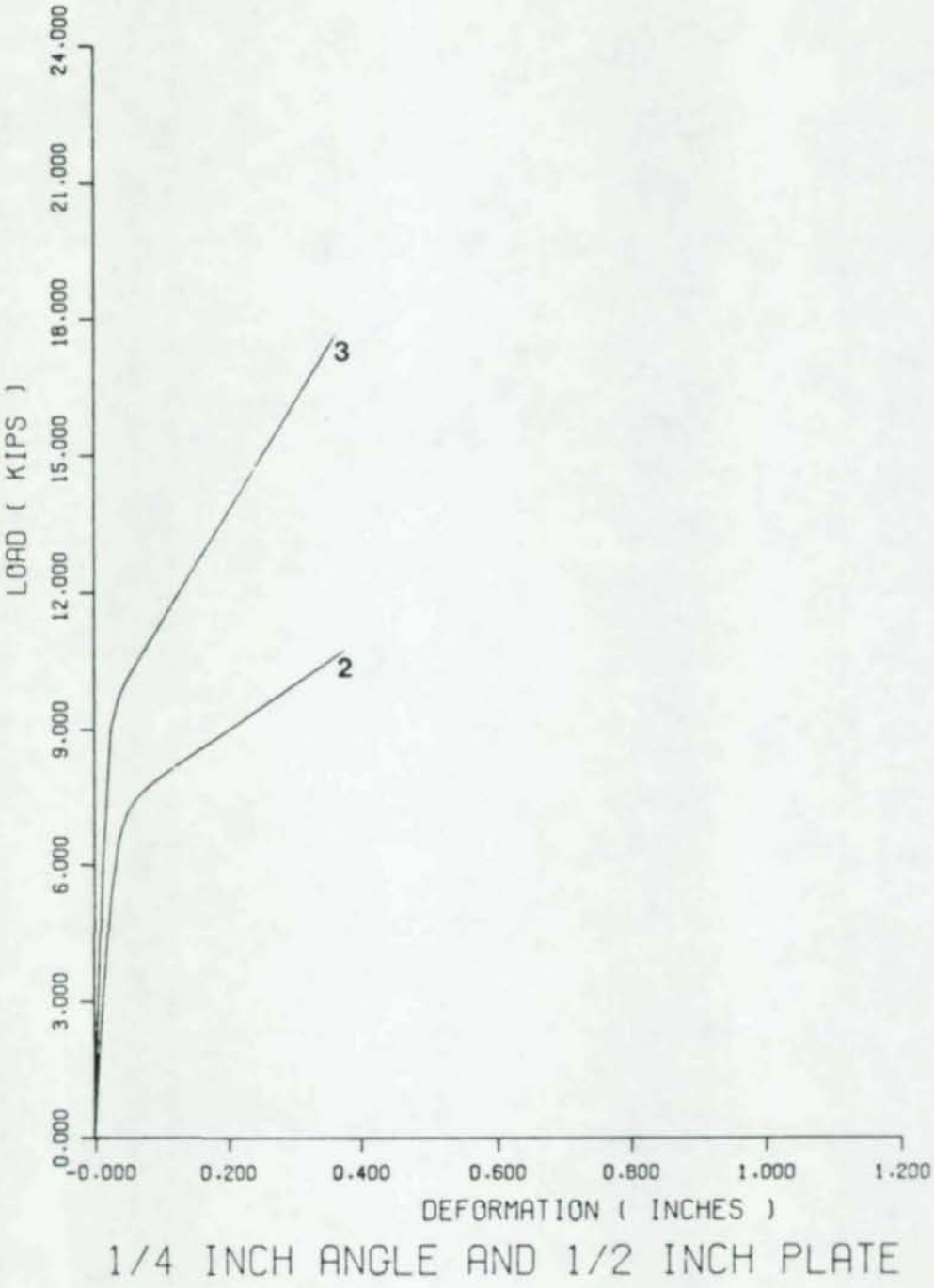
LOAD (KIPS)
0.000
3.000
6.000
9.000
12.000
15.000
18.000
21.000
24.000
-0.000
0.200
0.400
0.600
0.800
1.000
1.200
DEFORMATION (INCHES)
3
2
1/4 INCH ANGLE AND 1/2 INCH PLATE

Figure D-7

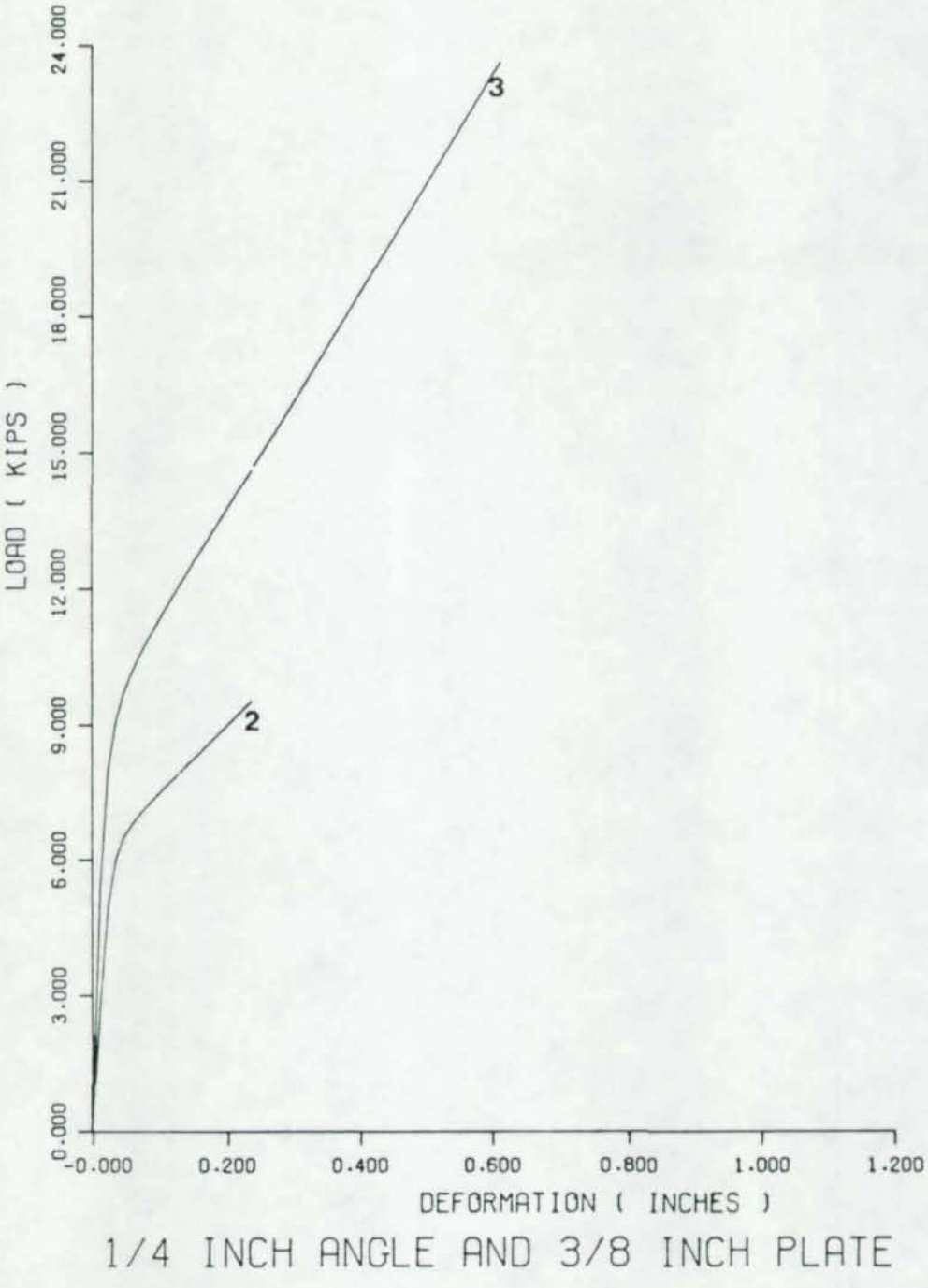
LOAD (KIPS)
0.000
3.000
6.000
9.000
12.000
15.000
18.000
21.000
24.000
0.000
0.200
0.400
0.600
0.800
1.000
1.200
DEFORMATION (INCHES)
2
3
1/4 INCH ANGLE AND 3/8 INCH PLATE

Figure D-8

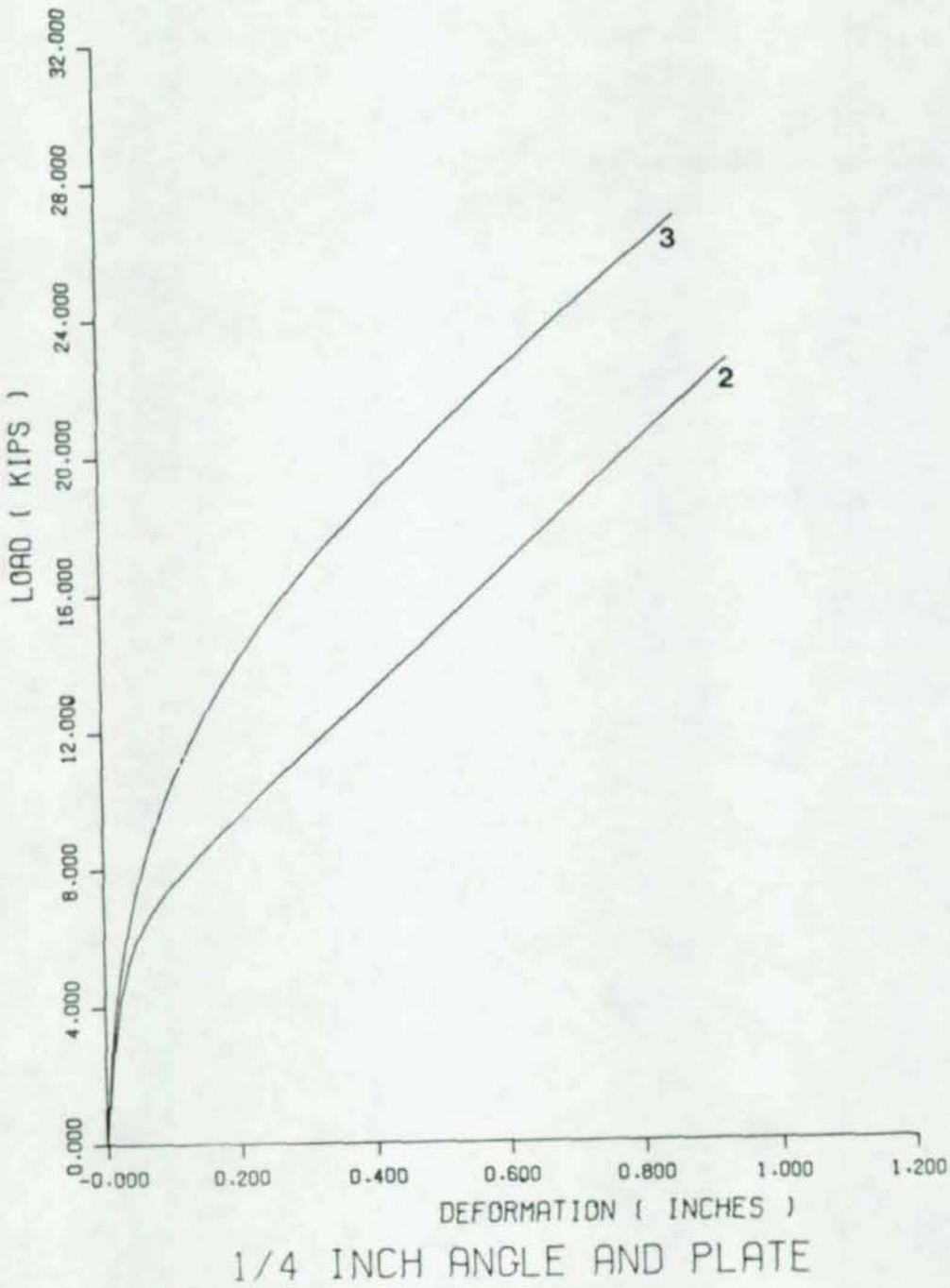
LOAD (KIPS)
0.000
4.000
8.000
12.000
16.000
20.000
24.000
28.000
32.000
-0.000
0.200
0.400
0.600
0.800
1.000
1.200
DEFORMATION (INCHES)
3
2
1/4 INCH ANGLE AND PLATE

Figure D-9

APPENDIX E

VARIATION IN LOAD-DEFORMATION CURVES WITH RESPECT TO BOLT DIAMETER OR STATE OF STRESS

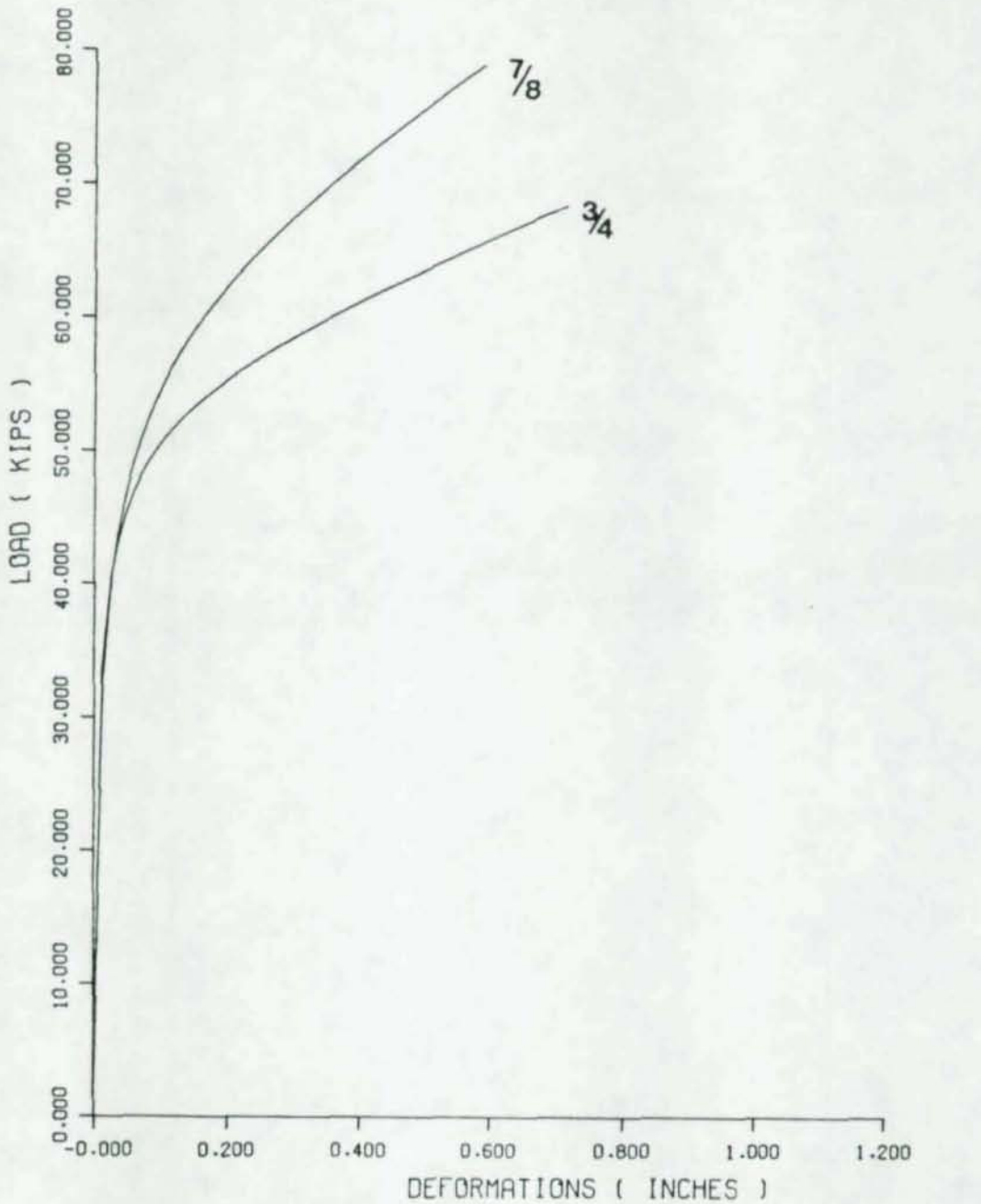

COMPRESSION TESTS: 3/4 AND 7/8 INCH BOLTS

Figure E-1

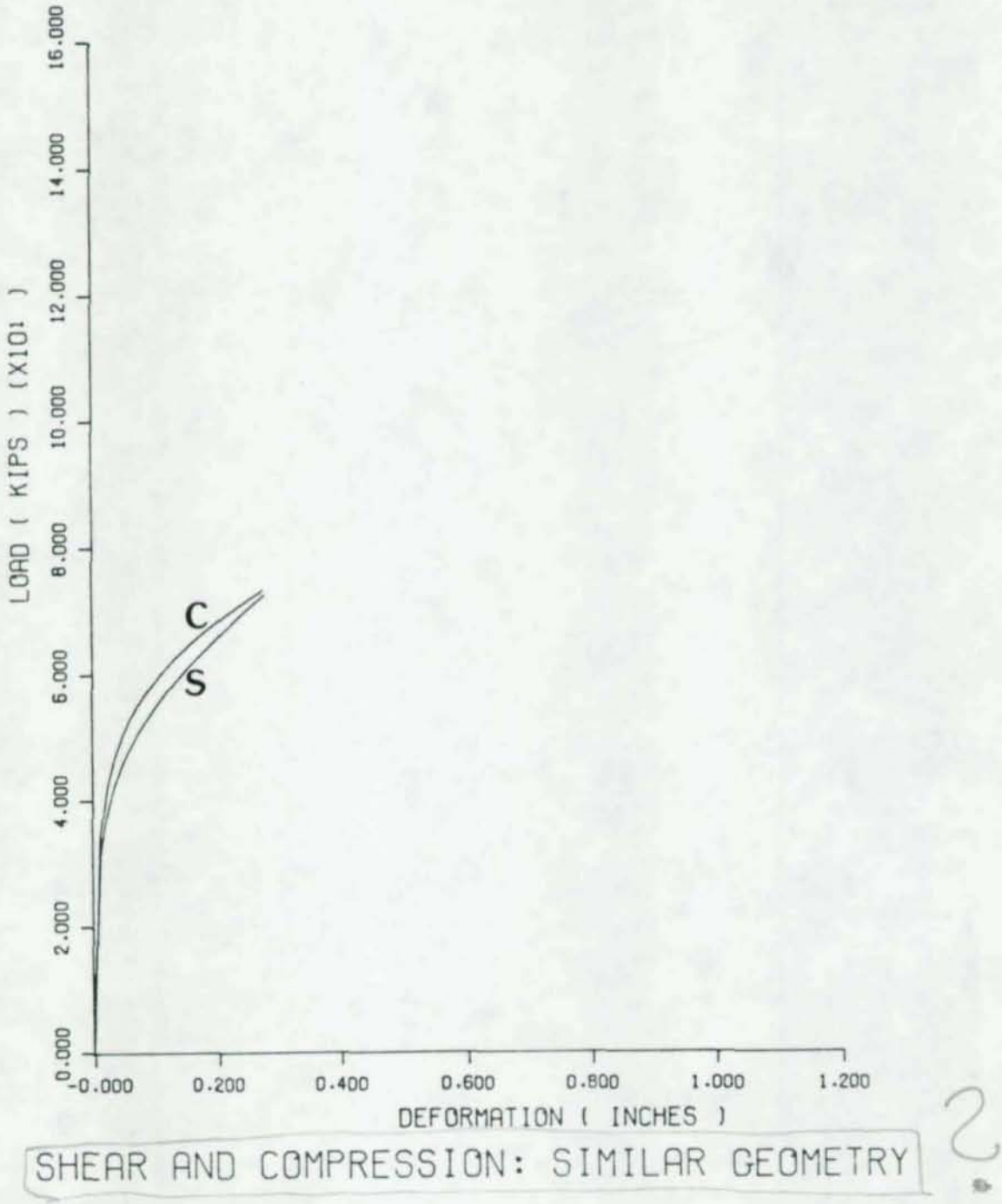
LOAD (KIPS) (X10¹)
16.000
14.000
12.000
10.000
8.000
6.000
4.000
2.000
0.000
C
S
-0.000
0.200
0.400
0.600
0.800
1.000
1.200
DEFORMATION (INCHES)
SHEAR AND COMPRESSION: SIMILAR GEOMETRY

Figure E-2

APPENDIX F

EXPLANATION OF THE RICHARD CURVE

In the analysis of nonlinear structural systems, the load-deformation curve must be represented mathematically. Although other approaches exist, the method used in this thesis was to fit a smooth analytical expresson (Richard and Abbott, 1975) to the experimentally obtained load-deformation curve. The equation of the curve used for the program RCFIT is as follows:

Equation F-1

$$R = \frac{K_1 \cdot \Delta}{\left[1 + \left|\frac{K_1 \Delta}{R_o}\right|^n\right]^{1/n}} + K_p \cdot \Delta$$

where: R = load

Δ = deformation

R_o = y-intercept

n = defines smoothness of the curve

K_p = the slope of the load-deformation curve in the extreme yielding range

K_1 = $K - K_p$, where K is the initial slope of the curve.

This equation allows the user to specify either strain hardening or strain softening by allowing the value of K_p to be positive or negative, respectively. A negative value of K_p is often used to help

fit the curve to the data even though the strain softening is not exhibited. The user has this ability because of the way K_1 is defined and used in the equation.

In conclusion, the equation used in RCFIT provides a simple and useful means of describing material load-deformation behavior accurately beyond the proportional limit.

REFERENCES CITED

Bjorhovde, R. Double Angle Beam-to-Column Connections. University of Alberta, Structural Engineering Report No. 73 (in preparation), Edmonton, Alberta, Canada, 1983.

Bjorhovde, R. and Chakrabarti, S. K. Tests of Full-Scale Gusset Plate Connections. Research Report (in preparation), University of Arizona, Tucson, Arizona, 1983.

Gillett, P. E., and Hornby, D. E. RCFIT, Department of Civil Engineering and Engineering Mechanics, University of Arizona, Tucson, Arizona, August 1978.

Lewitt, C. W., Chesson, E., and Munse, W. H. Restraint Characteristics of Flexible Riveted and Bolted Beam-to-Column Connections. Dept. of Civil Engineering, University of Illinois, Urbana, Ill., March 1966.

Munse, W. H., Bell, W. G., and Chesson, E. "Behavior of Beam-to-Column Connections," ASCE Structural Division Journal, March 1959.

Rathbun, J. C. "Elastic Properties of Riveted Connections," ASCE Journal, #1933, January 1935.

Richard, R. M. and Abbott, B. J. "Versatile Elastic-Plastic Stress-Strain Formula," ASCE Journal of Engineering Mechanics, August 1975.

Richard, R. M., Gillett, P. E., Kriegh, J. D., and Lewis, B. A. "The Analysis and Design of Single Plate Framing Connections," AISC Engineering Journal, No. 2, 1980.

Sommer, W. H. Behavior of Welded Header Plate Connections. Dept. of Civil Engineering, University of Toronto, Toronto, Canada, January 1969.

Vaserhelyi, I. "Tests of Gusset Plate Models," ASCE Structural Division Journal, February 1971.